MODELING OF PHOTOTRANSDUCTION

IN VISION SYSTEMS

A Thesis

presented to

the Faculty of the Graduate School

at the University of Missouri - Columbia

In Partial Fulfillment

of the Requirements for the Degree

Master of Science

---

by

LEI LU

Dr. Jinglu Tan, Thesis Supervisor

DECEMBER 2007

The undersigned, appointed by the Dean of the Graduate School, have examined the thesis entitled

MODELING OF PHOTOTRANSDUCTION

IN VISION SYSTEMS

presented by Lei Lu

A candidate for the degree of Master of Science

And hereby certify that, in their opinion, it is worthy of acceptance.

_____

Jinglu Tan, Biological Engineering

_____

Bo Lei, Vision Science and Ophthalmology

_____

Gang Yao, Biological Engineering

ACKNOWLEDGEMENTS

I would like to express my thanks to my advisor, Dr. Jinglu Tan, for his wisdom, guidance and encouragement during my entire Master's program. Thanks are extended to Dr. Bo Lei for his valuable guidance and contribution to the success of this research.

Acknowledgment is also extended to Dr. Gang Yao. I genuinely thank Dr. Yao for his valuable suggestions.

I want to thank Ms. Keqing Zhang, Mr. Brian Wirth and Mr. Ya Guo for their help with equipment setup, sample preparation, data acquisition, and their valuable suggestions.

Finally, special thanks are extended to my parents, my husband and my brother for their encouragement and support.

TABLE OF CONTENTS

ACKNOWLEDGEMENTS ii

LIST OF FIGURES vi

LIST OF TABLES x

LIST OF NOMENCLATURE xi

ABSTRACT xiii

Chapter

1. INTRODUCTION 1

2. LITERATURE REVIEW 4

2.1 Retinal Neurons 4

2.2 Photoreceptors: Rod and Cone 6

2.2.1 Structure 6

2.2.2 The circulating electrical current 7

2.3 Phototransduction 8

2.3.1 Activation 9

2.3.2 Termination and Modulation 10

2.4 History of the ERG 13

2.5 The ERG Recording 15

2.6 Components of the ERG 16

3. MODEL DEVELOPMENT 19

3.1 Existing Models 19

3.1.1 Hood and Birch's model 19

3.1.2 Lamb and Pugh's model 20
3.2 Proposed Model for ERG a-wave 27
4. MODEL VALIDATION 33
4.1 Methods 33
4.1.1 Experimental Subjects 33
4.1.2 The ERG Recording 34
4.1.3 Parameters Estimation 35
4.2 Experimental Results 39
4.2.1 Wild-type Mice 39
4.2.2 NOB1 Mice 41
4.2.3 Light-induced Retina-damaged Mouse 42
4.2.4 N-methyl-N-nitrosourea-induced Photoreceptor-degenerated Mice 44
4.3 Parameter Estimation and Model Verification 46
4.4 Detection of Photoreceptor Damage or Degeneration 53
4.5 Modeling of Termination and Modulation 58
4.6 Discussion 60
5. CONCLUSIONS AND RECOMMENDATIONS 63
5.1 Conclusions 63
5.2 Recommendations 64
APPENDIX
A. Matlab Program for Modeling of Phototransduction 65
1. Main Program 65
2. ERG a-wave model 76

3. Jacobian Matrix of control subjects 77

4. Jacobian Matrix of stress subjects 78

5. Solution of the model 78

6. Getting cG 79

7. Identifying the Parameters 79

B. Figures of Experimental and Estimated Data 85

1. Simulations of wild-type mice 85

2. Simulations of wild-type and light-damaged mice 87

3. Simulations of NOB1 and drug-damaged mice 90

BIBLIOGRAPHY 95

LIST OF FIGURES

Figure Page

1. Simple diagram of the organization of the retina. 4

2. Structure of rods and cones, and nature of the circulating current. 7

3. Activation steps of the phototransduction cascade in vertebrate photoreceptors (Pugh & Lamb, 2000). 9

4. Inactivation of R* of the phototransduction cascade in vertebrate photoreceptors (Pugh & Lamb, 2000). 11

5. Inactivation of G*-E* of the phototransduction cascade in vertebrate photoreceptors (Pugh & Lamb, 2000). 12

6. The ERG of a cat in response to a 2 sec light stimulus. 14

7. The ERG of a dark-adapted mouse. A brief (10μs) flash green light was given at 40 ms. The light intensity (Log) was 14.906 photons cm^{-2} s^{-1}. 16

8. Elimination of the ERG b-wave in mouse by injecting L-glutamate. A brief (10 ms) flash green light was given at 40 ms. The light intensity (Log) was 12.997 photons cm^{-2} s^{-1}. 17

9. Comparison of prediction by Eq. (3.9) with experimental ERG a-waves. Mouse rod a-waves (Lyubarsky & Pugh, 1996). 22

10. Comparison of predictions by Eq. (3.9) with the experimental ERG a-waves. Left: Human rod a-waves; Right: Human cone a-waves (Smith & Lamb, 1997). 23

11. Flash responses of a salamander rod at four dim intensities, compared with theoretical predictions. Φ =11, 23, 45 and 94 respectively. 26

12. Transition in the phototransduction. 27

13. The isolated ERG a-wave of wild-type mice. Stimulus: pulse. 40

14. The isolated ERG a-wave of wild-type mice. Stimulus: step. 40

15. Pulse responses of NOB1 mice. 41

16. Step responses of NOB1 mice. 42

17. Pulse responses of light-damaged wild-type mouse after APB....43

18. Step responses of light-damaged wild-type mouse after APB. 44

19. Pulse responses of drug-damaged NOB1 mice. 45

20. Step responses of drug-damaged NOB1 mice. 46

21. Wild-type mice after APB excited with pulse stimuli. 47

22. Wild-type mice after APB excited with step stimuli. 48

23. NOB1 mice excited with pulse stimuli. 48

24. NOB1 mice excited with step stimuli. 49

25. Subjects: wild-type after APB. Stimulus: pulse. Light Intensity (Log): 12.407 photons cm^{-2} s^{-1}. 52

26. Subjects: wild-type after APB. Stimulus: step. Light Intensity (Log): 13.891 photons cm^{-2} s^{-1}. 53

27. Subjects: wild-type after APB and light-damaged wild-type after APB. Stimulus: pulse. Light Intensity (Log): 12.407 photons cm^{-2} s^{-1}. 54

28. Subjects: wild-type after APB and light-damaged wild-type after APB. Stimulus: step. Light Intensity (Log): 13.891 photons cm^{-2} s^{-1}. 55

29. Subjects: NOB1 and drug-damaged. Drug dose: 60 mg/kg body weight. Stimulus: pulse. Light Intensity (Log): 12.997 photons cm^{-2} s^{-1}. 56

30. Subjects: NOB1 and drug-damaged. Drug dose: 60 mg/kg body weight. Stimulus: step. Light Intensity (Log): 12.997 photons cm^{-2} s^{-1}. 56

31. Subject: wild-type after APB. Stimulus: pulse. Light Intensity (Log): 13.891 photons cm^{-2} s^{-1}. 59

32. Subject: NOB1. Stimulus: step. Light Intensity (Log): 12.997 photons cm^{-2} s^{-1}. ..59

33. Subject: wild-type after APB. Stimulus: pulse. Light Intensity (Log): 14.906 photons cm^{-2} s^{-1}. 61

34. Subject: NOB1. Stimulus: step. Light Intensity (Log): 14.906 photons cm^{-2} s^{-1}. ..62

B1. Subjects: wild-type after APB. Stimulus: pulse. Light Intensity (Log): 12.997 photons cm^{-2} s^{-1}. 85

B2. Subjects: wild-type after APB. Stimulus: pulse. Light Intensity (Log): 13.891 photons cm^{-2} s^{-1}. 86

B3. Subjects: wild-type after APB. Stimulus: step. Light Intensity (Log): 12.407 photons cm^{-2} s^{-1}. 86

B4. Subjects: wild-type after APB. Stimulus: step. Light Intensity (Log): 12.997 photons cm^{-2} s^{-1}. 87

B5. Subjects: wild-type after APB and light-damaged wild-type after APB. Stimulus: pulse. Light Intensity (Log): 12.997 photons cm^{-2} s^{-1}.....88

B6. Subjects: wild-type after APBand light-damaged wild-type after APB. Stimulus: pulse. Light Intensity (Log): 13.891 photons cm^{-2} s^{-1}.....88

B7. Subjects: wild-type after APB and light-damaged wild-type after APB. Stimulus: step. Light Intensity (Log): 12.407 photons cm^{-2} s^{-1}.....89

B8. Subjects: wild-type after APB and light-damaged wild-type after APB. Stimulus: step. Light Intensity (Log): 12.997 photons cm^{-2} s^{-1}.....89

B9. Subjects: NOB1 and drug-damaged. Drug dose: 30 mg/kg body weight. Stimulus: pulse. Light Intensity (Log): 12.407 photons cm^{-2} s^{-1}.....90

B10. Subjects: NOB1 and drug-damaged. Drug dose: 30 mg/kg body weight. Stimulus: pulse. Light Intensity (Log): 12.997 photons cm^{-2} s^{-1}. 90

B11. Subjects: NOB1 and drug-damaged. Drug dose: 30 mg/kg body weight. Stimulus: pulse. Light Intensity (Log): 13.891 photons cm^{-2} s^{-1}. 91

B12. Subjects: NOB1 and drug-damaged. Drug dose: 30 mg/kg body weight. Stimulus: step. Light Intensity (Log): 12.407 photons cm^{-2} s^{-1}. 91

B13. Subjects: NOB1 and drug-damaged. Drug dose: 60 mg/kg body weight. Stimulus: step. Light Intensity (Log): 12.997 photons cm^{-2} s^{-1}. 92

B14. Subjects: NOB1 and drug-damaged. Drug dose: 30 mg/kg body weight. Stimulus: step. Light Intensity (Log): 13.891 photons cm^{-2} s^{-1}. 92

B15. Subjects: NOB1 and drug-damaged. Drug dose: 60 mg/kg body weight. Stimulus: pulse. Light Intensity (Log): 12.407 photons cm^{-2} s^{-1}. 93

B16. Subjects: NOB1 and drug-damaged. Drug dose: 60 mg/kg body weight. Stimulus: pulse. Light Intensity (Log): 13.891 photons cm^{-2} s^{-1}. 93

B17. Subjects: NOB1 and drug-damaged. Drug dose: 60 mg/kg body weight. Stimulus: step. Light Intensity (Log): 12.407 photons cm^{-2} s^{-1}. 94

B18. Subjects: NOB1 and drug-damaged. Drug dose: 60 mg/kg body weight. Stimulus: step. Light Intensity (Log): 13.891 photons cm^{-2} s^{-1}. 94

LIST OF TABLES

Table Page

1. Stimulus light intensities.....35

2. Parameters of wild-type mice. Stimulus: pulse.....50

3. Parameters of wild-type mice. Stimulus: step.....50

4. Parameters of NOB1 mice. Stimulus: pulse. 51

5. Parameters of NOB1 mice. Stimulus: step. 51

6. Parameter k_{11} for wild-type and light-damaged subjects. 57

7. Parameter k_{11} for NOB1 and 30 mg/kg body weight drug-damaged NOB1 subjects...57

8. Parameter k_{11} for NOB1 and 60 mg/kg body weight drug-damaged NOB1 subjects...58

LIST OF NOMENCLATURE

cG	concentration of free cyclic GMP
cG_{dark}	concentration of cG in darkness
C_1	number of complex C1
C_2	number of complex C2
E	total number of phosphodiesterase
E*	number of activated phosphodiesterase
G	total number of G-protein
G*	number of activated G-protein
GC	number of guanylyl cyclase
GCAP	guanylyl cyclase activating protein
k_1	activated rate of rhodopsin
k_2	inactivated rate of activated rhodopsin
k_3	activated rate of G-protein
k_4	inactivated rate of G-protein, and is equal to activated rate of phosphodiesterase
k_5	inactivated rate of phosphodiesterase
k_6	reaction velocity of cyclic GMP and activated phosphodiesterase
k_7	rate of hydrolysis of complex C1
k_8	reaction velocity of GC, GCAPs and complex C1
k_9	rate of synthesis of cG

k_{10}	rate in which guanylyl cyclase converts to be activated
k_{11}	gain
MSE	mean square error
R	total number of rhodopsin
R*	number of activated rhodopsin
u	intensity of the stimulus light

MODELING OF PHOTOTRANSDUCTION IN VISION SYSTEMS

Lei Lu

Dr. Jinglu Tan, Thesis Supervisor

ABSTRACT

To improve the usefulness of the electroretinogram (ERG) in identifying the sites and mechanisms of adaptation, development and disease processes, a quantitative model was developed based on the biochemical reaction kinetics in the phototransduction cascade and experimental data. A set of differential equations were derived to predict the electrical response of photoreceptors to light and system identification was employed to determine the model parameters. When applied to wild-type and retina-damaged mice, the proposed model effectively described the ERG a-wave over a range of light intensities and different stimulus patterns. From the model parameters, the retina-damaged subjects could be differentiated from the normal ones. It is anticipated that this model could help detect changes in the phototransduction process and enhance the utility of ERG in the clinic. It also provides insights into dynamics of the vision system.

CHAPTER 1

INTRODUCTION

The visual sight is the main information source for the human brain to sense the world. Compared with hearing and smelling, the vision is a highly important sensory system in perceiving the world.

While visual processing is very complex, it is initiated in the retina. Although the retina is only about 0.33 mm thick and 1100 square mm surface area (Kolb, Nelson & Fernandezs, 2000), its value is out of proportion to its size. It is well known that the retina senses light and converts an image into neural signals. The complex nervous system cannot function well without a healthy retina. Human lifestyle and performance could be affected in every aspect by any retinal disease. Scientists and natural philosophers have been interested in it for centuries.

In order to understand visual, many methods have been used (e.g. Hood & Birch, 1990; Lamb & Pugh, 1992). From the 1960s, the electroretinogram (ERG) has become a very important means. The ERG is the recording of light-induced electrical activities of the retinal, and the summation of the electrical signals generated by the different cells of the retina.

The ERG is the only objective measurement of the function of the retina in vivo. It does not depend on the function of the optic nerve, but it changes with age and in disease process. For years, doctors have used ERG to diagnose and track retinal diseases in clinic (Berson, 1975).

The recording of ERGs in the clinical setting has become much more popular as protocols are standardized and commercial equipments further developed (Birch, 1989), which leads to a better understanding of the relationship between the patterns of the ERG and the sites of disease action. These findings imply that it is possible to measure the parameters of both normal and abnormal retinas with the ERG, and thus to test quantitative hypotheses.

The ERG is known as the result of a summation of a few components (Einthoven & Jolly, 1908; Granit, 1933; Armington, 1974) and generated from extracellular currents. The a-wave is one of the major components of the ERG. It is generated from the photoreceptors (Granit, 1933; Penn & Hagins, 1969). As a result of intensive studies at the molecular level, the causes of phototransduction and the relationship between the ERG and the underlying biochemistry have become more clearly understood (Koutalos et al., 1995a; Koutalos et al., 1995b).

Advanced analytical approaches and models have been developed to describe the ERG a-wave responses (Hood & Birch, 1990; Lamb & Pugh, 1992; Nikonov, et al., 1998). However, there are limitations in these models. For example, some models are empirical thus the model parameters have no physical meanings. Some models are based on the biochemical mechanisms, but they are oversimplified.

The objective of this research is to provide a biophysical description of the photoreceptor response based on the kinetics of phototransduction and experimental data. The biochemical reactions in phototransduction are described by a set of mathematical equations, which is derived to depict the activation, termination and modulation phases of

phototransduction as a series of relatively simple physical and biochemical processes. The proposed modeling approach presents a quantitative description of the ERG a-wave.

Normal and retina-damaged mice were used to test the model. System identification was employed to determine the model parameters. For both wild-type and retina-damaged mice, the model effectively described the isolated ERG a-wave over a range of light intensities and different stimulus patterns. The estimated model parameters differentiated retina-damaged mice from normal ones. The model helps detect changes in the phototransduction process and may enhance the utility of ERG. It also provides insights into the dynamics of the visual signal process.

The thesis is divided into five chapters. The first chapter addresses the importance and the purpose of this research. Five subtopics are covered in Chapter 2 to provide readers much of the background for the following chapters. Following a review of two published models, a quantitative model is presented in Chapter 3, which describes the electrical response of photoreceptors to light. In Chapter 4, the experiment plan, subject preparation, and ERG recording are described, and parameters estimation based on the system identification and optimization is discussed. Experimental data are presented and compared with the prediction results by calibrated model. The research is summarized and recommendations for further work are made in the final chapter.

CHAPTER 2

LITERATURE REVIEW

2.1 Retinal Neurons

The retina is the inner layer of the back portion of the eyeball. Its function is to convert light rays into electrical impulses that are transmitted to the brain by way of the optic nerve. There are six general classes of neurons, which are organized into discrete layers or lamina, in the vertebrate retina (Fig. 1).

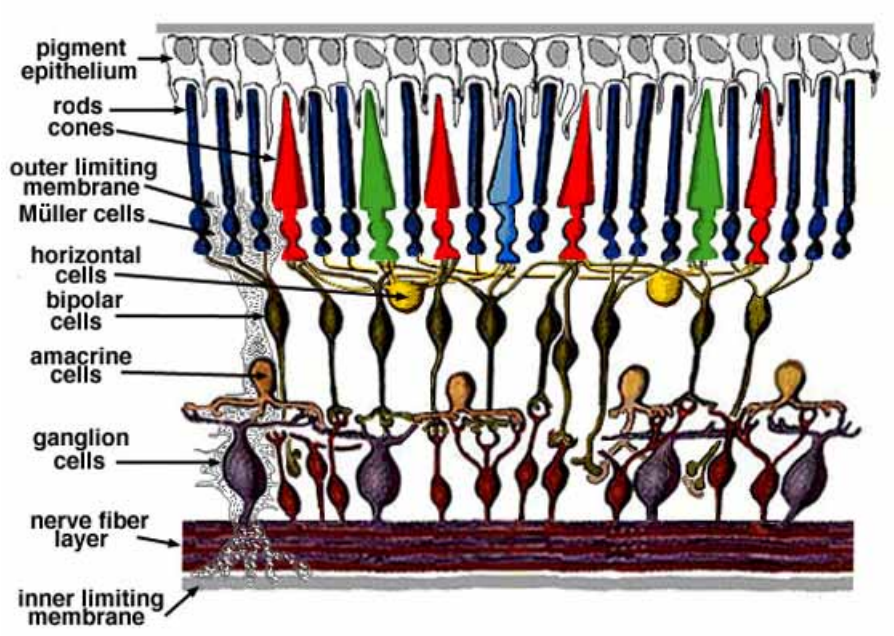

Fig. 1. Simple diagram of the organization of the retina. (http://webvision.med.utah.edu/sretina.html)

The five main classes are: photoreceptor cells, horizontal cells, bipolar cells, amacrine cells and ganglion cells (Cajal, 1972).

Photoreceptor cells are the light-sensitive cells. They absorb light and convert it to electrical signals that are eventually passed to the brain. There are two types of photoreceptors: rod and cone cells, which will be discussed later.

According to their functions, the horizontal cells can be divided into two classes: luminosity-type horizontal cells and chromaticity-type horizontal cells. In general, the former sense the amount of light striking the photoreceptors, and the latter have light-evoked responses with kinetics strongly dependent upon the color of the light stimuli.

The bipolar cells are in the second synaptic layer. They transfer image information from the photoreceptor cells to the ganglion cells. These cells can be divided into two functional classes: 'on' and 'off' bipolar cells. The classification is based on the character of the cell response to small spots of light positioned over the center of the cell's receptive field. When illumination increases, 'on' bipolar cells depolarize, and 'off' bipolar cell hyperpolarize.

The amacrine cells are named by their anatomy: they have an axonless cell body. Lateral and radial interconnections in the inner plexiform layer are composed of the amacrine cells. **A**macrine cells have a lot of different anatomical classes and functional counterparts.

The ganglion cells are the output neurons of the retina. They convey image information from the retina to the lateral geniculate nucleus in the thalamus. The ganglion cells are made up of diversiform anatomical subclasses whose precise functions have yet to be fully explored.

2.2 Photoreceptors: Rod and Cone

2.2.1 Structure

Rod photoreceptors are highly sensitive to light. They are functional in dim viewing conditions, and thus provide 'night vision'. There is only one class of rod photoreceptors.

Cone photoreceptors are functional in most viewing conditions, although they are not as sensitive to dim light as rods. In human, cones are able to detect color because three classes of cone photoreceptors express different photopigments.

The structures of the vertebrate rods and cones are similar (Figure 2). The photoreceptor has two functional compartments: the inner and outer segments. The mitochondria, nucleus and endoplasmic reticulum are in the inner segment, which connects to the synaptic terminal. The inner segment supplies energy and synthesizes protein. The mechanism of phototransduction, which is the process by which light is converted into electrical signals in a photoreceptor cell, occurs in the outer segment. (Snyder & Menzel, 1975; Enoch & Tobey, 1981).

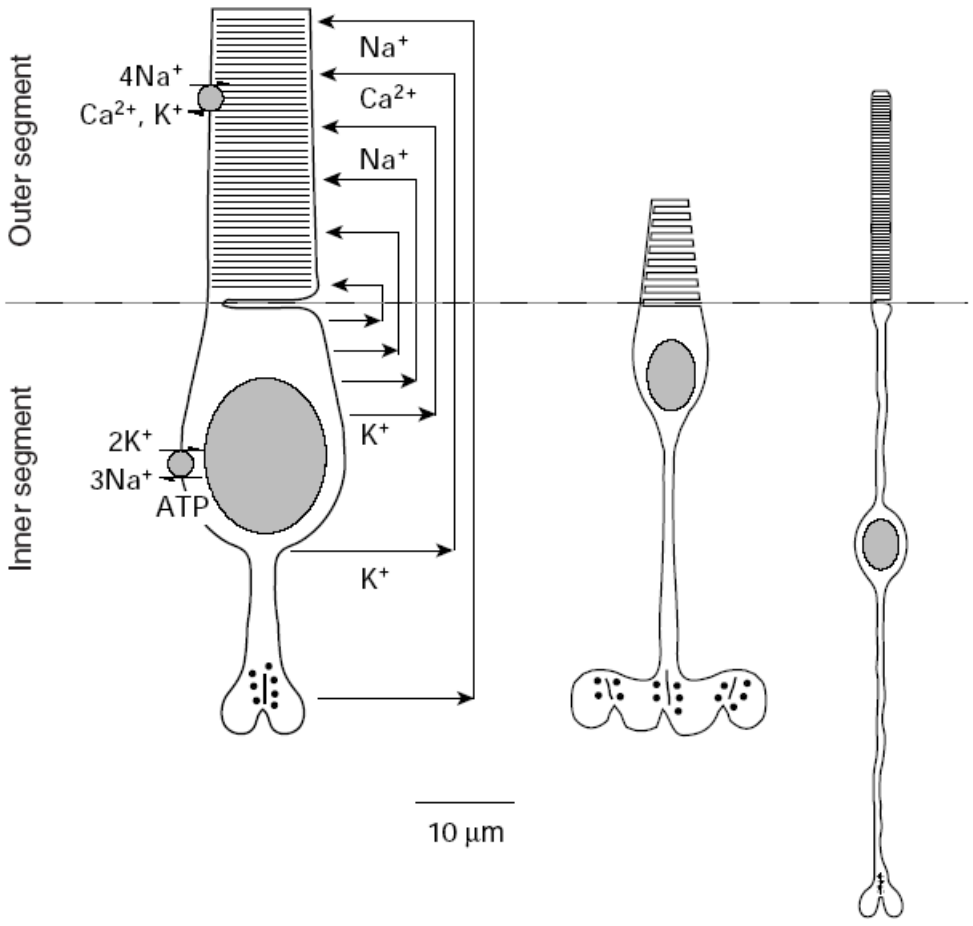

Fig. 2. Structure of rods and cones, and nature of the circulating current. From left to right: a salamander rod, a salamander red-sensitive cone and a mammalian rod (Pugh & Lamb, 2000).

2.2.2 The circulating electrical current

The protein compositions of the surface membrane in the inner and outer segments are greatly different. For ion permeation, there are only two active classes of protein in the outer segment membrane: the cGMP-gated channel (or cyclic nucleotide gated channel or CNGC) and the electrogenic Na^+/Ca^{2+}, K^+ exchange (NCKX). On the other hand, the membrane of the inner segment includes K^+ channels of two main

varieties as well as channels permeable to other cations, including Ca^{2+}. (Molday & Kaupp, 2000).

The cGMP-gated channel in the outer segment is controlled to open or close by the cytoplasmic messenger of phototransduction, cGMP. In resting dark conditions, the concentration of free cGMP is several μM, and a small proportion of the cGMP-gated channels are held open. The permeation of the ions (e.g. Na^{+}, Ca^{2+} and K^{+}) between the inner and outer segment through cGMP-gated channels will produce a current. Under this condition, the net current is inward (at the normal resting potential of vertebrate robs and cones, *ca* –35 to –40 mV) (Pugh & Lamb, 2000). When the concentration of free cGMP varies, the number of open cGMP-gated channels will change. Then the value and direction of the current will change correspondingly.

2.3 Phototransduction

When light comes in, the photoreceptor outer segments absorb the photons and generate an electrical response. This process is called phototransduction. 'G-protein cascade', which is a sequence of reactions initiated by a G-protein-coupled receptor (GPCR) protein, plays the most important role.

The phototransduction process in vertebrate photoreceptors includes three steps: activation, termination and modulation. Activation results in the response to the light. Each activated molecular species tends to shut down in the termination step. Modulation refers to the regulation of the entire signaling system. Termination and modulation are so closely related (especially in time) that they are often combined. Then the photo-

transduction process is considered to have two major stages: (a) activation and (b) termination and modulation (Pugh & Lamb, 2000).

2.3.1 Activation

Activation involves proteins and cGMP-gated channels. The principal proteins are rhodopsin, the G-protein and the phosphodiesterase. The process is illustrated in Fig. 3.

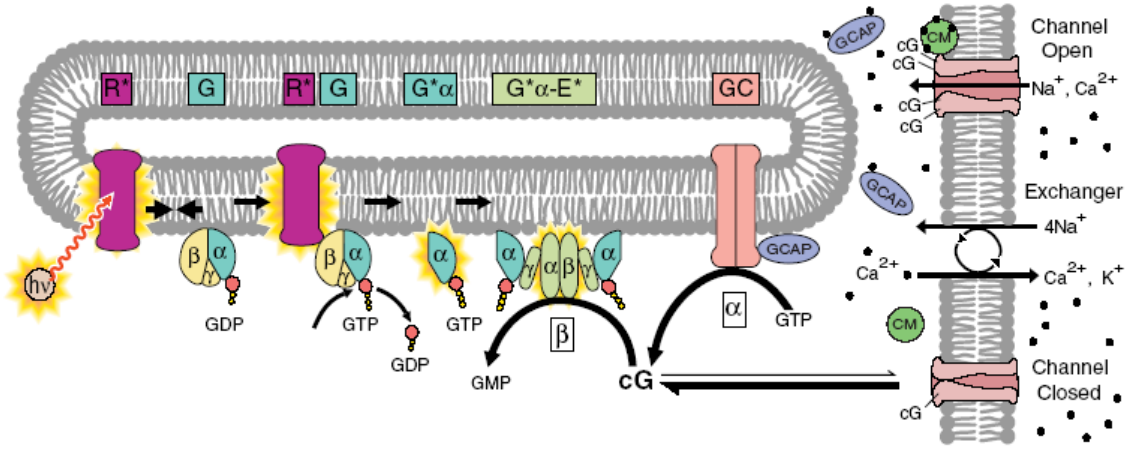

Fig. 3. Activation steps of the phototransduction cascade in vertebrate photoreceptors (Pugh & Lamb, 2000).

When a visual pigment molecule (rhodopsin) in a photoreceptor cell captures a photon, its bent 11-cis conformation will convert to the relatively straight all-*trans* form. Then the length of the chromophore molecule will extend slightly because of straightening. It stresses the opsin protein molecule from the interior and thereby triggers the conformational changes that result in enzymatic activities. In other words, rhodopsin changes to a state R* (activated rhodopsin) by photoisomerization.

Through diffusion, the activated rhodopsin contacts the G-protein on the disc membrane. The accessibility of the nucleotide binding site to the aqueous environment is increased. G-protein can release its GDP easily (Sprang, 1997; Hamm, 1998; Liri, Farfel

& Bourne, 1998). When the complex encounters a GTP in the cytoplasm, G-protein will bind GTP to produce an activated form G* ($=G\alpha - GTP$), which carries the signal forward, and separates from R* (Bornancin, Pfister & Chabre, 1989; Hofmann, 1986; Hofmann, 2000). At the end of this sequence the R* is released unaltered, and is therefore free to interact with other G molecules, and thereby catalyzing their activation. As a result, a single activated molecule of R* can trigger the activation of G* at a rate in the order of hundreds of molecules per second (Pugh & Lamb, 1993; Hofmann, 2000; Kahlert & Hofmann, 1991).

The cGMP phosphodiesterase, the 'effector protein' E, has two catalytic α and β subunits (Artemyev, et al., 1996; Beavo, 1995; Stroop & Beavo, 1992). Through the diffusion on the membrane surface, two G* subunits bind to γ subunits of the cGMP phosphodiesterase E. Then the two catalytic α and β subunits are activated. The activated form is E* ($=(G\alpha - GTP) - PDE\gamma$).

The cGMP-gated channel translates the message embodied in the cytoplasmic concentration of cGMP into an electrical signal. E* catalyzes the hydrolysis of cGMP (cG). The consequent reduction in cytoplasmic concentration of cGMP leads to the closure of cyclic nucleotide gated channels. Then the inward flux of Na^+ and Ca^{2+} will be blocked, leading to a reduction in the circulating electrical current.

2.3.2 Termination and Modulation

In the termination and modulation process, the activated proteins (e.g. R*, G* and E*) are shut off, and the concentration of cGMP is regulated.

According to the existing research, at least three proteins are involved in the termination or down-regulating activity of R*. They are rhodopsin kinase (RK), arrestin (Arr) and recoverin (Rec). In the dark-adapted state, most of the recoverin (Rec) is in Ca^{2+}-bound form at the membrane. Rec-2Ca forms a complex with rhodopsin kinase (RK), blocking its activity. Thus at the resting Ca^{2+} level, few molecules of RK are available to interact with R*.

During the light response, the reduction of the concentration of cGMP blocks the inward Na^{+} and Ca^{2+}, but a Na^{+}/Ca^{2+}, K^{+} exchanger continues to pump Ca^{2+} out, so that the cytoplasmic Ca^{2+} concentration declines. Then Rec releases its Ca^{2+}, and dissociates from RK. The elevated concentration of free RK increases the frequency of interaction between R* and RK, permitting more rapid phosphorylation of R*. Arrestin (Arr) then binds, substantially quenching the R* activity. This step is shown in Fig. 4.

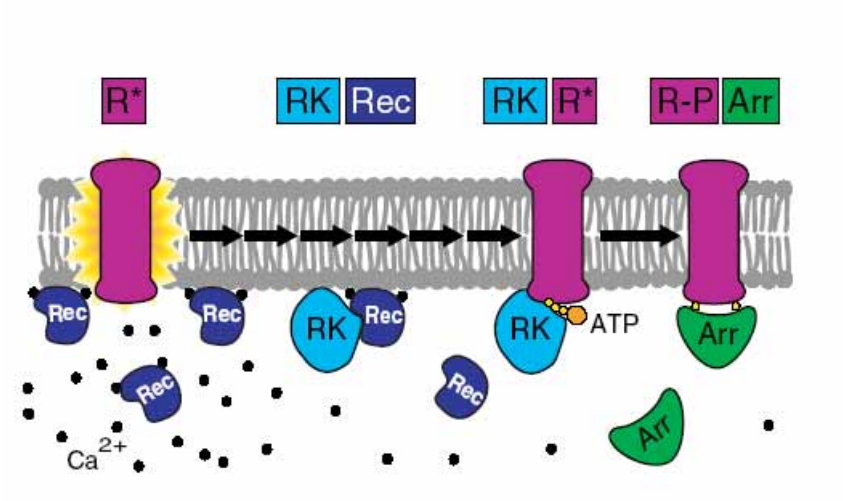

Fig. 4. Inactivation of R* of the phototransduction cascade in vertebrate photoreceptors (Pugh & Lamb, 2000).

RGS9 ('Regulator of G-protein Signaling, 9) (He, et al., 1998) and $G\beta 5$ ('type 5 G-protein β subunit ') (Makino et al., 1999) are the 'GTPase-accelerating protein'

(GAPs) factors. They bind to $(G\alpha - GTP) - PDE\gamma$ to form a quaternary complex: $RGS9 - G\beta - (G\alpha - GTP) - PDE\gamma$. Formation of this complex may allow access of water to GTP-binding sites, which are located in the interior of the $G\alpha$ subunit. It rapidly hydrolyzes the GTP to GDP, returning the $G\alpha$ subunit to its inactivated form. The inactivated $G\alpha - GDP$ dissociates from E, so that the E* and G* are inactivated simultaneously. This process is shown in Figure 5.

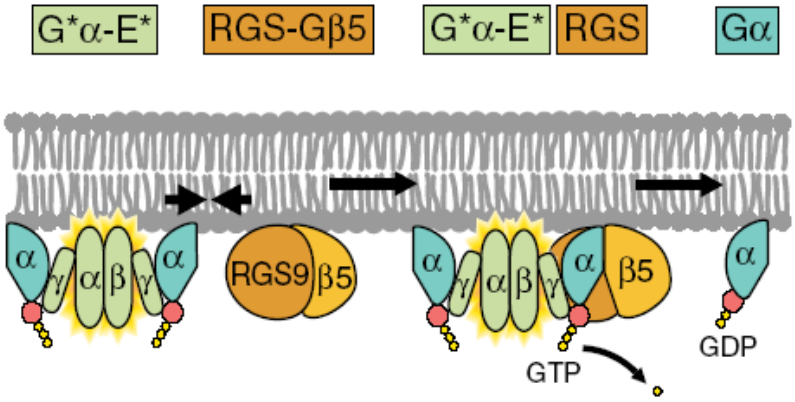

Fig. 5. Inactivation of G*-E* of the phototransduction cascade in vertebrate photoreceptors (Pugh & Lamb, 2000).

Regulation of cGMP synthesis need guanylyl cyclase (GC) and its activating proteins (GCAPs). GC is an enzyme. GCAPs (guanylyl cyclase activating proteins) belong to a large family of calcium-binding proteins, which includes calmodulin (CM) and recoverin (Rec).

In the darkness, a high proportion of guanylyl cyclase activating proteins molecules binds with Ca^{2+} ions because of the relatively high concentration of Ca^{2+}. This form of complex is soluble in the cytoplasm and does not interact with the guanylyl cyclase. But the Ca^{2+} concentration will drop during light response. Guanylyl cyclase activating proteins release Ca^{2+} ions and become the calcium-free form. Then they can

bind a cytoplasmic site on the GC, thereby switching on its enzymatic activity. So GC will synthesize cGMP from GTP (Gorczyca, et al., 1994; Gorczyca, et al., 1995; Palczewski, et al., 1994). The increasing cGMP concentration will cause the cGMP-gated channels to open.

2.4 History of the ERG

The historical review, given by Perlman (Perlma, 2005), indicated that in 1865, Frithiof Holmgren, an Uppsala physiology professor, found the response of the eye to the light stimulus when he put the recording electrodes on the front and the back of a frog eye. But he did not understand what his recording was until 1870 (Holmgren, 1870). So the real birth date of the ERG is 1870 (Granit, 1991). Shortly after, Dewar and Mckendrick also discovered the phenomenon (Dewar & Mckendrick, 1873; Granit, 1947).

Limitations of instrumentation prevented further advances until 1903, Gotch analyzed the ERG further with the capillary electrometer, and first proposed that the ERG included two waves: the early negative wave and the later positive wave of large amplitude (Gotch, 1903; Granit, 1947).

Einthoven and Jolly (1908) were first to report that the ERG wave consisted of three waves: a-wave, b-wave and c-wave. They postulated that light stimuluss caused a series of responses associated with the formation of products A, B and C, and every electrical wave indicated a change in a ‘relevant’ product.

Piper, whose opinion was different from Einthoven and Jolly’s, published his analysis in 1911 (Piper, 1911). He considered that all the ERG components lasted for the duration of the light stimulus (Armington, 1974).

In 1933, Granit published his study of the ERG components. He used a chemical agent to anesthetize the cat at the different levels, and recorded the corresponding ERG waves. According to the experiment, Granit indicated that the ERG was made up of three components: P-I, P-II and P-III (Figure 6). In other words, the P-I component is a slow cornea-positive wave. P-II is also a corneal-positive wave that rises relatively fast to peak amplitude and then recovers to an intermediate potential while the light stimulus is still on. The last component, P-III, which was the most resistant to the level of anesthesia, is a cornea-negative wave that develops faster than the other two and remains as a negative potential for as long as the light stimulus is on.

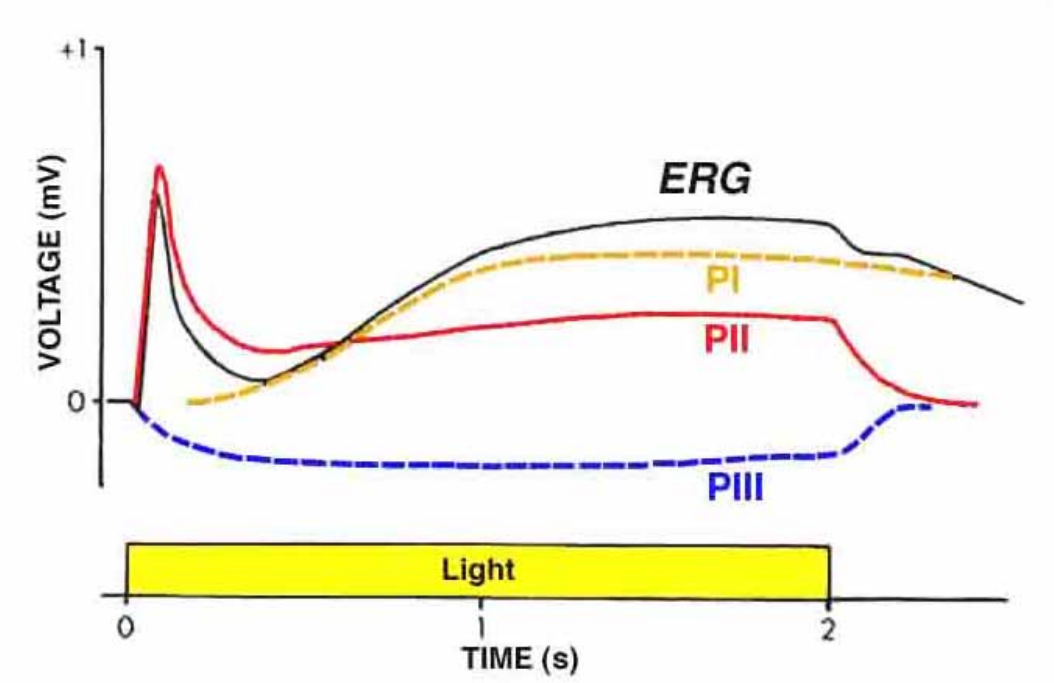

Fig. 6. The ERG of a cat in response to a 2 sec light stimulus. The components, P-I, P-II and P-III, are separated by deepening the state of anesthesia (Granit, 1933).

The component analyses have been modified with the development of the ERG analysis. However, the early works have been the foundation for analysis used to the present day. In particular, Granit's study is still the basis for the analysis of ERG.

2.5 The ERG Recording

In the late nineteenth century and the early twentieth century, it was hard to measure the rapid changes accurately because of the measurement instrument, the slow galvanometers. The researchers had to use many eyes in series to observe the response.

Gotch was first to describe the full phasic display of the ERG. He measured the light response of the frog eye exactly by a capillary electrometer in 1903 (Gotch, 1903). In the same year, Einthoven developed his string galvanometer, which was fast and sensitive enough to record the ERG. When the amplifiers for the ERG and fast recording instrument were developed, the ERG waves could be obtained accurately.

Dewar recorded the first successful ERG of a human by placing the reference electrode on the abrade skin in 1877. However, he did not publish the results. The first human ERG curve was published by Kahn and Löwenstein in 1924 (Kahn & Lőwenstein, 1924; de Rouck, 1991). In their method, one electrode was placed in a distal temporal point of an anesthetized eyeball. It could not be applied in the clinical setting, although their purpose was clinical application.

Around the same time, the other materials and methods were developed. With the better understanding of the major components of the ERG, progress in the recording devices and the introduction of the haptic (scleral) contact lens electrode by Riggs (Gouras, 1970), the clinical electroretinography was developed. This kind of contact lens contained a silver disk connected to a hole in the contact lens. A fine flexible wire supported by beeswax was used as a lead from the electrode. When the lens was inserted

into the eyes, the silver made contact with the isotonic sodium chloride solution between it and the cornea (de Rouck, 1991).

The ERG was introduced as a routine method in the ophthalmology clinic by Karpe (Karpe, 1945) in 1945. In the recently years, other types of corneal or scleral electrodes have been introduced that are generally more comfortable for the patient.

2.6 Components of the ERG

Figure 7 shows an example of a dark-adapted mouse ERG.

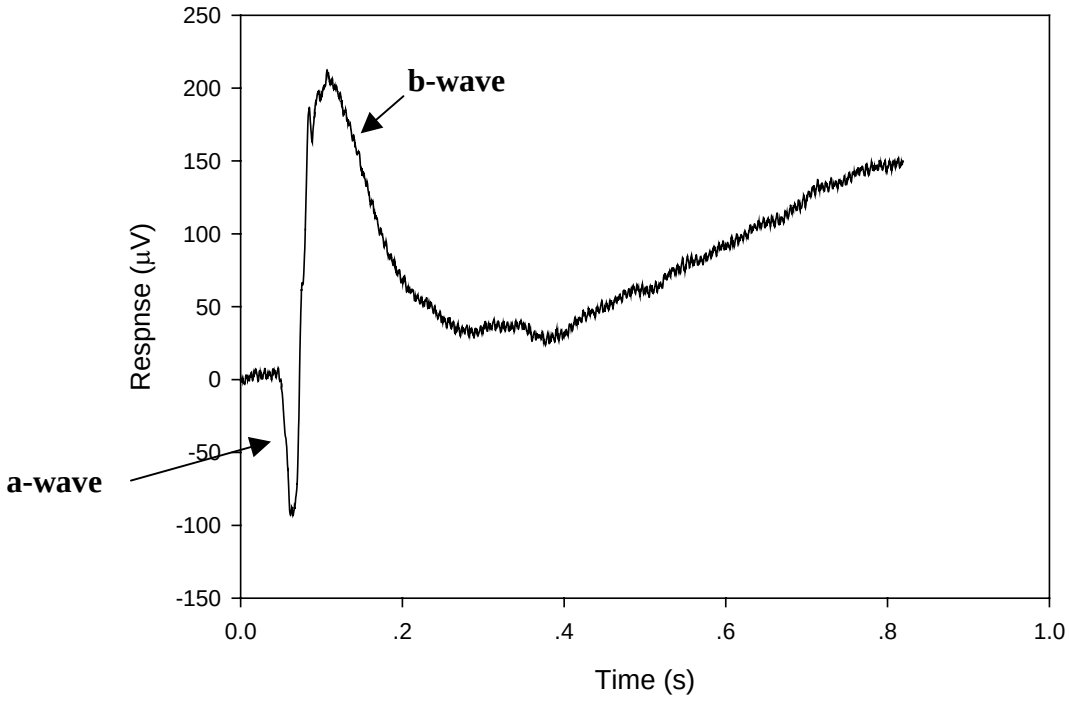

Fig. 7. The ERG of a dark-adapted mouse.
A brief (10μs) flash green light was given at 40 ms.
The light intensity (Log) was 14.906 photons cm^{-2} s^{-1}.

According to the origins, the major components of ERG are: a-wave, b-wave and c-wave.

The a-wave is generated by the photoreceptors (Tomita, 1950; Brown & Wiesel, 1961a, 1961b; Brown & Murakami, 1964; Brown, 1968). Because L-glutamate is the neurotransmitter of the photoreceptors, the synaptic transmission from the photoreceptors can be blocked effectively when agonists or antagonists of L-glutamate are injected to the vitreous cavity. Figure 8 shows the ERG responses from a dark-adapted mouse that was recorded 1 hour after injecting L-glutamate.

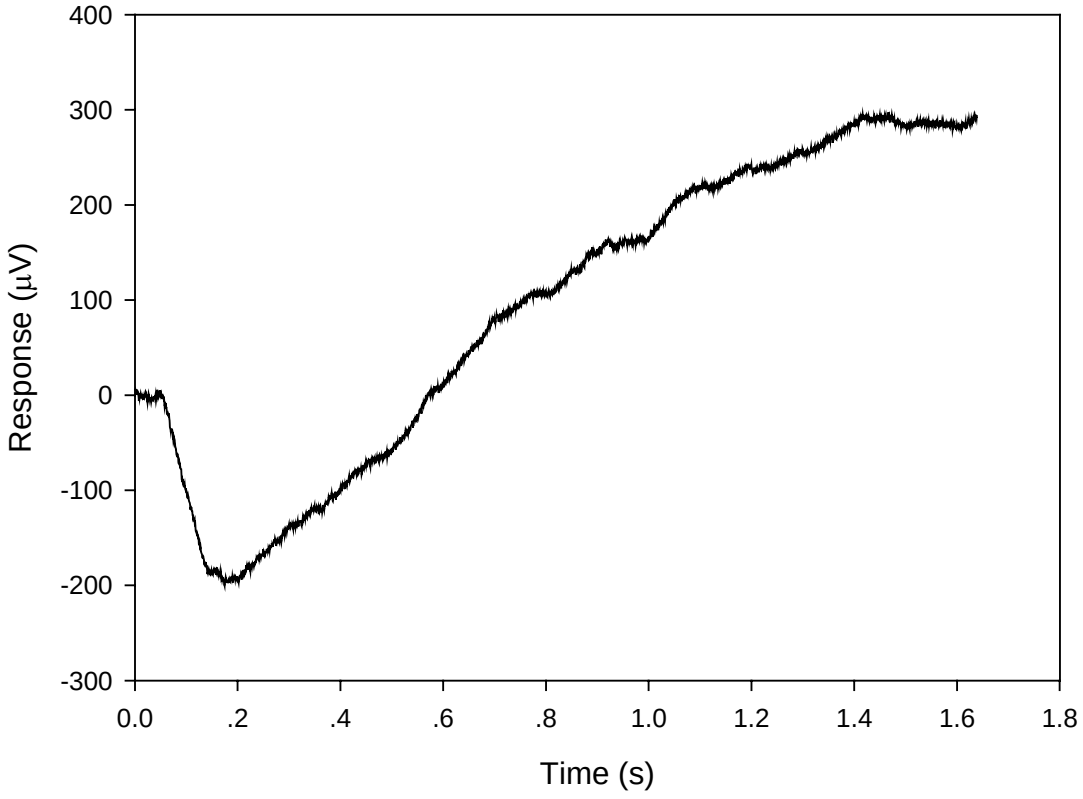

Fig. 8. Elimination of the ERG b-wave in mouse by injecting L-glutamate. A brief (10 ms) flash green light was given at 40 ms. The light intensity (Log) was 12.997 photons cm^{-2} s^{-1}.

The b-wave is originated from bipolar cells that are post-synaptic to the photoreceptors. It is widely used in clinical and experimental analysis of retinal function. The c-wave is originated in the pigment epithelium.

Besides the three major waves, other components can be identified in the ERG depending on the experimental recording conditions: the early receptor potential (ERP), the oscillatory potentials (OPs), the d-wave, the Scotopic threshold response (STR) and the m-wave.

Among the minor components of the ERG, only the oscillatory potentials and the d-wave are used for the clinical assessment of retinal function. The others are more difficult to isolate in the routine clinical setup and are measured only for research purposes.

The focus of this research was on the photoreceptor response. Only the isolated a-wave was analyzed and modeled.

CHAPTER 3

MODEL DEVELOPMENT

3.1 Existing Models

The analysis of the ERG has been advanced greatly in the past 50 years. The objective assessment of retinal function has always been of great interest to clinicians and researchers. The functional integrity of different retinal structures can be separated by analyzing ERGs of normal and abnormal photoreceptors. The ERG allows the testing of quantitative hypotheses about normal functions and diseases. It helps to understand the information processing mechanisms and/or the sites of retinal disorders.

Many analytical approaches have been proposed. For the leading edge of a-wave, there have been two main models. The first one was proposed in 1990 by Hood and Birch (Hood & Birch, 1990; Hood & Birch, 1992; Hood & Birch, 1993). The second one was developed by Lamb and Pugh in 1992 (Lamb & Pugh, 1992) and modified later (Nikonov, et al., 1998).

3.1.1 Hood and Birch's model

In 1990, Hood and Birch proposed their model that comprised two components. The first component is a linear process described by the impulse response function of a low-pass filter g(t) normalized to a peak response of 1.0 as:

$$g(t) = [\frac{t}{t_p} e^{(1-\frac{t}{t_p})}]^{(n-1)} \tag{3.1}$$

where t_p is the time to peak response, and *n* is the number of stages.

The second component is a nonlinear function. The photoreceptor response is given by

$$p3(t) = [1 - e^{-\frac{\ln 2}{\sigma_{p3}} i \cdot g(t)}] \cdot rm_{p3} \quad (3.2)$$

where rm_{p3} is the peak response, σ_{p3} is the flash energy that evokes a peak response of $0.5\, rm_{p3}$, and *i* is the intensity of a brief flash energy.

This model fits the a-wave responses. It provides support for the notion that a-wave reflects the rod photocurrent. However, it is of limited value in understanding the biochemical mechanisms. There are no explicit physical or biological basis for the parameters t_p, *n*, σ_{p3} and rm_{p3} (Hood & Birch, 1990).

3.1.2 Lamb and Pugh's model

In 1992, Lamb and Pugh proposed a model that described the steps of molecular reaction involved in activation of phototransduction as follows.

Step 1: Activation of rhodopsin:

$$R^*(t) = \Phi[1 - e^{-\frac{t}{t_R}}] \quad (3.3)$$

where *R*(t)* is number of photoactivated rhodopsin molecules per outer segmet,

Φ is number of photoisomerizations produced by a brief flash, and

t_R is delay time in the formation of activated rhodopsin.

Step 2: Activation of the G-protein by rhodopsin

$$G^*(t) = \Phi\, \nu_{RG}(t - t_{RG}) \text{ for } t > t_{RG} \quad (3.4)$$

where *G*(t)* is number of activated G-protein molecules per outer segment,

ν_{RG} is rate of production of G* by a single R*, and

t_{RG} is sum of delay time in the formation of R* and G*.

Step 3: Activation of E by $G_{\alpha} * \cdot GTP$

$$E^*(t) = \Phi \nu_{RP}(t - t_{RGP}) \qquad \text{for } t > t_{RGP} \qquad (3.5)$$

where *E*(t)* is number of activated phosphodiesterase catalytic subunits per outer segment,

ν_{RP} is rate of production of E* due to a single R*, and

t_{RGP} is sum of delay time in the formation of R*, G* and E*.

Step 4: Cyclic GMP concentration

$$\frac{cG(t)}{cG_{dark}} = \exp[-\frac{1}{2}\Phi \nu_{RP}\beta_{sub}(t - t_{RGP})^2] \qquad \text{for } t > t_{RGE} \qquad (3.6)$$

where *cG(t)* is concentration of free cGMP in the outer segment,

cG_{dark} is concentration of free cGMP in the outer segment in darkness,

and β_{sub} is rate constant of a single catalytic subunit of *E* in a well-stirred volume.

The cGMP-activated current *F(t)* as a fraction of resting (dark) level of cG is:

$$F(t) = [\frac{cG(t)}{cG_{dark}}]^n \qquad (3.7)$$

$$= \exp[-\frac{1}{2}\Phi \nu_{RP}\beta_{sub} n(t - t_{eff})^2], \qquad t_{eff} = t_R + t_G + t_E + t_r + t_B + t_c \qquad (3.8)$$

$$= \exp[-\frac{1}{2}\Phi A(t - t_{eff})^2], \qquad t > t_{eff} \tag{3.9}$$

where n is Hill coefficient of opening of the cGMP-activated channel, and

t_{eff} is effective delay time.

Figures 9 and 10 show recording of the a-wave from mouse and human subjects. Comparison of the model predictions with experimental data shows that the leading edge of the response is well fitted by the model.

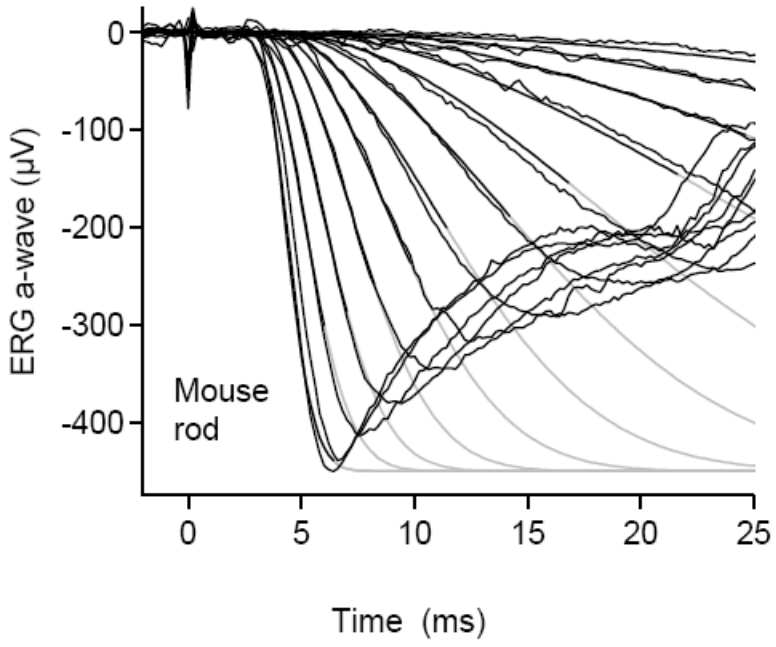

Fig. 9. Comparison of prediction by Eq. (3.9) with experimental ERG a-waves. Mouse rod a-waves (Lyubarsky & Pugh, 1996).

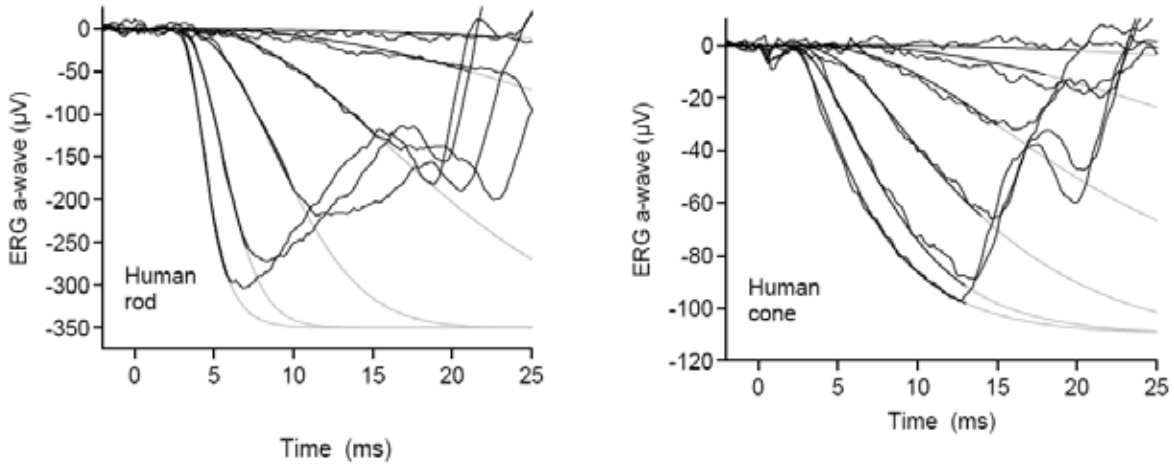

Fig. 10. Comparison of predictions by Eq. (3.9) with the experimental ERG a-waves. Left: Human rod a-waves; Right: Human cone a-waves (Smith & Lamb, 1997).

This model was derived by mathematically representing the well known phototransduction cascade. It depicts the rising phase kinetics of a family of a-wave responses.

However, the model has several limitations. First, it ignores the inactivation processes for simplifying the analytical solution. At least five recovery processes have been ignored: (i) termination of R* activity; (ii) the Ca^{2+}-dependent modulation of R* shut-off via recoverin; (iii) resting hydrolysis of cGMP; (iv) the Ca^{2+}-dependent activation of GC via GCAPs; and (v) termination of G*-E* activity. Second, the longitudinal diffusion in the outer segment is neglected. Third, it neglects modulation and thus cannon be applied at extremely high flash intensities.

With new knowledge of the recovery phases of photoresponses, Nikonov et al. modified this model in 1998.

After considering the mass inactivation reactions for R* and G*-E*, the equation for E*(t) was modified as:

$$E^*(t) = \Phi \nu_{RE} C_{RE} [e^{-t/\tau_E} - e^{-t/\tau_R}] \tag{3.10}$$

where ν_{RE} is the rate of generation of E* per fully activated R*, and $C_{RE} = [\tau_E \tau_R / (\tau_E - \tau_R)]$ is a constant.

The equation for synthesis and hydrolysis of cGMP (Lamb & Pugh, 1992) is

$$\beta_{sub} = \frac{\frac{1}{2} K_{cat} / K_m}{N_{AV} V_{cyto} B_{cG}} \tag{3.11}$$

$$\Delta\beta(t) = E^*(t) \cdot \beta_{sub} \tag{3.12}$$

$$\frac{dcG}{dt} = \alpha(t) - \beta(t) \cdot cG \tag{3.13}$$

$$= \Delta\alpha(t) - \Delta\beta(t) \cdot cG + \beta_0 (cG_0 - cG) \tag{3.14}$$

where $\alpha(t)$ is the rate of synthesis by guanylyl cyclase, $\beta(t)$ is the rate constant of hydrolysis, and the subscript '0' denotes the initial steady-state condition. Since dynamic change occurs in the concentration of Ca^{2+} during the light response, the incremental cyclase activity $\Delta\alpha(t)$ cannot be ignored as done previously.

Based on the assumption that only calcium flows into or out the cytoplasm through the cGMP-gated channels and the NCKX exchanger, the change rate of the free calcium concentration can be written as:

$$\frac{dCa}{dt} = -\frac{\frac{1}{2} f_{Ca} J_{cG}(t) - J_{ex}(t)}{\Im V_{cyto} B_{Ca}} \tag{3.15}$$

where Ca represents $[Ca^{2+}]_i$, J_{ex} denotes the electrogenic exchange current, f_{Ca} denotes the fraction of the current, J_{cG}, through the cGMP-gated channels that is carried by Ca^{2+}, B_{Ca} denotes the buffering power of the cytoplasm for calcium, and $\Im$ denotes Faraday's constant (the charge carried by a mole of monovalent cations) (Miller & Korenbrot, 1994; Lagnado et al., 1992; Koutalos et al., 1995). Further,

$$\frac{J_{ex}(t)}{J_{ex,sat}} = \frac{Ca(t)}{Ca(t) + K_{ex}} \tag{3.16}$$

where $J_{ex,sat}$ symbolies the maximal exchange current, and K_{ex} symbolizes the half-saturating Ca^{2+} concentration of the exchanger.

The free calcium concentration and the activity of GC have the following relationship:

$$\alpha(t) = \alpha_{\min} + \frac{\alpha_{\max} - \alpha_{\min}}{1 + (Ca(t) / K_{cyc})^{n_{cyc}}} \tag{3.17}$$

where $\alpha_{\min}$ is the residual component of cyclase activity at very high calcium concentration, $(\alpha_{\max} - \alpha_{\min})$ is the calcium-sensitive component of cyclase activity, K_{cyc} is the calcium concentration for half-maximal activation, and n_{cyc} is the cooperativity coefficient.

The solution of Eq. (3.7), (3.10), (3.11), (3.12), (3.13), (3.14), (3.15), (3.16) and (3.17) is the flash response in the presence of inactivation reactions. Figure 11 shows the electrical responses of a salamander rod compared with theoretical predictions.

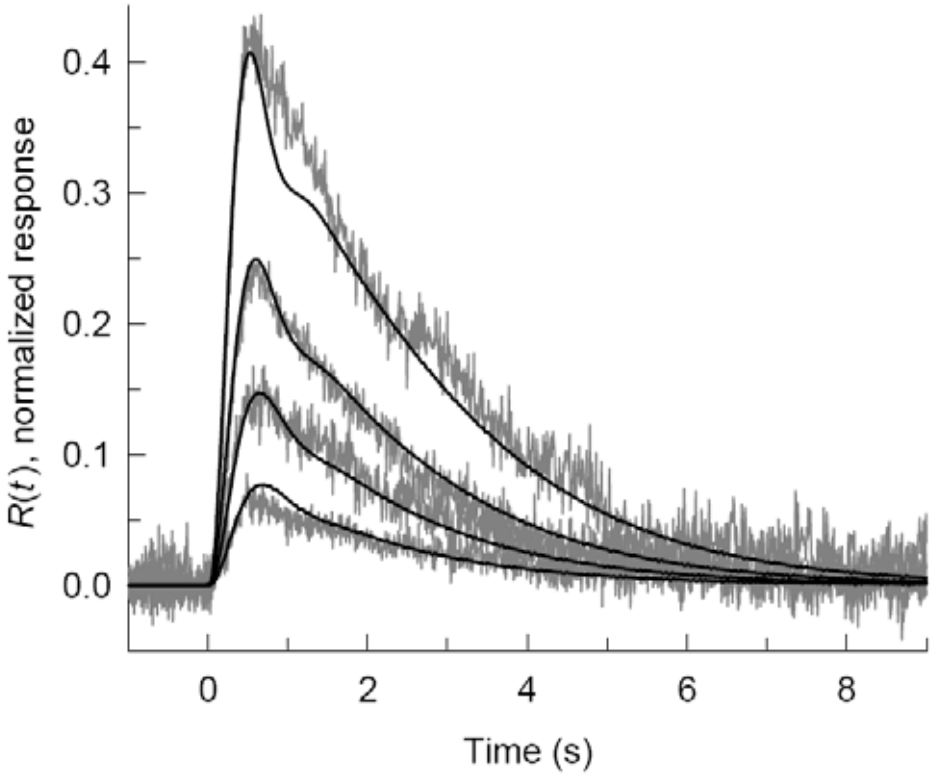

Fig. 11. Flash responses of a salamander rod at four dim intensities, compared with theoretical predictions. Φ **=11, 23, 45 and 94 respectively.** $\nu_{\mathbf{RE}} = \mathbf{150 s^{-1}}$**;** $\mathbf{A = 0.16 s^{-2}}$**;** $\tau_{\mathbf{R}} = \mathbf{0.35 s}$**;** $\tau_{\mathbf{E}} = \mathbf{1.7 s}$**;** $\mathbf{1/\beta_{dark} = 0.9 s}$**.** **(Nikonov, et al., 1998).**

This model describes the activation and inactivation steps in the flash responses based on molecular-level reactions. It was originally applied to salamander rod response, but it fits a-wave in human ERG as well (Smith & Lamb, 1997).

The model is improved but still has limitations. First, this model ignores the dynamic modulation of the R* shut-off reaction. It also ignores any stochastic features of R* inactivation (Pugh & Lamb, 2000). Secondly, because of the finite quantity of RGS9, Gβ5 and E, the inactivation time of the 'excess' G* may be delayed relative to the time, τ_E, that applies at lower flash intensities. Thirdly, τ_e and τ_R in Eq. (3.8) are inter-

changeable. It's difficult to determine τ_e and τ_R individually. Fourthly, Eq. (3.14) oversimplifies the behaviour of the exchange current, which exhibits at least two components of delay following a saturating flash (Nikonow, Engheta & Pugh, 1998).

3.2 Proposed Model for ERG a-wave

To improve the usefulness of the electroretinogram (ERG) in identifying the sites and mechanisms of adaptation, development and disease processes, a new quantitative model was developed based on the biochemical reaction kinetics in the phototransduction cascade and experimental data. It considered the activation and inactivation of phototransduction. During the process of phototransduction, the reactions of proteins and enzymes are depicted in Figure 12.

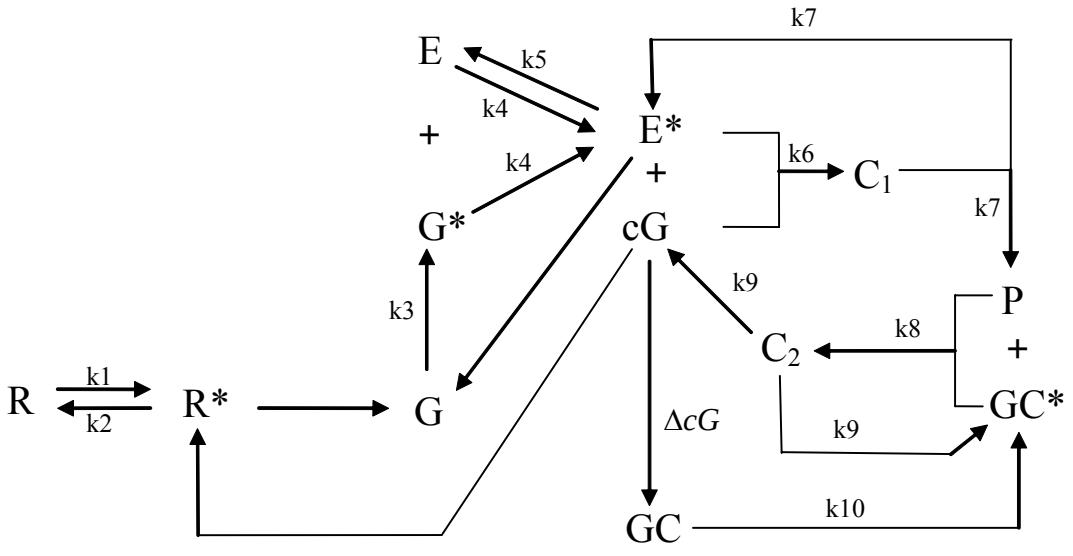

Fig. 12. Transition in the phototransduction.

A photon induces the rhodopsin (R) to undergo a conformational change to a state, R*, in which it is enzymatically activated. The production of R* is proportional to the light intensity and the number of rhodopsin.

$$\frac{dR^*}{dt} = k_1 u(R - R^*) \tag{3.18}$$

where R is the total number of Rodopsin,

R^* is the number of activated Rodopsin,

k_1 is the activated rate of Rodopsin, and

u is the intensity of the stimulus light.

R* contacts the G-protein on the membrane surface. The two molecules bind, thereby increasing the accessibility of the nucleotide binding site to the aqueous environment so that the GDP can be dissociated easily. After losing the GDP, G will bind to R* tighter, until the complex encounters a GTP in the cytoplasm. Binding of a GTP in place of the GDP triggers a conformational change that leads to separation of the G-GTP from R*, and also to separation of the α - and $\beta\gamma$ -subunits ($G\alpha - GTP$ and $G\beta\gamma$). $G\alpha - GTP$ represents the activated form of the G-protein that carries the signal forward, and for brevity we denote it as G*. The production of G* is proportional to the numbers of R* and G.

$$\frac{dG^*}{dt} = k_3 R^* (G - G^*) \tag{3.19}$$

where G is the total number of G-protein,

G^* is the number of activated G-protein, and

k_3 is the activation rate of G-protein.

During this process, R* is unaltered. R* can interact with other G-proteins. One R* can activate hundreds of G-proteins.

Two G* subunits bind to the two inhibitory γ subunits of the phosphodiesterase (E), thereby activating the corresponding α and β catalytic subunits, forming G*-E* ($(G\alpha - GTP) - PDE\gamma$). We call the activated form E*. The generation rate of E* is proportional to the number of E and the square of the number of G*; i.e.,

$$\frac{dE^*}{dt} = k_4 G^{*2} (E - E^*) \tag{3.20}$$

where E is the total number of E,

E^* is the number of activated E, and

k_4 is the activation rate of E. At the same time, G* will be consumed at the same rate, or

$$\frac{dG^*}{dt} = -k_4 G^{*2} (E - E^*) \tag{3.21}$$

E* will catalyze the hydrolysis of cGMP (cG). In this reaction, reversible formation of a complex between E* and substrate cG is followed by irreversible formation of the product C1. This is accompanied with regeneration of the enzyme, thus

$$E^* + cG \xrightarrow{k6} C1 \xrightarrow{k7} E^* + P$$

The concentration of cGMP in cytoplamic will reduce. The rates of the concentration of cGMP, the complex C_1 and E* are:

$$\frac{dcG}{dt} = -k_6 E^* cG \tag{3.22}$$

$$\frac{dC_1}{dt} = k_6 E^* cG - k_7 C_1 \tag{3.23}$$

$$\frac{dE^*}{dt} = -k_6 E^* cG + k_7 C_1 \tag{3.24}$$

where cG is the concentration of free cGMP,

C_1 is the number of complex C1,

k_6 is the reaction velocity of cG and E*, and

k_7 is the rate of the hydrolysis of complex C1.

Bound by $RGS9$ and $G\beta 5$, form E*-G* will be easily inactivated as described below

$$\frac{dE^*}{dt} = -k_5 E^* \tag{3.25}$$

with k_5 being the inactivation rate of E*.

During light response, the concentration of cG will drop, and it will cause the concentration of cytoplasmic Ca^{2+} to reduce. Rec and GCAPs will release Ca^{2+} that are bound to them. Rec contacts with R*, and causes the phosphorylation of R*. With the biding of Arr, R* will be inactivated. The calcium-free form of GCAP will bind to the cytoplasmic domain of GC, and switch the enzymatic activity of GC. The two processes can be written as

$$\frac{dR^*}{dt} = -k_2 \cdot R^* (cG_{dark} - cG) \tag{3.26}$$

$$\frac{dGC^*}{dt} = k_{10}^* (cG_{dark} - cG) \cdot (GC - GC^*) \tag{3.27}$$

where GC is the number of Guanylyl cyclase,

cG_{dark} is the concentration of cG in the darkness,

k_2 is the inactivated rate of R*, and

k_{10} is the rate in which GC converts to GC*.

Then GC* will synthesize cGMP from GTP.

$$GC^* + P \xrightarrow{k8} C2 \xrightarrow{k9} cG + GC^*$$

where P is decomposer of cGMP. So it can be represented by $(cG_{dark} - cG)$. Then this process can be written as

$$\frac{dC_2}{dt} = k_8 \cdot GC^* (cG_{dark} - cG) - k_9 C_2 \tag{3.28}$$

$$\frac{dGC^*}{dt} = -k_8 \cdot GC^* \cdot (cG_{dark} - cG) + k_9 \cdot C_2 \tag{3.29}$$

$$\frac{dcG}{dt} = k_9 \cdot C_2 \tag{3.30}$$

where k_8 is the reaction velocity of GC, GCAPs and the complex C1, and

k_9 is the synthesis rate of cG.

Based on the action of cGMP (Owen, 1987; Yau & Baylor, 1989; Pugh & Lamb, 1990), we know that the change in intracellular concentration of cGMP will control the opening or closure of the ion channel, which will cause the change of circulating electrical current between the inner and outer segments. The normalized circulating current, denoted by F(t), is a function of $\frac{cG(t)}{cG_{dark}}$ (Lamb & Pugh, 1992).

Here we use *f(t)* to denote the unnormalized ERG response to the stimulus signal. In darkness, the value of *f(t)* is equal to zero. The value of *f(t)* will change with the light stimulus. There is an polynomial relationship between *f(t)* and cG. From previous studies (Fesenko, et al., 1985; Yau & Baylor, 1989), power factor of 3 is a good choice; i.e.,

$$f(t) = k_{11} cG^3 - k_{11} cG^3{}_{dark} \tag{3.31}$$

where k_{11} is gain.

Rewriting the equations derived, we have the photoreceptor response model as:

$$\frac{dR^*}{dt} = k_1 u(R - R^*) - k_2 R^*(cG_{dark} - cG) \tag{3.32}$$

$$\frac{dG^*}{dt} = k_3 R^*(G - G^*) - k_4 G^{*2}(E - E^*) \tag{3.33}$$

$$\frac{dE^*}{dt} = k_4 G^{*2}(E - E^*) - k_5 E^* - k_6 E^* cG + K_7 C_1 \tag{3.34}$$

$$\frac{dC_1}{dt} = k_6 E^* cG - k_7 C_1 \tag{3.35}$$

$$\frac{dGC^*}{dt} = -k_8(cG_{dark} - cG)GC^* + k_9 C_2 + k_{10}(cG_{dark} - cG)(GC - GC^*) \tag{3.36}$$

$$\frac{dC_2}{dt} = k_8 \cdot GC^*(cG_{dark} - cG) - k_9 C_2 \tag{3.37}$$

$$\frac{dcG}{dt} = -k_6 cG \cdot E^* + k_9 C_2 \tag{3.38}$$

$$f(t) = k_{11} cG^3 - k_{11} cG_{dark}{}^3 \tag{3.39}$$

Based on the biochemical reaction kinetics in the phototransduction cascade, eight differential equations above are derived to predict the electrical response of photoreceptors to light. In the flowing chapter, system identification will be employed to determine the model parameters ($k_1 \sim k_{11}$) values from experimental data.

CHAPTER 4

MODEL VALIDATION

The photoreceptor response model derived in the previous chapter was validated with experimental data. Both healthy and photoreceptor-damaged subjects were used. The model parameters were estimated from the ERG recordings. The ability of the model in describing photoreceptor responses was verified, and its usefulness in differentiating normal and diseased subjects was analyzed.

4.1 Methods

4.1.1 Experimental Subjects

A series of a-waves were recorded from three wild-type (normal) mice, three NOB1 mice, one mouse with light-induced retina damage (light-damaged) and six mice with N-methyl-N-nitrosourea-induced photoreceptor-degeneration (drug-damaged).

The wild-type mice were 61-day-old males. Their right eyes were injected APB (DL-2-AMINO-4-PHOSPHONO-BUTYRIC ACID) to isolate the a-wave. The ERG recordings were carried out one hour after APB injection.

The NOB1 mice were 61-day-old. Their bipolar cells were disabled so that the b-wave in ERG is suppressed.

The light-induced retina-damaged mouse was a wild-type subject whose eyes were dilated by 1% tropicamide. After then it was exposed under white light which intensity was 11000 lux meter for 24 hours, and its photoreceptors were partially

damaged. The subject was a 89-day-old female mouse. The ERG recordings were recorded one hour after injecting APB.

The N-methyl-N-nitrosourea-induced photoreceptor-degenerated mice (drug-damaged subjects) were 67-day-old NOB1 mice. Three of them had been injected 30 mg/kg body weight of N-methyl-N-nitrosourea 5 days before ERG recordings. The others had been injected 60 mg/kg body weight of N-methyl-N-nitrosourea 2 days before ERG recordings.

4.1.2 The ERG Recording

ERGs were recorded in a darkroom except for a dim red light illuminating the computer keyboard. Each subject was dark-adapted overnight. Both eyes were measured, but only one eye was excited with a light stimulus and analyzed.

The mice were anesthetized with a mixture of 75 mg/kg ketamine and 13.6 mg/kg xylazine. Pupils were dilated with 1% tropicamide. The gold wire loop electrode was placed on the surface of the cornea, the differential electrode was placed under the skin on the forehead, and the neutral electrode was inserted subcutaneously near the tail.

The electrical signals were amplified and digitized at 2.5 kHz with a data-acquisition board (National Instrument, Austin, TX). The ERG signals were averaged three to ten times to reduce noise. The subjects were placed on a heating pad to keep the body temperature at 38°C.

A green LED visual stimulator was used. Two stimulus durations were used. One was 10 ms, and the other was 800 ms. The short one is referred to as the pulse stimulus, and the long one as the step stimulus although it was only a wide pulse. The light

luminance was calibrated with a photo diode (818-ST-UV/CM, Newport Corp., Irvine, CA, USA) coupled with a power meter (2835-C, Newport Corp.). For the dark-adapted ERG recording, the interstimulus interval (ISI) was at least 6 seconds for low pulse intensities and 5 minutes for high step intensities. The distance between the light source and the mouse eyes was 4.5 cm. Three levels of stimulus were used as listed in Table 1.

Table. 1 Stimulus light intensities

Intensity (nd)	Supply Volt (V)	Light Intensity (Log) (photons cm^{-2} s^{-1})
3	3	12.407
2	4	12.997
1	4	13.891

4.1.3 Parameters Estimation

A system of differential equations may be expressed in the form:

$$\frac{d\mathbf{Y}}{dt} = \mathbf{g}(t, \mathbf{Y}, \mathbf{k}) \tag{4.1}$$

where d**Y**/dt is a vector of derivatives of **Y,**

g is a vector of functions,

t is the independent variable,

Y is a vector of dependent variables, and

k is a vector of parameters.

If the initial or boundary conditions are given and if the vector **k** can be estimated, then the differential equations can be integrated numerically to give the solutions, which are

$$\mathbf{Y} = \mathbf{f}(t, \mathbf{k}) \tag{4.2}$$

If the model only includes one dependent variable, the sum of squared residuals can be given by

$$\Phi = \varepsilon' \varepsilon = \mathbf{(Y^*\text{-}Y)'(Y^*\text{-}Y)} \tag{4.3}$$

where **Y*** is a vector of experimental observations of the dependent variables, and

Y is a vector of calculated values of the dependent variables obtained from Eq. (4.2).

There are several techniques for minimization of the sum of squared residuals described by Eq. (4.3). They include the method of steepest descent, the Gauss-Newton method, Newton's method, and the Marquardt method.

Since the gradient of a scalar function gives the direction of the greatest increase of the function at any point, the steepest descent method tries to reach a lower function value by moving in the opposite direction. Therefore, the initial vector of parameter estimates is corrected in the direction of the negative gradient of Φ:

$$\Delta\mathbf{k} = -b\frac{\partial\Phi}{\partial\mathbf{k}} \tag{4.4}$$

where b is a suitable constant factor and $\Delta\mathbf{k}$ is the correction vector to be applied to the estimated value of **k** to obtain a new estimate of the parameter vector:

$$\mathbf{k}^{(m+1)} = \mathbf{k}^{(m)} + \Delta\mathbf{k} \tag{4.5}$$

where m is the iteration counter. Combining Eqs. (4.3) and (4.5) results in:

$$\Delta\mathbf{k} = 2b\mathbf{J}'(\mathbf{Y}^* - \mathbf{Y}) \tag{4.6}$$

where **J** is the Jacobian matrix of partial derivatives of **Y** with respect to **k** evaluated at all *n* points where experimental observations are available:

$$\mathbf{J} = \begin{bmatrix} \dfrac{\partial Y_1}{\partial k_1} & \cdots & \dfrac{\partial Y_1}{\partial k_b} \\ \cdots & \cdots & \cdots \\ \dfrac{\partial Y_n}{\partial k_1} & \cdots & \dfrac{\partial Y_n}{\partial k_b} \end{bmatrix} \tag{4.7}$$

To find a vector of parameters **k** to minimize the sum of squared residuals Φ, the vector **k** may be found by setting:

$$\frac{\partial \Phi}{\partial \mathbf{k}} = 0 \tag{4.8}$$

The Gauss-Newton method uses a Taylor series expansion to approximate the function, which is nonlinear with respect to the parameters:

$$\mathbf{Y}(t, \mathbf{k}) = \mathbf{Y}(t, \mathbf{k}^{(m)} + \Delta\mathbf{k}) = \mathbf{Y}(t, \mathbf{k}^{(m)}) + \frac{\partial \mathbf{Y}}{\partial \mathbf{k}}\Big|_{\mathbf{k}^{(m)}} \Delta\mathbf{k} = \mathbf{Y} + \mathbf{J}\Delta\mathbf{k} \tag{4.9}$$

where the Taylor series has been truncated after the second term. The nonlinear problem is thus converted into a linear problem. Combining Eqs. (4.3) and (4.9) gives:

$$\Phi = (\mathbf{Y}^* - \mathbf{Y} - \mathbf{J}\Delta\mathbf{k})'(\mathbf{Y}^* - \mathbf{Y} - \mathbf{J}\Delta\mathbf{k}) \tag{4.10}$$

Taking the partial derivative of Φ with respect to $\Delta\mathbf{k}$, setting it equal to zero, and solving for $\Delta\mathbf{k}$, we obtain:

$$\Delta\mathbf{k} = (\mathbf{J}'\mathbf{J})^{-1}\mathbf{J}'(\mathbf{Y}^* - \mathbf{Y}) \tag{4.11}$$

The Marquardt method is an interpolation between the Gauss-Newton and the steepest descent methods. A diagonal matrix ($\lambda\mathbf{I}$) is added to the matrix ($\mathbf{J'J}$) in Eq. (4.11):

$$\Delta\mathbf{k} = (\mathbf{J}'\mathbf{J} + \lambda\mathbf{I})^{-1}\mathbf{J}'(\mathbf{Y}^* - \mathbf{Y}) \tag{4.12}$$

The value of λ is chosen at each iteration so that the corrected parameter vector will result in a lower sum of squares in the following iteration.

The Marquardt method consists of the following steps:

1. Assume initial guesses for the parameter vector **k**.
2. Assign a large value, say 1000, to λ. This means that in the first iteration the steepest descent method is predominant and would assure that the method is moving toward the lower sum of squared residuals.
3. Evaluate the Jacobian matrix **J** from the equation(s) of the model.
4. Use Eq. (4.11) to obtain the correction vector $\Delta\mathbf{k}$.
5. Evaluate the new estimate of the parameter vector from Eq. (4.5).

   $$\mathbf{k}^{(m+1)} = \mathbf{k}^{(m)} + \Delta\mathbf{k}$$

6. Calculate the new value of Φ. If ($\Phi^{(m+1)} < \Phi^{(m)}$), reduce the value of λ, by a factor of 4, for example. If $\Phi^{(m+1)} > \Phi^{(m)}$, keep the old parameters [$\mathbf{k}^{(m+1)} = \mathbf{k}^{(m)}$] and increase the value of λ, by a factor of 2, for example.
7. Repeat steps 3-6 until either (or both) of the following conditions is satisfied:
   a. Φ does not change appreciably.
   b. $\Delta\mathbf{k}$ becomes very small.

We can find that when the value of λ is small compared with the elements of matrix (**J'J**), the Marquardt method approaches the Gauss-Newton method; when λ is very large, it is identical to the steepest descent. (Constantinides & Mostoufi, 2000).

The Marquardt method was chosen in this research. It is noticed that the proposed model is nonlinear. It includes eleven unknown parameters, k_1, k_2, k_3, k_4, k_5, k_6, k_7, k_8, k_9, k_{10}, and k_{11}, to be determined by using the Marquardt method to fit the model to the experimental data.

4.2 Experimental Results

4.2.1 Wild-type Mice

The wild-type mice were healthy subjects. Figures 13 and 14 are the isolated ERG a-wave after intravitreal injection of APB to the wild-type mice to pulse and step stimuli, respectively.

The responses were obtained with three different stimulus light intensities. The pink line represents the stimulus duration. In Figure 13, the stimulus was a pulse of 10 ms, and in Figure 14, the stimulus lasted 800 ms, which we refer as a step.

From the responses, we see that the ERG a-wave amplitude generally increases with the intensity of the stimulus light. For the same intensity, the recovery time of the responses to step stimulus is longer than the responses to pulse stimulus.

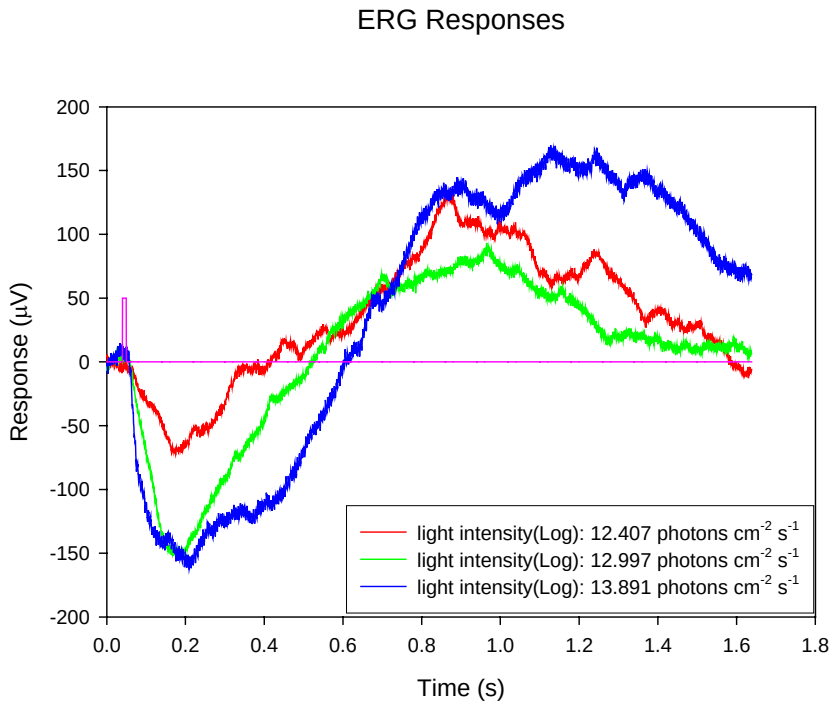

Fig. 13. The isolated ERG a-wave of wild-type mice. Stimulus: pulse.

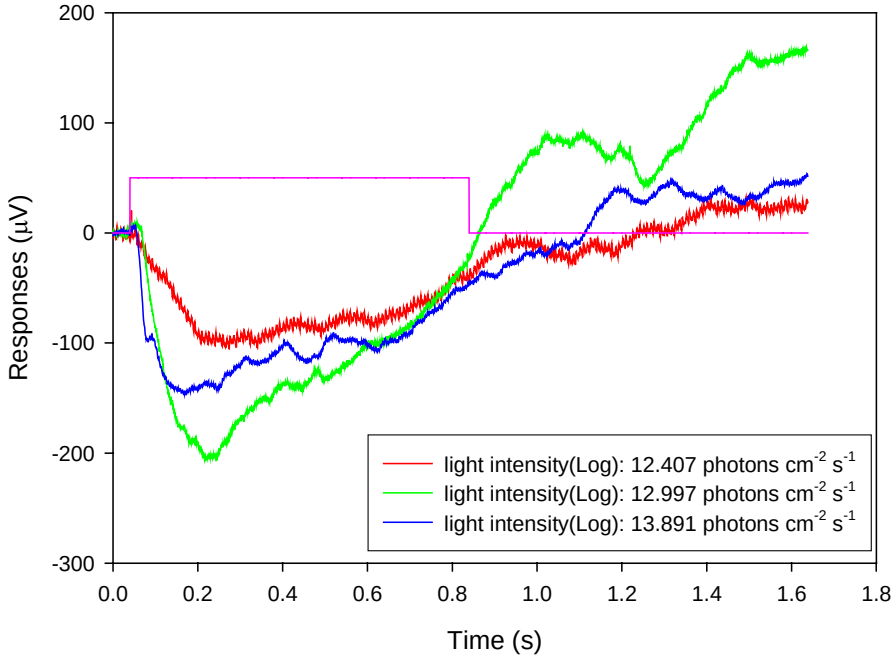

Fig. 14. The isolated ERG a-wave of wild-type mice. Stimulus: step.

4.2.2 NOB1 Mice

Figures 15 and 16 show the responses of the NOB1 mice to the pulse and step stimuli, respectively.

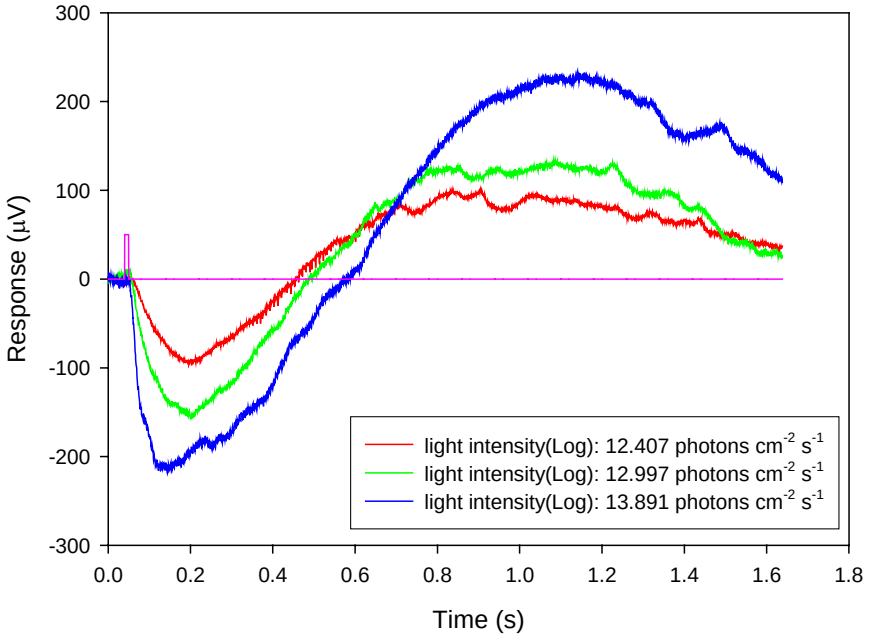

Fig. 15. Pulse responses of NOB1 mice.

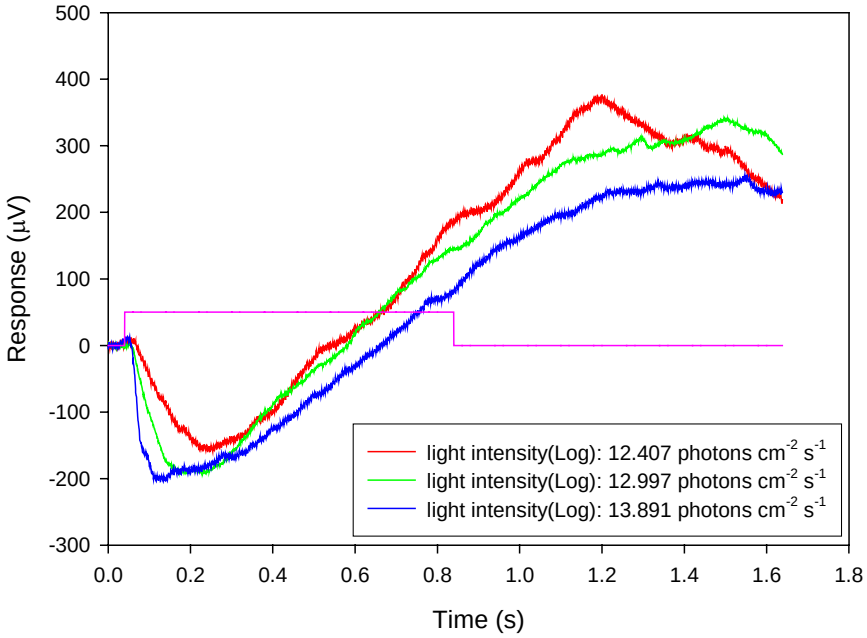

Fig. 16. Step responses of NOB1 mice.

The amplitude of responses and recovery time are similar to those of wild-type mice. These were expected since the photoreceptors of the NOB1 subjects were normal. The bipolar cell function in the NOB1 was disabled, and thus the b-waves were missing. The positive-going responses were, however, obvious and did not appear to be suppressed or reduced. The overall responses seem more consistent and less noisy than the wild type.

4.2.3 Light-induced Retina-damaged Mouse

The existing studies demonstrated that the photoreceptors on adult retinas could be damaged when exposed to bright light (Li, et al., 2001; Marc, et al., 2003). Many

factors, including the duration of the exposure, the intensity, the wavelength of the luminous environment and the type of exposure, affect the severity of the retina damage. Light damages are rhodopsin-mediated and, thus, are initiated in the outer segments of the photoreceptors, where the light stimulus is transduced (Noell et al., 1966).

In this research, a wild-type mouse was exposed to 11,000 lux white light for 24 hours to induce photoreceptor damage. Figures 17 and 18 show its responses to the pulse and step stimuli, respectively.

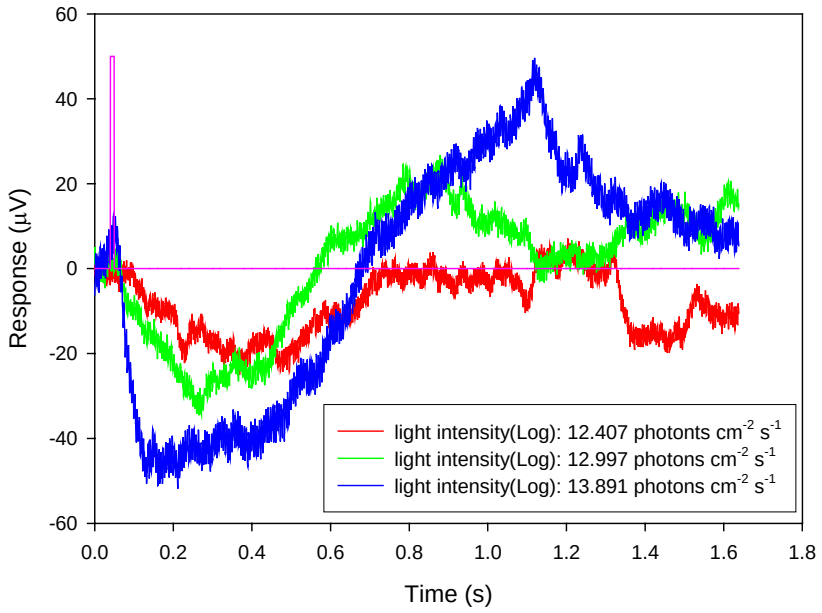

Fig. 17. Pulse responses of light-damaged wild-type mouse after APB.

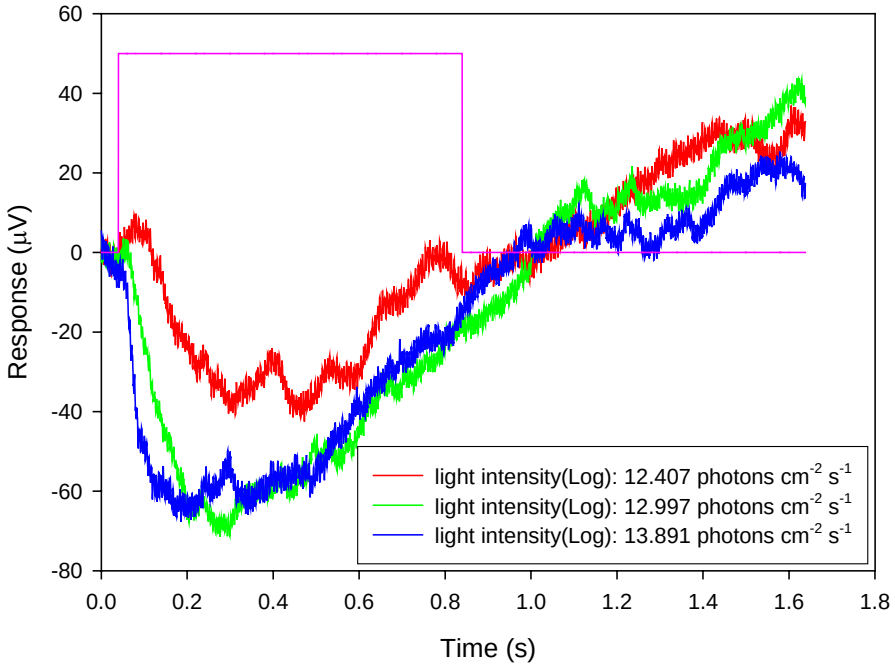

Fig. 18. Step responses of light-damaged wild-type mouse after APB.

Compared with the wild-type and NOB1 subjects, the amplitudes of responses were reduced greatly under the same light intensity. This indicates that the photoreceptors were partially damaged by exposure to intense light. The other features of the responses were similar to those of the wild-type and NOB1 mice.

4.2.4 N-methyl-N-nitrosourea-induced Photoreceptor-degenerated Mice

N-methyl-N-nitrosourea can cause photoreceptor apoptosis. The initial lesion area is the photoreceptor nuclei and later the outer segment (LaVil, Hollyfield & Anderson, 2003). Finally, all the elements of the phototransduction cascade are affected.

Figs. 19 and 20 show the responses of N-methyl-N-nitrosourea-induced photoreceptor-degenerated mice to pulse and step stimuli, respectively. The mice were injected 60mg/kg body weight of N-methyl-N-nitrosourea 2 days before ERG recordings. The red, green and blue lines are the responses for light intensities (Log) 12.407, 12.997 and 13.891 photons cm^{-2} s^{-1}, respectively.

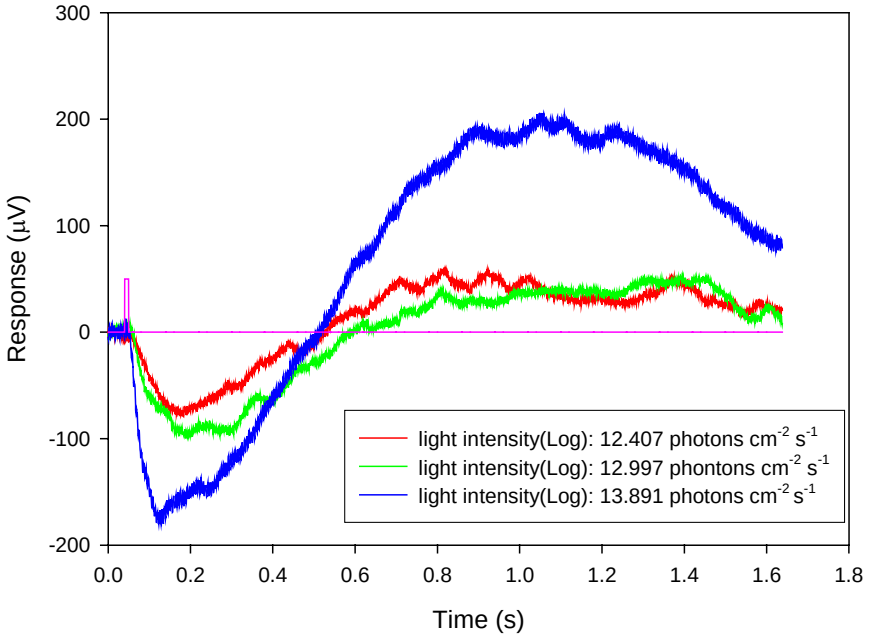

Fig. 19. Pulse responses of drug-damaged NOB1 mice.

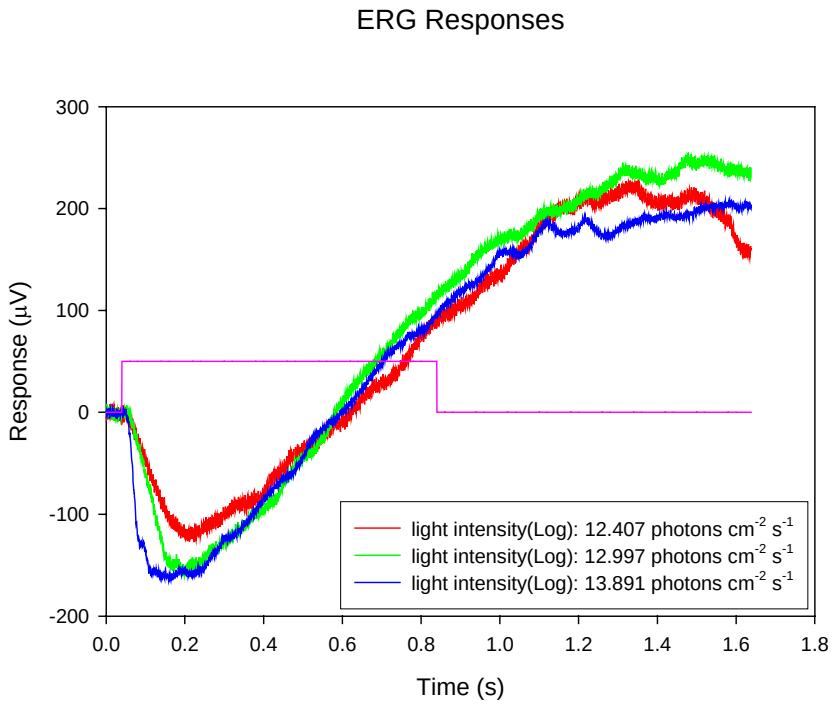

Fig. 20. Step responses of drug-damaged NOB1 mice.

The figures also show the same properties as those for the light-damaged mouse. The amplitude of each response was reduced and the recovery time to the step stimulus was longer than that to the pulse stimulus.

4.3 Parameter Estimation and Model Verification

Although b-wave was tried to block, part of the b-wave or other waves might still exist in the measurement. Since the proposed model is for photoreceptor response or a-wave, only the data from the beginning to the trough point were used for parameter estimation so that the influences of other waves are minimized.

By using the Marquardt method to fit the experimental data, the optimized estimate parameters were obtained. Figures 21 – 24 show the comparison of model predictions with experimental data.

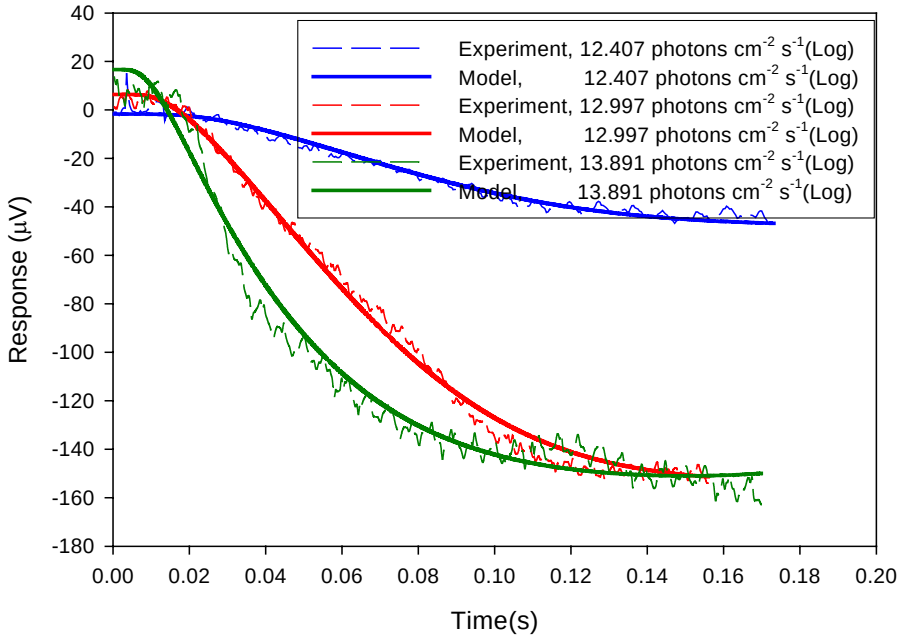

Fig. 21. Wild-type mice after APB excited with pulse stimuli.

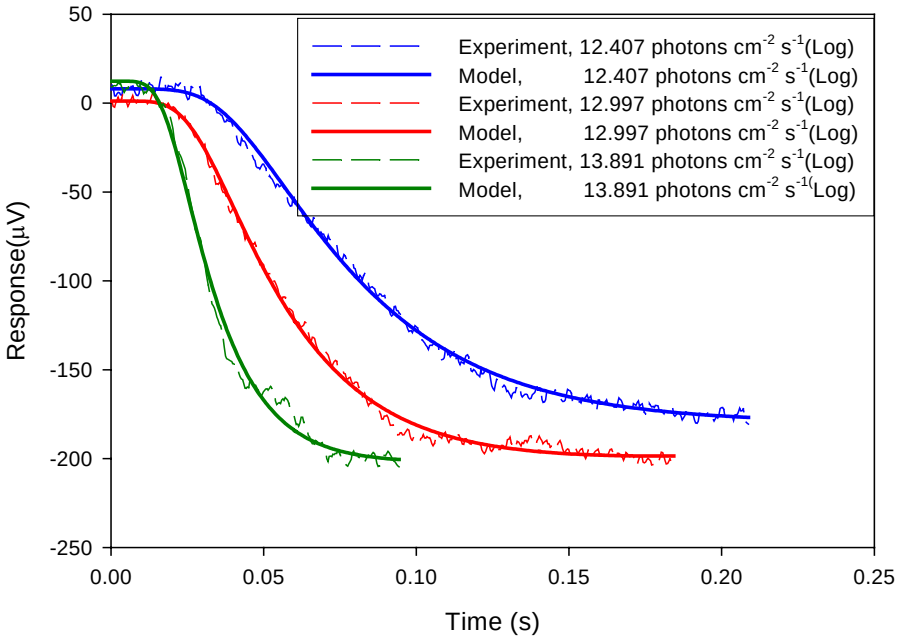

Fig. 22. Wild-type mice after APB excited with step stimuli.

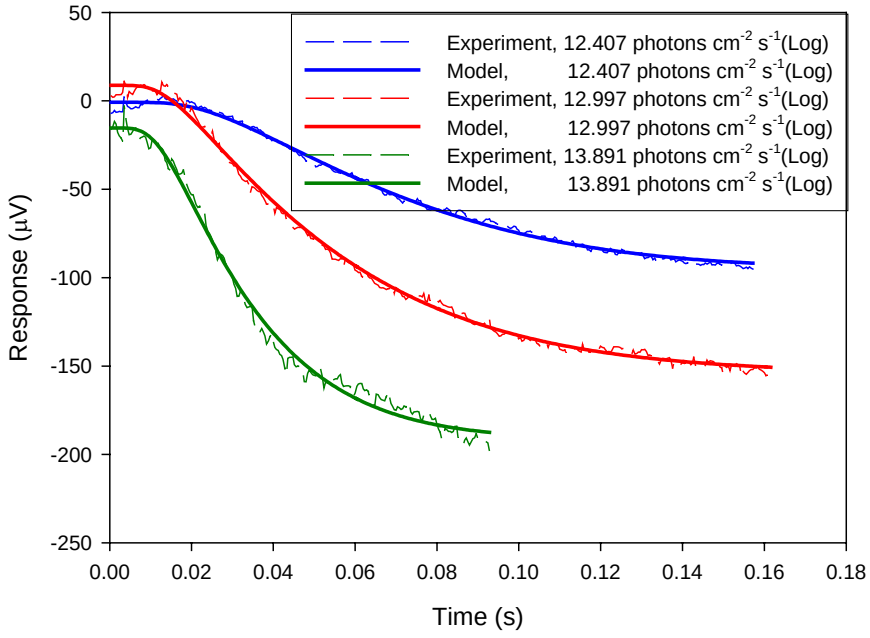

Fig. 23. NOB1 mice excited with pulse stimuli.

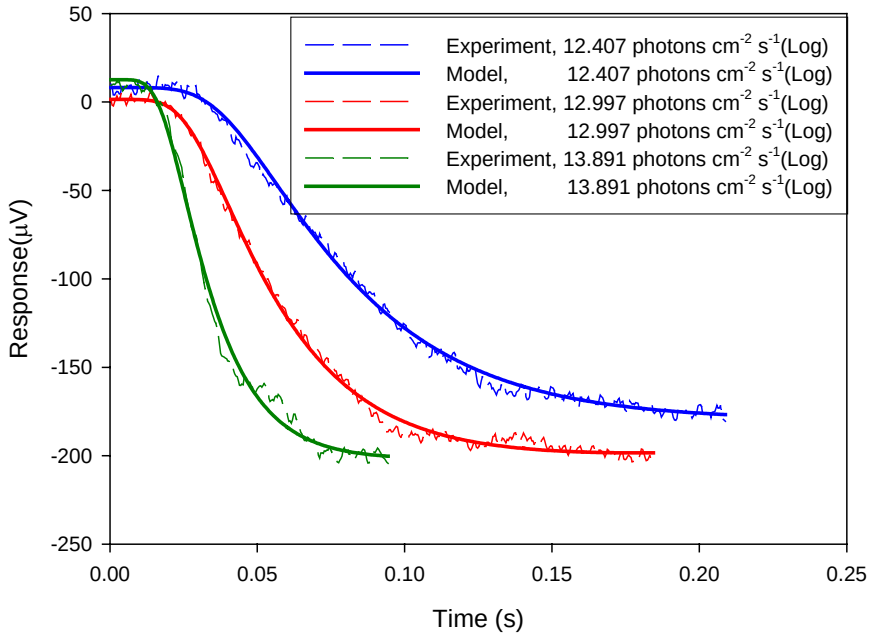

Fig. 24. NOB1 mice excited with step stimuli.

From the plots, we can see that the model data fit the experimental data very well for both the wild-type and NOB1 subjects under different stimulus conditions. The mean squared error ranges from 3.8100 to 124.3458 (or from 1.99% to 16.58%). This shows that model was capable of describing the photoreceptor responses under the different conditions.

The estimated parameters for the wild-type and NOB1 mice, and different stimulus conditions are listed in Tables 2 – 5.

Table. 2 Parameters of wild-type mice. Stimulus: pulse.

Para	Light Intensity (Log) (photons cm^{-2} s^{-1})					
	12.407		12.997		13.891	
	Subject1	Subject2	Subject1	Subject2	Subject1	Subject2
k_1	18.3676	18.4025	18.4491	18.3832	18.3283	16.3062
k_2	1.1815	1.1828	1.184	1.1819	1.9671	1.3632
k_3	8.3927	8.4788	8.6398	8.45	5.1632	2.5163
k_4	0.6045	0.6643	0.9077	0.6972	6.9181	32.1012
k_5	0.0780	0.1089	0.2156	0.1091	5.5910	3.2539
k_6	22.9787	22.9652	22.8848	22.9500	9.6142	6.9733
k_7	26.5974	26.5769	26.5199	26.5674	22.4460	29.1640
k_8	6.4978	6.5102	6.5905	6.4408	8.0346	38.9136
k_9	10.1016	10.1098	10.165	10.0636	9.7512	19.9541
k_{10}	0.5447	0.7217	1.5497	0.7271	1.6349	0.1380
k_{11}	1.0425	0.7236	1.8757	1.8801	2.8074	2.5600
MSE	16.0129	5.3735	8.6053	7.2401	53.3718	73.338

Table. 3 Parameters of wild-type mice. Stimulus: step.

Para	Light Intensity (Log) (photons cm^{-2} s^{-1})					
	12.407		12.997		13.891	
	Subject1	Subject2	Subject1	Subject2	Subject1	Subject2
k_1	3.9346	4.7320	2.8170	2.067	4.4261	2.2085
k_2	1.9245	2.0178	1.9575	1.9296	1.7171	1.7126
k_3	4.8145	5.1310	5.0068	4.1917	7.0696	5.679
k_4	7.1729	3.5545	9.1043	7.5771	10.1420	9.8822
k_5	8.8803	9.6661	9.0438	8.8032	8.9704	8.5732
k_6	13.4774	5.7895	5.7381	11.8761	5.0601	12.7393
k_7	7.1815	6.4410	6.0339	7.0086	7.5851	8.1834
k_8	6.9855	6.6340	7.8843	7.0116	10.2066	9.7448
k_9	1.5719	0.1227	0.6683	1.0298	0.5065	1.2743
k_{10}	4.5752	3.9834	5.3529	4.5532	7.0602	6.5531
k_{11}	3.4102	1.5152	3.0382	2.3408	2.7635	2.4091
MSE	8.5723	33.73	27.1408	26.4601	124.3458	57.9934

Table. 4 Parameters of NOB1 mice. Stimulus: pulse.

Para	Light Intensity (Log) (photons cm^{-2} s^{-1})								
	12.407			12.997			13.891		
	Subject1	Subject2	Subject3	Subject1	Subject2	Subject3	Subject1	Subject2	Subject3
k_1	12.2420	17.7909	21.5044	15.5560	15.5908	15.9454	12.9289	11.2366	10.5567
k_2	1.2505	2.4122	1.3522	2.0986	2.0996	2.3223	2.7212	2.8258	2.8552
k_3	12.7646	27.7105	22.5931	9.4347	9.5131	10.9205	1.6649	2.3156	2.4818
k_4	1.5119	0.6481	1.0396	1.2839	1.3308	2.4323	17.9779	12.7676	13.2934
k_5	4.7877	23.3689	10.5812	6.3263	6.3525	9.6149	3.2684	6.3934	6.3099
k_6	16.3945	57.4287	18.6099	20.0847	20.0796	15.1194	15.3082	16.0120	15.7540
k_7	11.0793	1.5086	0.5814	10.6667	10.6063	1.1014	17.3234	7.6637	7.4492
k_8	4.4274	42.1596	4.7670	8.7526	8.7532	9.5294	0.0257	9.7533	9.2883
k_9	0.9867	6.3932	3.1341	0.5707	0.5667	0.7078	22.0346	3.0145	0.1550
k_{10}	2.8239	0.0107	4.1834	9.2468	9.2475	10.1333	16.3274	10.2479	9.8214
k_{11}	1.4761	1.3051	1.4946	2.2249	1.8758	2.5951	3.4751	2.8486	3.2631
MSE	3.8100	25.0466	16.3908	9.9255	9.2504	8.0964	43.0814	27.8889	44.4964

Table. 5 Parameters of NOB1 mice. Stimulus: step.

Para	Light Intensity (Log) (photons cm^{-2} s^{-1})								
	12.407			12.997			13.891		
	Subject1	Subject2	Subject3	Subject1	Subject2	Subject3	Subject1	Subject2	Subject3
k_1	3.9694	3.5775	5.1352	2.0001	1.6865	1.8919	0.2194	0.6350	0.4737
k_2	1.8203	1.7713	1.7000	1.7128	1.7214	1.7220	1.9512	1.6929	0.6293
k_3	5.7199	6.5997	6.9093	5.4922	5.1815	5.2564	10.4736	5.7180	10.2605
k_4	5.2817	8.9933	3.3694	9.6439	8.9556	8.9728	23.0909	14.0617	22.8879
k_5	9.8573	8.9882	8.1680	8.5955	8.7272	8.7299	3.7860	7.8457	6.8579
k_6	9.6902	8.8406	6.9456	12.3509	11.2859	11.2021	22.0456	20.5334	16.2091
k_7	7.9758	7.9116	7.8242	8.1887	8.1632	8.1567	14.4514	8.2798	2.5689
k_8	0.4406	9.5344	0.2598	9.7787	9.6445	9.6494	13.3776	9.9186	6.1004
k_9	3.7801	0.5582	1.3946	1.5741	0.0185	0.1929	3.1749	2.6117	3.8761
k_{10}	4.4938	6.1975	4.2447	6.6101	6.3929	6.4023	5.9142	6.8159	12.2792
k_{11}	2.9478	1.8621	2.5329	3.2188	3.0251	2.9678	3.3899	2.7144	3.1906
MSE	12.6598	21.3515	26.7120	12.8018	46.9969	23.1264	37.6746	21.8293	76.6384

From the preceding tables and figures, we see that the responses and the parameters varied even for the same subject under the same conditions. While the model could fit individual data sets very well, it is not meaningful to attempt to represent this unpredictable biological variability. As a result, all ERG recordings for the same type of subjects under the same conditions were collectively used to fit one model. Figures 25 and 26 are example simulations for the wild-type mice under different conditions. Additional plots can be found in Appendix B.

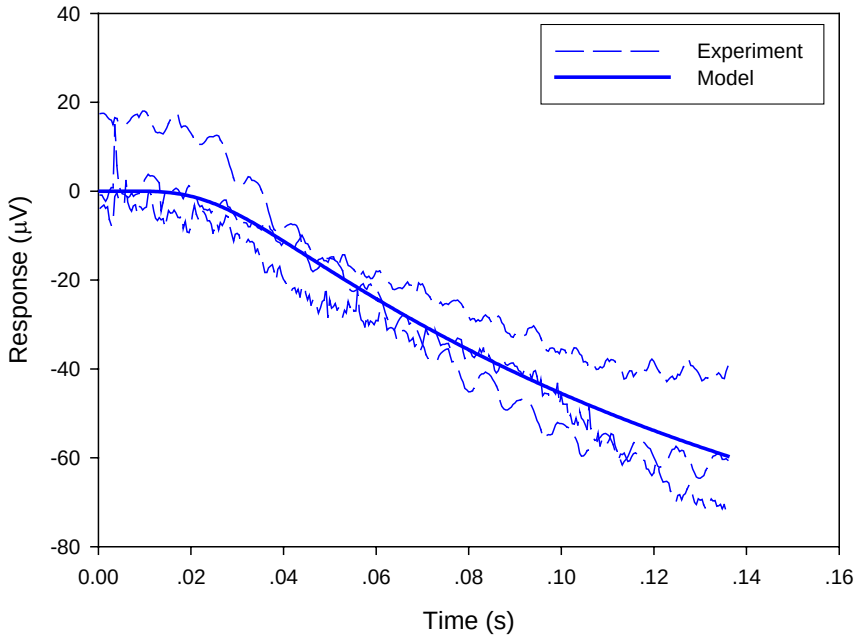

Fig. 25. Subjects: wild-type after APB. Stimulus: pulse. Light Intensity (Log): 12.407 photons cm^{-2} s^{-1}.

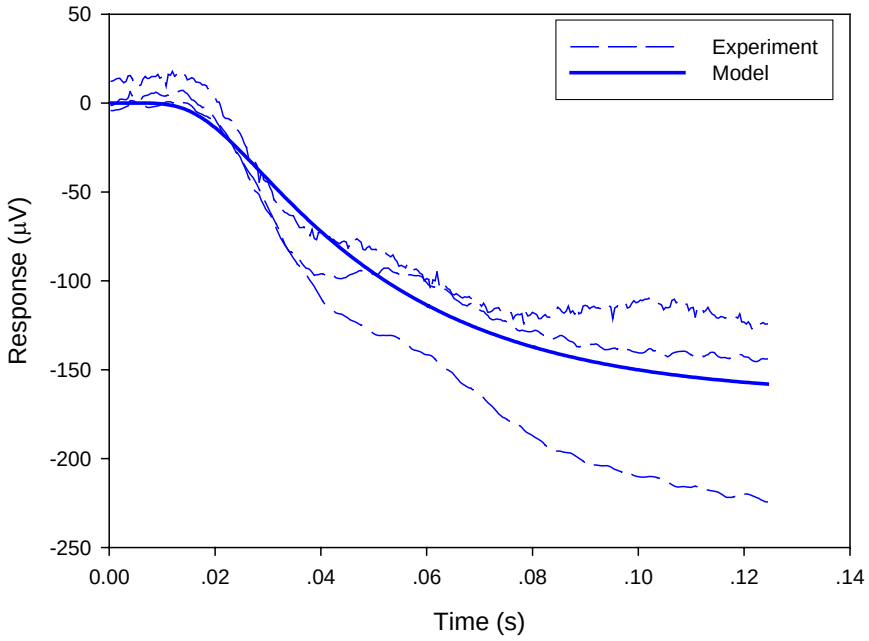

Fig. 26. Subjects: wild-type after APB. Stimulus: step. Light Intensity (Log): 13.891 photons cm^{-2} s^{-1}.

From Figures 25 and 26, it can be seen that the model represents the average or overall response of different subjects. The parameters were selected to minimize the total errors. This further demonstrates the flexibility and usefulness of the model in describing visual photoreceptor responses.

4.4 Detection of Photoreceptor Damage or Degeneration

Part of the photoreceptors in the light-damaged subject was damaged. This should reduce the magnitude of response or parameter k_{11} in the model since k_{11} is the gain and reflects the response of the photoreceptors to the stimulus. The parameters from the wild-type subjects were used as initial parameters, only k_{11} was changed to fit responses of the

light-induced retina-damaged mouse. Two of the simulation plots are in Figures. 27 and 28.

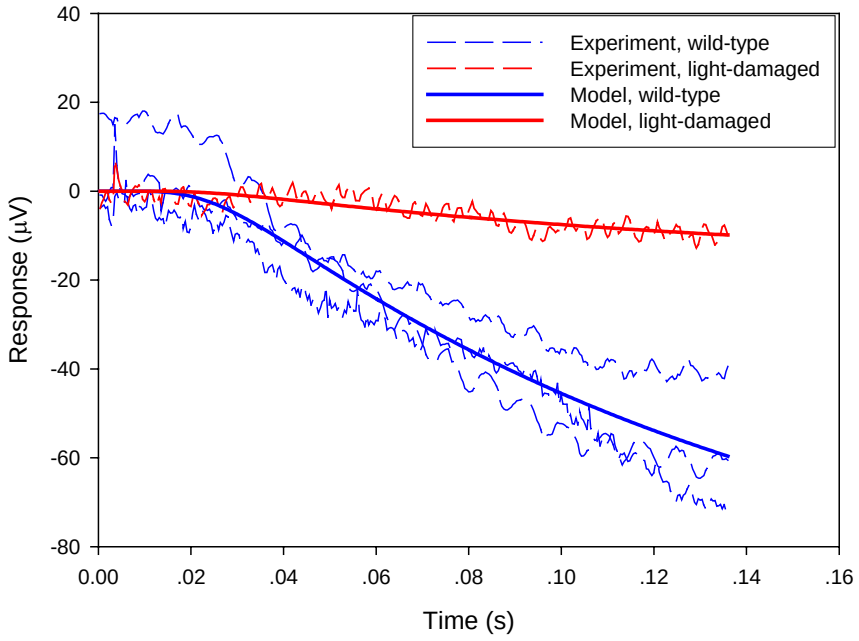

Fig. 27. Subjects: wild-type after APB and light-damaged wild-type after APB. Stimulus: pulse. Light Intensity (Log): 12.407 photons cm^{-2} s^{-1}.

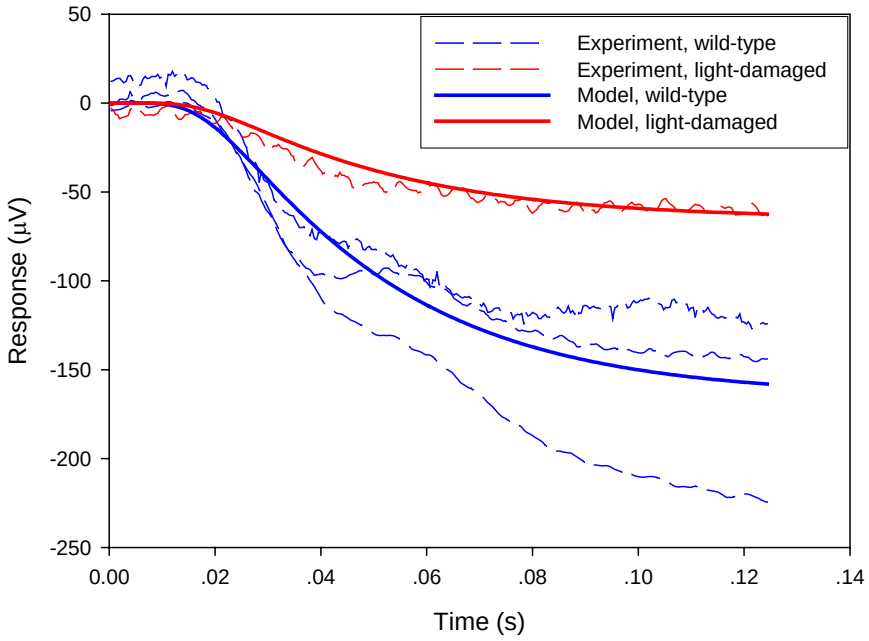

Fig. 28. Subjects: wild-type after APB and light-damaged after APB. Stimulus: step. Light Intensity (Log): 13.891 photons cm^{-2} s^{-1}.

Similarly, by injecting N-methyl-N-nitrosourea, part of the photoreceptors in the NOB1 subjects was damaged. In this experiment, three NOB1 mice were injected 30 mg/kg body weight and ERGs were recorded 120 hours after drug injection. Another three were injected 60 mg/kg body weight and ERGs were taken 48 hours after drug injection. Figures 29 and 30 show the simulation results.

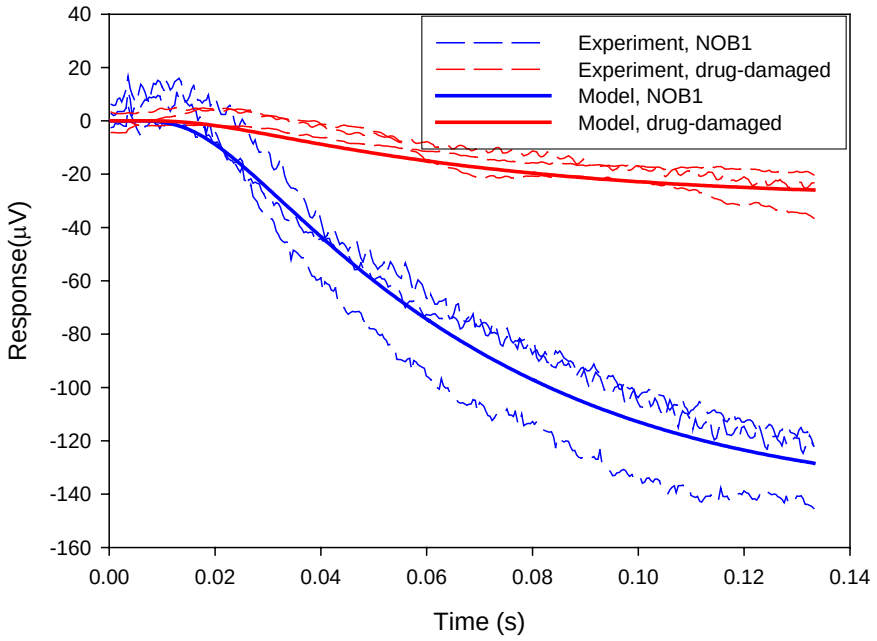

Fig. 29. Subjects: NOB1 and drug-damaged. Drug dose: 60 mg/kg body weight. Stimulus: pulse. Light Intensity (Log): 12.997 photons cm^{-2} s^{-1}.

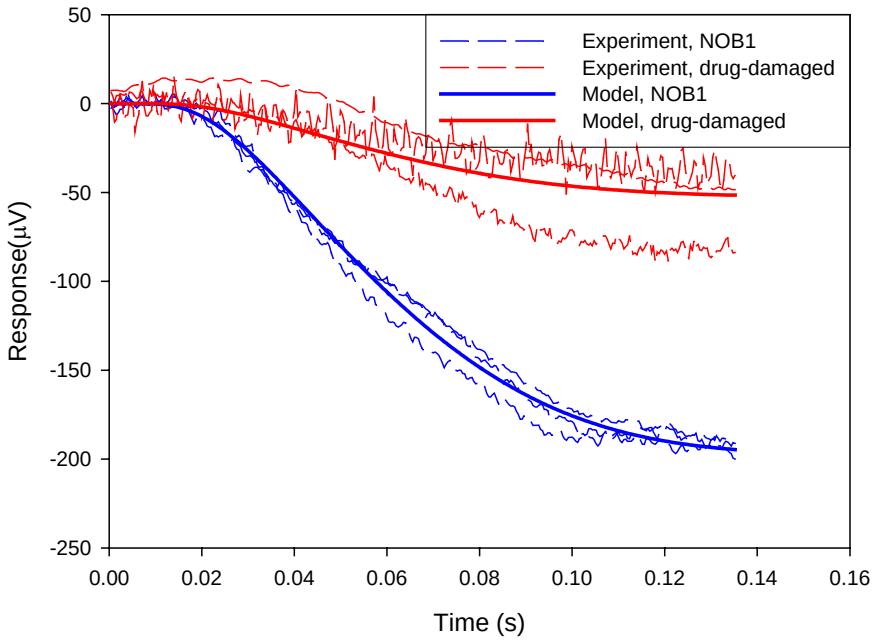

Fig. 30. Subjects: NOB1 and drug-damaged. Drug dose: 60 mg/kg body weight. Stimulus: step. Light Intensity (Log): 12.997 photons cm^{-2} s^{-1}.

Two figures are shown here as examples. Additional figures for different conditions are in Appendix B. The figures show that the model effectively describes the photoreceptor responses of both normal and photoreceptor-damaged subjects. Furthermore, variation of parameter k_{11} is sufficient to account for photoreceptor damage, which is consistent with the theoretical basis of the model.

Tables 6 – 8 list the values of coefficient k_{11} obtained from different types of subjects under different light intensities and patterns.

Table. 6 Parameter k_{11} for wild-type and light-damaged subjects.

Light pattern	Subject	Light Intensity (Log) (photons cm^{-2} s^{-1})		
		12.407	12.997	13.891
Pulse	Wild-type mice	1.5634	1.7661	2.0920
	Light-damaged mouse	0.2591	0.3861	0.7399
Step	Wild-type mice	2.1232	2.5897	2.5782
	Light-damaged mouse	0.3226	0.9401	1.0183

Table. 7 Parameter k_{11} for NOB1 and 30 mg/kg body weight drug-damaged NOB1 subjects.

Light pattern	Subject	Light Intensity (Log) (photons cm^{-2} s^{-1})		
		12.407	12.997	13.891
Pulse	NOB1 mice	1.4145	2.1391	3.0866
	Drug-damaged NOB1 mice	0.858	1.4399	1.6676
Step	NOB1 mice	2.3477	3.1497	2.7182
	Drug-damaged NOB1 mice	1.8321	1.3820	1.8480

Table. 8 Parameter k_{11} for NOB1 and 60 mg/kg body weight drug-damaged NOB1 subjects.

Light pattern	Subject	Light Intensity (Log) (photons cm^{-2} s^{-1})		
		12.407	12.997	13.891
Pulse	NOB1 mice	0.9537	2.1860	3.2000
	Drug-damaged NOB1 mice	0.3141	0.4423	0.5738
Step	NOB1 mice	2.3848	3.0898	2.8780
	Drug-damaged NOB1 mice	0.6527	0.8182	0.5984

From above tables, we see that the k_{11} values for the subjects with normal photoreceptors (including wild-type and NOB1 mice) are consistently larger than those for the photoreceptor-damaged subjects under the same conditions. Moreover, the k_{11} values for the subjects injected with 30 mg/kg body weight drug were always higher than those for the subjects injected with 60 mg/kg body weight drug. This means that the model can show malfunction of photoreceptor. While the photoreceptor damages were not quantified to show how they related to k_{11}, it appears that k_{11} can also indicate the degree of photoreceptor damage.

4.5 Modeling of Termination and Modulation

In the termination and modulation process, the activated proteins (e.g. R*, G* and E*) are deactivated, and cGMP is synthesized. As a result, the ERG response should reduce and move towards a steady state. To test if the model describes these phases of the phototransduction, the parameters estimated from the initial a-wave part of the response

were used to simulate the response for a much longer period. Figures 31 and 32 show two simulation plots compared with experimental data.

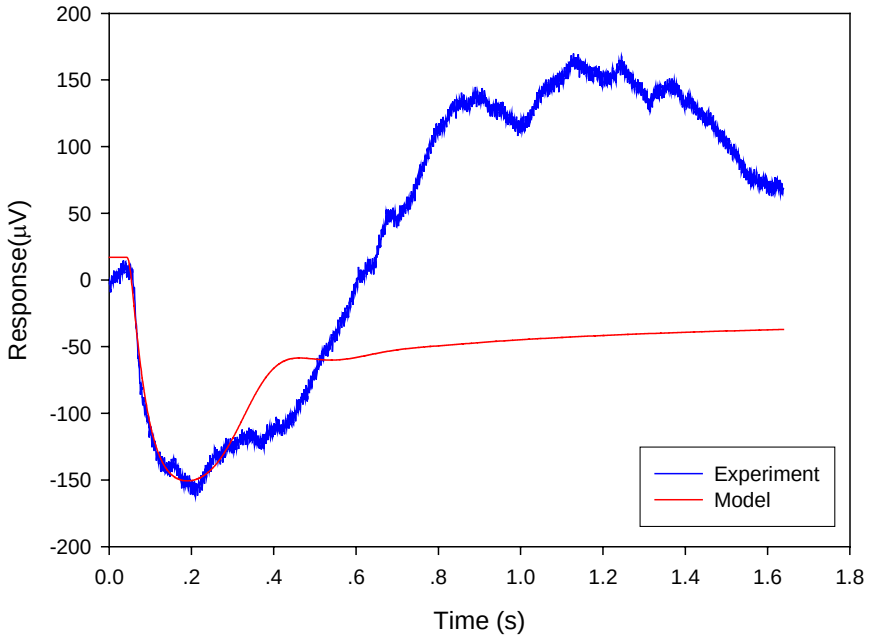

Fig. 31. Subject: wild-type after APB. Stimulus: pulse. Light Intensity (Log): 13.891 photons cm^{-2} s^{-1}.

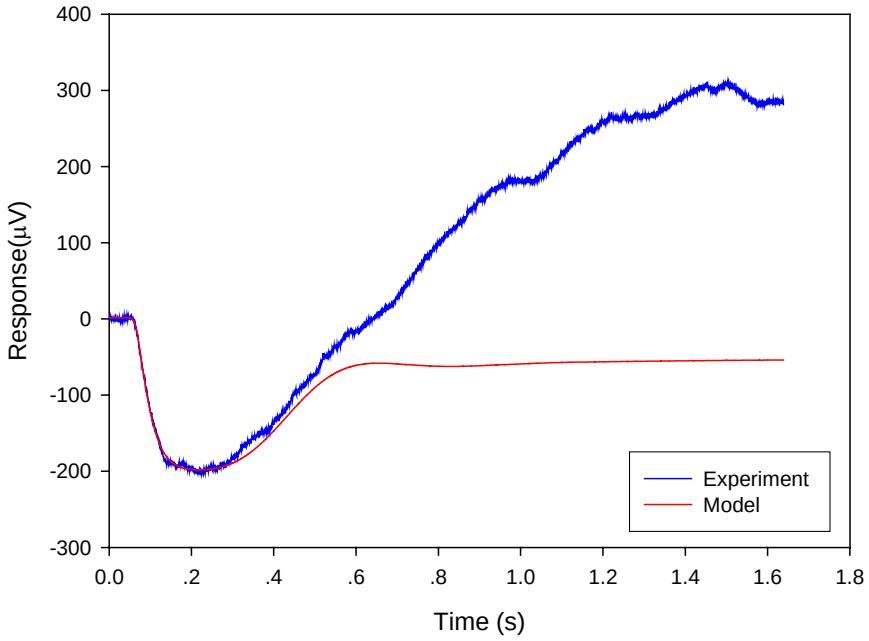

Fig. 32. Subject: NOB1. Stimulus: step.
Light Intensity (Log): 12.997 photons cm^{-2} s^{-1}.

The simulation shows the predicted long-term behavior of the photoreceptor response or the ERG without the influences of the bipolar and other cells. It agrees with Lamb and Pugh's model as shown in Fig. 11. The trend is consistent with expectation of recovery to a steady state. Although further verification is needed, the proposed model could describe the termination and modulation phases of the phototransduction process as well.

4.6 Discussion

Since this model is based on phototransduction process, it only represents the a-wave of ERG. It does not describe the b-wave and other components.

In this experiment, the stimulus light was a green LED. The intensity (Log) levels ranged from 12.407 photons cm^{-2} s^{-1} – 13.891 photons cm^{-2} s^{-1}. If the Light Intensity level was higher (e.g., 14.906 photons cm^{-2} s^{-1}, 15.662 photons cm^{-2} s^{-1}), the ERG a-wave could be different from that under lower power levels. Figures 33 and 34 are ERG plots for a stimulus of 14.906 photons cm^{-2} s^{-1}.

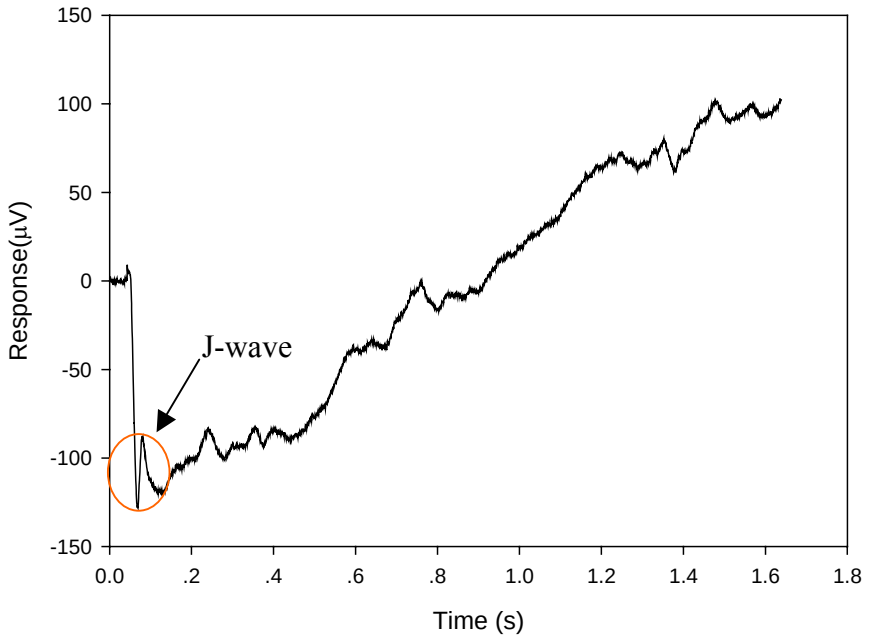

Fig. 33. Subject: wild-type after APB. Stimulus: pulse. Light Intensity (Log): 14.906 photons cm^{-2} s^{-1}.

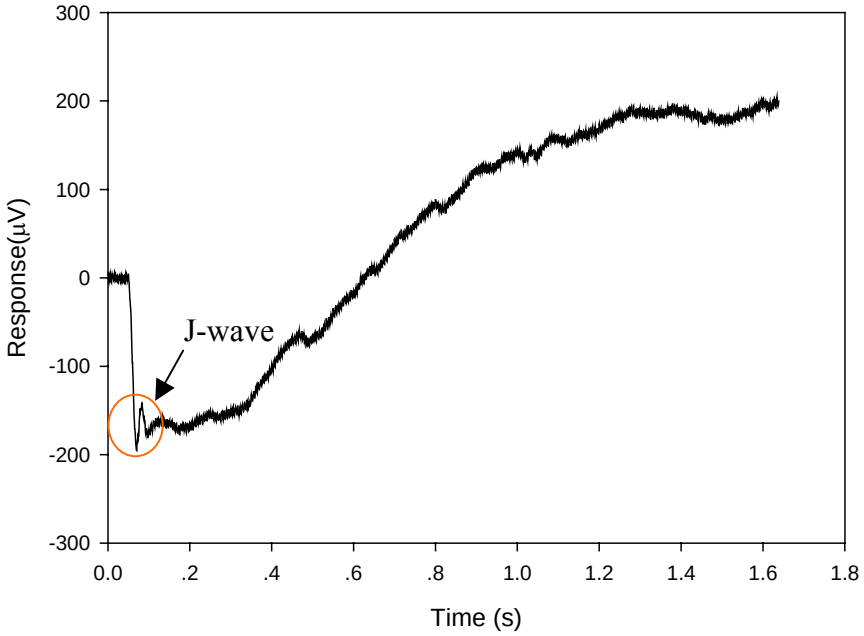

Fig. 34. Subject: NOB1. Stimulus: step.
Light Intensity (Log): 14.906 photons cm^{-2} s^{-1}.

The figures show that some additional variations exist. These variations are not considered in the proposed model. Therefore, a good description cannot be obtained from the model for very high-intensity stimulus.

CHAPTER 5

CONCLUSIONS AND RECOMMENDATIONS

5.1 Conclusions

In this research, a mathematical model was developed for the rod photoreceptor phototransduction process based on the biochemical reaction kinetics in the photo-transduction cascade. Unlike the existing models, which are either empirical fittings of the ERG a-waves and thus lack a physical basis or based on some over simplification of the phototransduction process, the proposed model does not only describe the activation phase of the process but also accounts for possible changes in the termination and modulation phases. Results from the analysis and experimental validation of the model lead to the following conclusions:

1. The model can effectively describe the photoreceptor responses under different combinations of excitation pattern and intensity.
2. The model parameters, which describe the rates or quantum efficiencies of reactions in the cascade, can indicate physical changes in the process. In this work, model parameter changes clearly reflected light or chemical induced photoreceptor damages.
3. While further verification is needed, the model appears to represent the termination and modulation phases of phototransduction in a theoretically meaningful manner.
4. The model is promising for enhancing the diagnostic usefulness of ERG.

5.2 Recommendations

The model developed and experiments conducted are still limited in scope. Further research is warranted. Specifically, the following future research efforts are recommended:

1. High excitation intensities seemed to result in significantly different photoreceptor responses, which the current model may not effectively describe. Further experiments and analysis of the changes under high-intensity conditions would be beneficial.
2. To establish the effectiveness of the model under a wide range of conditions, further experimental verification is needed. In particular, measurements of the proteins and enzymes would provide a direct validation of the state-variable values and thus greatly enhance the parameter estimation and the overall validity of the model.
3. Effective chemical, genetic or mathematical methods are needed to isolate the photoreceptor response (a-wave) from the other responses, especially those generated by the bipolar and other cells.

APPENDIX A. Matlab Program for Modeling of Phototransduction

1. Main Program

```
%%%%%%%%%%%%%%%%%%%%%%%%%%%%%%%%%%%%
% File name: DA_f2.m
% Author: Lei Lu
% Data: June 2006
% Function: This is the main program to perform the
%               nonlinear least optimization.
%%%%%%%%%%%%%%%%%%%%%%%%%%%%%%%%%%%%

clear;
clc;

fre_samp=2500;                          % sampling frequence
dt=1/fre_samp;                          % interval time

row_start=0;                            % the start row of data
row_end=4095;                           % the end row of data
column_start=0;                         % the start column of data
column_end=0;                           % the end column of data

data_leng=row_end-row_start+1;          % the length of "data"

t=zeros(data_leng, 1);                  % initial the matrix of time t
u=zeros(data_leng, 1);                  % initial the matrix of stimulus signal u
f1=zeros(data_leng, 1);                 % initial the matrix of response f
f2=zeros(data_leng, 1);
f3=zeros(data_leng, 1);
f4=zeros(data_leng, 1);
f5=zeros(data_leng, 1);
f6=zeros(data_leng, 1);

%%%%%%%%%%%  the pathway of file 3nd 3v (pulse)
% file_11=('C:\2006-5-10_WildType\05100601B008.PRN');
% file_12=('C:\2006-5-18_WildType\05180601\05180601B002.PRN');
% file_13=('C:\2006-5-18_WildType\05180602\05180602A013.PRN');

% file_14=('C:\2006-7-13\2006-7-13(1)\07130601B006.PRN');

% file_11=('C:\2006-5-15_NOB1\05150601\05150601B013.PRN');
% file_12=('C:\2006-5-15_NOB1\05150602\05150602B000.PRN');
% file_13=('C:\ch\data\2006-5-15_NOB1\05150603\05150603B000.PRN');
%
% file_14=('C:\2006-8-3\08030601\08030601B000.PRN');
% file_15=('C:\2006-8-3\08030602\08030602B012.PRN');
% file_16=('C:\2006-8-3\08030603\08030603B001.PRN');
```

```
% file_14=('C:\2006-8-3\08030604\08030604B003.PRN');
% file_15=('C:\2006-8-3\08030605\08030605B000.PRN');
% file_16=('C:\2006-8-3\08030606\08030606B001.PRN');

%%%%%%%%%%%%%%  the pathway of file 2nd 4v (pulse)
% file_11=('C:\2006-5-10_WildType\05100601B010.PRN');
% file_12=('C:\2006-5-18_WildType\05180601\05180601B003.PRN');
% file_13=('C:\ 2006-5-18_WildType\05180602\05180602B005.PRN');

% file_14=('C:\2006-7-13\2006-7-13(1)\07130601B009.PRN');

% file_11=('C:\ 2006-5-15_NOB1\05150601\05150601B015.PRN');
% file_12=('C:\2006-5-15_NOB1\05150602\05150602B004.PRN');
% file_13=('C:\2006-5-15_NOB1\05150603\05150603B002.PRN');

% file_14=('C:\2006-8-3\08030601\08030601B002.PRN');
% file_15=('C:\2006-8-3\08030602\08030602B014.PRN');
% file_16=('C:\2006-8-3\08030603\08030603B004.PRN');

% file_14=('C:\2006-8-3\08030604\08030604B004.PRN');
% file_15=('C:\2006-8-3\08030604\08030604B006.PRN');
% file_16=('C:\2006-8-3\08030605\08030605B007.PRN');

%%%%%%%%%%%%%%  the pathway of file 1nd 4v (pulse)
% file_11=('C:\2006-5-10_WildType\05100601B012.PRN');
% file_12=('C:\2006-5-18_WildType\05180601\05180601B005.PRN');
% file_13=('C:\2006-5-18_WildType\05180602\05180602A018.PRN');

% file_14=('C:\2006-7-13\2006-7-13(1)\07130601B011.PRN');

% file_11=('C:\2006-5-15_NOB1\05150601\05150601B017.PRN');
% file_12=('C:\2006-5-15_NOB1\05150602\05150602B006.PRN');
% file_13=('C:\2006-5-15_NOB1\05150603\05150603B004.PRN');

% file_14=('C:\2006-8-3\08030601\08030601B006.PRN');
% file_15=('C:\2006-8-3\08030602\08030602B016.PRN');
% file_16=('C:\2006-8-3\08030603\08030603B006.PRN');

% file_14=('C:\2006-8-3\08030604\08030604B007.PRN');
% file_15=('C:\2006-8-3\08030605\08030605B008.PRN');
% file_16=('C:\2006-8-3\08030606\08030606B007.PRN');

%%%%%%%%%%%%%%  the pathway of file 3nd 3v (step)
% file_11=('C:\2006-5-10_WildType\05100601B009.PRN');
% file_12=('C:\2006-5-18_WildType\05180601\05180601B001.PRN');
% file_13=('C:\2006-5-18_WildType\05180602\05180602A015.PRN');
%
% file_14=('C:\2006-7-13\2006-7-13(1)\07130601B007.PRN');

% file_11=('C:\2006-5-15_NOB1\05150601\05150601B014.PRN');
% file_12=('C:\2006-5-15_NOB1\05150602\05150602B003.PRN');
% file_13=('C:\2006-5-15_NOB1\05150603\05150603B001.PRN');

% file_14=('C:\2006-8-3\08030601\08030601B001.PRN');
% file_15=('C:\2006-8-3\08030602\08030602B013.PRN');
```

```
% file_16=('C:\2006-8-3\08030603\08030603B002.PRN');

% file_14=('C:\2006-8-3\08030604\08030604B002.PRN');
% file_15=('C:\2006-8-3\08030605\08030605B001.PRN');
% file_16=('C:\2006-8-3\08030606\08030606B003.PRN');

%%%%%%%%%%%%%%  the pathway of file 2nd 4v (step)
% file_11=('C:\2006-5-10_WildType\05100601B006.PRN');
% file_12=('C:\2006-5-18_WildType\05180601\05180601B004.PRN');
% file_13=('C:\2006-5-18_WildType\05180602\05180602A017.PRN');

% file_14=('C:\2006-7-13\2006-7-13(1)\07130601B010.PRN');

% file_11=('C:\2006-5-15_NOB1\05150601\05150601B016.PRN');
% file_12=('C:\2006-5-15_NOB1\05150602\05150602B005.PRN');
% file_13=('C:\2006-5-15_NOB1\05150603\05150603B003.PRN');

% file_14=('C:\2006-8-3\08030601\08030601B003.PRN');
% file_15=('C:\2006-8-3\08030602\08030602B015.PRN');
% file_16=('C:\2006-8-3\08030603\08030603B005.PRN');

% file_14=('C:\2006-8-3\08030604\08030604B005.PRN');
% file_15=('C:\2006-8-3\08030605\08030605B005.PRN');
% file_16=('C:\2006-8-3\08030606\08030606B006.PRN');

%%%%%%%%%%%%%%  the pathway of file 1nd 4v (step)
% file_11=('C:\2006-5-10_WildType\05100601B013.PRN');
% file_12=('C:\2006-5-18_WildType\05180601\05180601B006.PRN');
% file_13=('C:\2006-5-18_WildType\05180602\05180602A008.PRN');
%
% file_14=('C:\2006-7-13\2006-7-13(1)\07130601B012.PRN');

% file_11=('C:\2006-5-15_NOB1\05150601\05150601B018.PRN');
% file_12=('C:\2006-5-15_NOB1\05150602\05150602B007.PRN');
% file_13=('C:\2006-5-15_NOB1\05150603\05150603B005.PRN');
%
% file_14=('C:\2006-8-3\08030601\08030601B007.PRN');
% file_15=('C:\2006-8-3\08030602\08030602B017.PRN');
% file_16=('C:\2006-8-3\08030603\08030603B007.PRN');

% file_14=('C:\2006-8-3\08030604\08030604B008.PRN');
% file_15=('C:\2006-8-3\08030605\08030605B009.PRN');
% file_16=('C:\2006-8-3\08030606\08030606B008.PRN');

%%%%%%%%%%%%%%%

data_1=csvread(file_11, row_start, column_start, [row_start, column_start, row_end, column_end]);
data_2=csvread(file_12, row_start, column_start, [row_start, column_start, row_end, column_end]);
data_3=csvread(file_13, row_start, column_start, [row_start, column_start, row_end, column_end]);
                                                    % read the control data file and save to "data"

for i=1:data_leng
   t(i)=i*dt;                                       % input the value of t
   f1(i)=data_1(i);                                 % input the value of f
   f2(i)=data_2(i);
   f3(i)=data_3(i);
```

```
end;

data_min1=min(data_1);                  % the value of trough of a-wave (file 1)
data_min2=min(data_2);                  % the value of trough of a-wave (file 2)
data_min3=min(data_3);                  % the value of trough of a-wave (file 3)

p_s1=0;
p_s2=0;
p_s3=0;
p_s4=0;
p_s5=0;
p_s6=0;
for j=1:data_leng                       % the number of point to reach the trough of a-wave
   if data_1(j)==data_min1
      p_s1=j;
   end;
end;
for j=1:data_leng
   if data_2(j)==data_min2
      p_s2=j;
   end;
end;
for j=1:data_leng
   if data_3(j)==data_min3
      p_s3=j;
   end;
end;

disp(' ')
disp(' The number of stress file: ')
disp('      1 - one')
disp('      2 - three')
numFile=input(' Enter your choice: ');
disp(' ')
if numFile==1
      data_4=csvread(file_14, row_start, column_start, [row_start, column_start, row_end, column_end]);

      for i=1:data_leng
         f4(i)=data_4(i);
      end;

      data_min4=min(data_4);            % the value of trough of a-wave (file 4)

      for j=1:data_leng
         if data_4(j)==data_min4
            p_s4=j;
         end;
      end;

      p_s=[p_s1 p_s2 p_s3 p_s4];

      t_p_s=min(p_s)*dt;                % display the time to reach trough of a-wave

      data_min_matr=[data_min1 data_min2 data_min3 data_min4];
      data_min=min(data_min_matr);
```

```
else if numFile==2
      data_4=csvread(file_14, row_start, column_start, [row_start, column_start, row_end, column_end]);
      data_5=csvread(file_15, row_start, column_start, [row_start, column_start, row_end, column_end]);
      data_6=csvread(file_16, row_start, column_start, [row_start, column_start, row_end, column_end]);
                              % read the data file and save to "data"
      for i=1:data_leng
         f4(i)=data_4(i);
         f5(i)=data_5(i);
         f6(i)=data_6(i);
      end;

      data_min4=min(data_4);              % the value of trough of a-wave (file 4)
      data_min5=min(data_5);              % the value of trough of a-wave (file 5)
      data_min6=min(data_6);              % the value of trough of a-wave (file 6)

      for j=1:data_leng
         if data_4(j)==data_min4
            p_s4=j;
         end;
      end;
      for j=1:data_leng                   % the number of point to reach the trough of a-wave
         if data_5(j)==data_min5
            p_s5=j;
         end;
      end;
      for j=1:data_leng
         if data_6(j)==data_min6
            p_s6=j;
         end;
      end;

      p_s=[p_s1 p_s2 p_s3 p_s4 p_s5 p_s6];

      t_p_s=min(p_s)*dt;                  % display the time to reach trough of a-wave

      data_min_matr=[data_min1 data_min2 data_min3 data_min4 data_min5 data_min6];
      data_min=min(data_min_matr);
   end;
end;

disp(' ')
disp(' The stimulus light type: ')
disp('      1 - pulse')
disp('      2 - step')
LightType=input(' Enter your choice: ');
disp(' ')
switch LightType
   case 1
      disp('Please choose the intensity: ');
      disp('  1 - 3nd 3v')
      disp('  2 - 2nd 4v')
      disp('  3 - 1nd 4v')
      inten=input(' Enter your choice:');
      switch inten
      case 1
         for i=1:data_leng
```

```
            if i>=100 & i<=125
               u(i)=1*1.504;                % input the value of u. u=1.504 when stimulus signal is 3 nd
            end;
         end;
      case 2
         for i=1:data_leng
            if i>=100 & i<=125
               u(i)=1*5.71;                 % input the value of u. u=5.71 when stimulus signal is 2 nd
            end;
         end;
      case 3
         for i=1:data_leng
            if i>=100 & i<=125
               u(i)=1*46.87;                % input the value of u. u=46.87 when stimulus signal is 1 nd
            end;
         end;
      end;
   case 2
      disp('Please choose the intensity: ');
      disp('  1 - 3nd 3v')
      disp('  2 - 2nd 4v')
      disp('  3 - 1nd 4v')
      inten=input(' Enter your choice:');
      switch inten
      case 1
         for i=1:data_leng
            if i>=100 & i<=2100
               u(i)=1*1.504;                % input the value of u. u=1.504 when stimulus signal is 3 nd
            end;
         end;
      case 2
         for i=1:data_leng
            if i>=100 & i<=125
               u(i)=1*5.71;                 % input the value of u. u=5.71 when stimulus signal is 2 nd
            end;
         end;
      case 3
         for i=1:data_leng
            if i>=100 & i<=125
               u(i)=1*46.87;                % input the value of u. u=46.87 when stimulus signal is 1 nd
            end;
         end;
      end;
end;

if numFile==1
   figure(1)                                % plot the ERG figure
   plot(t, u, t, f1, t, f2, t, f3, t, f4);
   title('mouse ERG');
   xlabel('time(s)');
   ylabel('response');
else if numFile==2
      figure(1)
      plot(t,u,t,f1,t,f2,t,f3,t,f4,t,f5,t,f6);
      title('mouse ERG');
      xlabel('time(s)');
```

```
      ylabel('response');
   end;
end;

data_s_leng=min(p_s)-100+1;

data_m1=zeros(data_s_leng, 1);          % initial the matrix of new data set (data_s)
data_m2=zeros(data_s_leng, 1);
data_m3=zeros(data_s_leng, 1);
data_m4=zeros(data_s_leng, 1);
data_m5=zeros(data_s_leng, 1);
data_m6=zeros(data_s_leng, 1);

t_s=zeros(data_s_leng, 1);              % initial the matrix of new time set (t_s)
u_s=zeros(data_s_leng, 1);              % initial the matrix of new response set (u_s)

if numFile==1
   for i=1:data_s_leng
      t_s(i)=i*dt;                      % input the true data to the new time set

      data_m1(i)=data_1(i+100-1);       % input the true data to the new data set
      data_m2(i)=data_2(i+100-1);
      data_m3(i)=data_3(i+100-1);
      data_m4(i)=data_4(i+100-1);

      u_s(i)=u(i+100-1);                % input the true data to the new response set
   end;
else if numFile==2
      for i=1:data_s_leng
         t_s(i)=i*dt;                   % input the true data to the new time set

         data_m1(i)=data_1(i+100-1);    % input the true data to the new data set
         data_m2(i)=data_2(i+100-1);
         data_m3(i)=data_3(i+100-1);
         data_m4(i)=data_4(i+100-1);
         data_m5(i)=data_5(i+100-1);
         data_m6(i)=data_6(i+100-1);

         u_s(i)=u(i+100-1);             % input the true data to the new response set
      end;
   end;
end;

if numFile==1
   figure(2)                            % plot the figure from the start to the trough of a-wave
   plot(t_s,u_s,t_s,data_m1,'-r',t_s,data_m2,'-r',t_s,data_m3,'-r',t_s,data_m4,'-b');
   title('mouse ERG');
   xlabel('time(s)');
   ylabel('response(s)');
else if numFile==2
      figure(2)                         % plot the figure from the start to the trough of a-wave
      plot(t_s,u_s,t_s,data_m1,'-r',t_s,data_m2,'-r',t_s,data_m3,'-r',t_s,data_m4,'-b',t_s,data_m5,'-
b',t_s,data_m6,'-b');
      title('mouse ERG');
      xlabel('time(s)');
      ylabel('response(s)');
```

```
   end;
end;

%%%%%%%%%%%%%%%%%%%%%%%%%%%%%
% simulate the ERG by using the assumption parameters
%%%%%%%%%%%%%%%%%%%%%%%%%%%%%

TNum=[50 5 1 4 0.25];                    % according the true proportion to initial R, G, E, cG and GC

IniState=[0 0 0 0 0 0 TNum(4)];

%%%%%%%%%%%%%%%%%%%%%%%%%%%%%
% pulse response
%%%%%%%%%%%%%%%%%%%%%%%%%%%%%

%%%%%%%%%%%%%%%%%% 3nd 3v
% k=[1.1466 3.0324 10.7332 23.4031 7.9535 26.9701 3.8903 9.4393 1.2727 6.0401 0.9249 0.1540]; % for
LD (MSE_Ctrl=199.7567 MSE_Stress=3.7728)
% k=[5.6122 1.7471 8.8844 18.8103 2.3178 2.8186 9.3028 11.4408 0.6341 8.0004 1.5634 0.2591]; % for
LD (MSE_Ctrl=191.1859 MSE_Stress=3.9178)

% k=[15.6102 1.2491 10.0982 0.9594 9.996 22.733 0.2102 4.4278 0.9889 2.8246 1.4145 0.858]; % for
half (MSE_Ctrl=436.1915 MSE_Stress=1.0414e+003)

% k=[12.3432 1.3007 4.3712 5.5563 9.5692 22.1812 0.0864 4.4281 0.9918 2.8257 0.9537 0.3141]; % for
   regular (MSE_Ctrl=253.7762 MSE_Stress=145.1571)

%%%%%%%%%%%%%%%%%% 2nd 4v
% k=[2.3961 1.0305 4.5150 14.8441 17.6206 5.8011 9.8993 11.8405 4.0722 8.1732 1.7661 0.3861]; % for
LD (MSE_Ctrl=2.1233e+003 MSE_Stress=5.3374)

% k=[14.4791 1.2542 7.7744 1.4327 9.8489 22.3831 0.2005 4.4280 0.9899 2.8249 2.1391 1.4399]; % for
half (MSE_Ctrl=477.0287 MSE_Stress=166.1797)

% k=[13.7936 1.2581 6.1277 1.5547 9.7998 22.2476 0.0540 4.4280 0.9895 2.8247 2.1860 0.4423]; % for
regular (MSE_Ctrl=458.6649 MSE_Stress=77.0374)

%%%%%%%%%%%%%%%%%% 1nd 4v
% k=[0.2103 1.9360 10.6392 18.7975 2.2586 11.4064 8.3364 11.4374 1.1552 7.9616 2.0920 0.7399]; %
for LD (MSE_Ctrl=1.7972e+003 MSE_Stress=21.3347)

% k=[13.9828 1.2700 2.8248 5.3405 9.3643 22.6414 0.1710 4.4283 0.9920 2.8250 3.0866 1.6676]; % for
half (MSE_Ctrl=547.5439 MSE_Stress=4.8713e+003)

% k=[14.4896 1.2679 4.9433 4.0565 9.5483 22.6414 0.0508 4.4275 0.9899 2.8252 3.2000 0.5738]; % for
regular (MSE_Ctrl=364.2747 MSE_Stress=315.6097)

%%%%%%%%%%%%%%%%%%%%%%%%%%%%%
% step response for Light Damage
%%%%%%%%%%%%%%%%%%%%%%%%%%%%%

%%%%%%%%%%%%%%%%%% 3nd 3v
% k=[4.5498 1.9081 5.4999 13.9659 6.4388 5.4053 9.8374 11.7478 4.2840 8.5539 2.1232 0.3226]; % for
LD(MSE_Ctrl=1.0717e+004 MSE_Stress=56.9093)
```

```
% k=[7.2845 0.7639 11.1707 0.8126 5.5602 27.8938 14.3162 9.4395 1.3659 6.1127 2.3477 1.8321]; % for
half (MSE_Ctrl=564.8997 MSE_Stress=1.4881e+003)

% k=[6.2593 0.5496 12.8171 0.7178 3.3565 33.4908 12.5410 9.3530 0.6668 5.9552 2.3848 0.6527]; % for
regular (MSE_Ctrl=565.3747 MSE_Stress=1.2605e+003)

%%%%%%%%%%%%%%% 2nd 4v
% k=[1.689 2.157 6.3111 15.2094 2.984 6.4627 9.0743 11.7056 4.1772 8.4934 2.5897 0.9401]; % for LD
(MSE_Ctrl=2.5738e+003 MSE_Stress=3.4028)

% k=[4.6703 0.0698 10.2552 1.0230 1.8892 32.7690 20.1365 9.3989 1.1316 6.0600 3.1497 1.3820]; % for
half (MSE_Ctrl=145.2273 MSE_Stress=2.6926e+003)

% k=[4.0362 0.1258 9.6381 1.2470 2.8077 31.7324 18.7830 9.4116 1.2032 6.0732 3.0898 0.8182]; % for
regular(MSE_Ctrl=133.7882 MSE_Stress=748.658)

%%%%%%%%%%%%%%% 1nd 4v
% k=[0.2992 1.9212 9.2450 20.2615 1.0213 10.6691 8.4774 11.4411 0.5530 8.0009 2.5782 1.0183]; % for
LD (MSE_Ctrl=2.4625e+003 MSE_Stress=28.1598)

% k=[2.7766 0.7681 6.8994 4.3037 5.1879 27.5068 14.6559 9.4402 1.3728 6.1139 2.7182 1.8480]; % for
half (MSE_Ctrl=997.2897 MSE_Stress=6.7652e+003)

k=[0.2135 1.7794 11.4841 18.4111 3.3368 27.8216 13.9584 9.4498 1.3852 6.1231 2.8780 0.5984]; % for
regular (MSE_Ctrl=620.149 MSE_Stress=623.9785)

%%%%%%%%%%%%%%%%%%%%%%%%%%%%%%%%%%%%
% use the paremeters to get the simulation ERG response
% and plot it
%%%%%%%%%%%%%%%%%%%%%%%%%%%%%%%%%%%%
CtrlK=[k(1) k(2) k(3) k(4) k(5) k(6) k(7) k(8) k(9) k(10) k(11)];
StressK=[k(1) k(2) k(3) k(4) k(5) k(6) k(7) k(8) k(9) k(10) k(12)];

cG_Ctrl=Diff_solution(IniState,u_s,t_s,data_s_leng,CtrlK,dt,TNum);
cG_Stress=Diff_solution(IniState,u_s,t_s,data_s_leng,StressK,dt,TNum);

figure(3)
plot(t_s,u_s,t_s,cG_Ctrl,'-r',t_s,cG_Stress,'-b');
txt2=sprintf('simulate the mouse ERG signal \n by using the assumption parameters');
title(txt2);
xlabel('time(s)');
ylabel('response');

%%%%%%%%%%%%%%%%%%%%%%%%%%%%%%%%%%%%
% plot the simulation response and the real response
% in the same figure
%%%%%%%%%%%%%%%%%%%%%%%%%%%%%%%%%%%%

if numFile==1
   figure(4)
   plot(t_s,u_s,t_s,cG_Ctrl,'-r',t_s,cG_Stress,'-b',t_s,data_m1,'-r',t_s,data_m2,'-r',t_s,data_m3,'-
r',t_s,data_m4,'-b');
   xlabel('time(s)');
   ylabel('response');
else if numFile==2
       figure(4)
```

```
      plot(t_s,u_s,t_s,cG_Ctrl,'-r',t_s,cG_Stress,'-b',t_s,data_m1,'-r',t_s,data_m2,'-r',t_s,data_m3,'-
r',t_s,data_m4,'-b',t_s,data_m5,'-b',t_s,data_m6,'-b');
      xlabel('time(s)');
      ylabel('response');
   end;
end;

%%%%%%%%%%%%%%%%%%%%%%%%%%%%%%%%%%%%
% identify the paremeters and compare the simulation
% response with the real response
%%%%%%%%%%%%%%%%%%%%%%%%%%%%%%%%%%%%

nIdify=12;                                  % the number of identification paremeters

imse_1=1000000;                             % the limited error mean square
imse=imse_1;

if numFile==1
   [k_f,
imse_2]=simu_f12(t_s,nIdify,IniState,k,imse,u_s,data_m1,data_m2,data_m3,data_m4,data_s_leng,dt,TNu
m)
                                            % identify the paremeter set by "simu_2" function

   if imse_2>imse
      imse=1/2*(imse_1+imse_2);
      [k_f,
imse_2]=simu_f12(t_s,nIdify,IniState,k_f,imse,u_s,data_m1,data_m2,data_m3,data_m4,data_s_leng,dt,TN
um)
                                            % identify the paremeter set by "simu_2" function
   end;
else if numFile==2
      [k_f,
imse_2]=simu_f32(t_s,nIdify,IniState,k,imse,u_s,data_m1,data_m2,data_m3,data_m4,data_m5,data_m6,da
ta_s_leng,dt,TNum)
                                            % identify the paremeter set by "simu_2" function

      if imse_2>imse
         imse=1/2*(imse_1+imse_2);
         [k_f,
imse_2]=simu_f32(t_s,nIdify,IniState,k_f,imse,u_s,data_m1,data_m2,data_m3,data_m4,data_m5,data_m6,
data_s_leng,dt,TNum)
                     % identify the paremeter set by "simu_2" function
      end;
   end;
end;

CtrlK=[k_f(1) k_f(2) k_f(3) k_f(4) k_f(5) k_f(6) k_f(7) k_f(8) k_f(9) k_f(10) k_f(11)]
StressK=[k_f(1) k_f(2) k_f(3) k_f(4) k_f(5) k_f(6) k_f(7) k_f(8) k_f(9) k_f(10) k_f(12)]

cG_Ctrl=Diff_solution(IniState,u_s,t_s,data_s_leng,CtrlK,dt,TNum);
cG_Stress=Diff_solution(IniState,u_s,t_s,data_s_leng,StressK,dt,TNum);


if numFile==1
   M=zeros(length(cG_Ctrl), 7);
   M(:, 1)=t_s(:, 1);
```

```
   M(:, 2)=data_m1(:, 1);
   M(:, 3)=data_m2(:, 1);
   M(:, 4)=data_m3(:, 1);
   M(:, 5)=data_m4(:, 1);
   M(:, 6)=cG_Ctrl(:, 1);
   M(:, 7)=cG_Stress(:, 1);

   dlmwrite('ident.txt', M);

else if numFile==2
   M=zeros(length(cG_Ctrl), 9);
   M(:, 1)=t_s(:, 1);
   M(:, 2)=data_m1(:, 1);
   M(:, 3)=data_m2(:, 1);
   M(:, 4)=data_m3(:, 1);
   M(:, 5)=data_m4(:, 1);
   M(:, 6)=data_m5(:, 1);
   M(:, 7)=data_m6(:, 1);
   M(:, 8)=cG_Ctrl(:, 1);
   M(:, 9)=cG_Stress(:, 1);

   dlmwrite('ident.txt', M);
   end;
end;

SEQ_Ctrl=0;
SEQ_Stress=0;

for i=1:length(cG_Ctrl)
   SEQ_Ctrl=SEQ_Ctrl+((cG_Ctrl(i)-data_m1(i))*(cG_Ctrl(i)-data_m1(i))+(cG_Ctrl(i)-
data_m2(i))*(cG_Ctrl(i)-data_m2(i))+(cG_Ctrl(i)-data_m3(i))*(cG_Ctrl(i)-data_m3(i)));

   if numFile==1
      SEQ_Stress=SEQ_Stress+((cG_Stress(i)-data_m4(i))*(cG_Stress(i)-data_m4(i)));
      figure(5)
      plot(t_s, data_m1,'-r',t_s,data_m2,'-r',t_s,data_m3,'-r',t_s,data_m4,'-b','LineWidth',0.5);
      xlabel('time(s)');
      ylabel('response');
      hold on;
      M=zeros(length(cG_Ctrl), 7);
      for j=1:length(cG_Ctrl)
         M(j, 1)=t_s(j);
         M(j, 2)=data_m1(j);
         M(j, 3)=data_m2(j);
         M(j, 4)=data_m3(j);
         M(j, 5)=data_m4(j);
         M(j, 6)=cG_Ctrl(j);
         M(j, 7)=cG_Stress(j);
      end;
      figure(5)
      plot(t_s,cG_Ctrl,'-r',t_s, cG_Stress,'-b','LineWidth',2);
      hold off;

   else if numFile==2
         SEQ_Stress=SEQ_Stress+((cG_Stress(i)-data_m4(i))*(cG_Stress(i)-data_m4(i))+(cG_Stress(i)-
data_m5(i))*(cG_Stress(i)-data_m5(i))+(cG_Stress(i)-data_m6(i))*(cG_Stress(i)-data_m6(i)));
```

```
        figure(5)
        plot(t_s, data_m1,'-r',t_s,data_m2,'-r',t_s,data_m3,'-r',t_s,data_m4,'-b',t_s,data_m5,'-b',t_s,data_m6,'-
b','LineWidth',0.5);
        xlabel('time(s)');
        ylabel('response');
        hold on;
        M=zeros(length(cG_Ctrl), 9);
        for j=1:length(cG_Ctrl)
           M(j, 1)=t_s(j);
           M(j, 2)=data_m1(j);
           M(j, 3)=data_m2(j);
           M(j, 4)=data_m3(j);
           M(j, 5)=data_m4(j);
           M(j, 6)=data_m5(j);
           M(j, 7)=data_m6(j);
           M(j, 8)=cG_Ctrl(j);
           M(j, 9)=cG_Stress(j);
        end;
        figure(5)
        plot(t_s,cG_Ctrl,'-r',t_s, cG_Stress,'-b','LineWidth',2);
        hold off;
      end;
   end;
end;

dlmwrite('ident.txt', M);

MSE_Ctrl=SEQ_Ctrl/(data_s_leng-2)
MSE_Stress=SEQ_Stress/(data_s_leng-2)
```

2. ERG a-wave model

```
%%%%%%%%%%%%%%%%%%%%%%%%%%%%%%%%%%%%%%%%%%%%%%%%
% File name: ERG_model.m
% Author: Lei Lu
% Data: June 2006
% Function: differential equations of ERG a-wave model
%%%%%%%%%%%%%%%%%%%%%%%%%%%%%%%%%%%%%%%%%%%%%%%%

function dy = ERG_model(t, y, k, u, TNum)

% t: time;

% y(1): number of activated R(R*);
% y(2): number of activated G(G*);
% y(3): number of activated E(E*);
% y(4): number of the complex C1 that is the product of E* and cG;
% y(5): number of free guangylyl cyclase (GC);
% y(6): number of the complex C2 that is the product of free GC, GCAPs and the complex C1;
% y(7): concentration of free cG;
```

```
% k(1): activated rate of R;
% k(2): inactivated rate of R*;
% k(3): activated rate of G;
% k(4): inactivated rate of G*; it's equal to the activated rate of E;
% k(5): inactivated rate of E;
% k(6): reaction velocity of cG and E* (the result is to produce the complex C1);
% k(7): rate of the hydrolysis of the complex C1;
% k(8): reaction velocity of GC, GCAPs and the complex C1;
% k(9): rate of the synthesis of cG;
% k(10): rate of which GC converts to GC*;

% u: stimulus signal;

% TNum(1): number of total R;
% TNum(2): number of total G;
% TNum(3): number of total E;
% TNum(4): concentration of free cG in dark;
% TNum(5): number of free GC;

dy=[k(1)*u*(TNum(1)-y(1))-k(2)*y(1)*(TNum(4)-y(7))
      k(3)*y(1)*(TNum(2)-y(2))-k(4)*y(2)*y(2)*(TNum(3)-y(3))
      k(4)*(TNum(3)-y(3))*y(2)*y(2)-k(5)*y(3)-k(6)*y(3)*y(7)+k(7)*y(4)
      k(6)*y(3)*y(7)-k(7)*y(4)
     -k(8)*(TNum(4)-y(7))*y(5)+k(9)*y(6)+k(10)*(TNum(4)-y(7))*(TNum(5)-y(5))
      k(8)*y(5)*(TNum(4)-y(7))-k(9)*y(6)
     -k(6)*y(3)*y(7)+k(9)*y(6)];
```

3. Jacobian Matrix of control subjects

```
%%%%%%%%%%%%%%%%%%%%%%%%%%%%%%%%%%%%
% File name: JocabCtrlFunction.m
% Author: Lei Lu
% Data: June 2006
% Function: getting Jacobian matrix of control subjects
%%%%%%%%%%%%%%%%%%%%%%%%%%%%%%%%%%%%

function JocbCtrl=JocbCtrlFunction(IniState,u,t,t_long,k,nIdify,dt,TNum)

JocbCtrl=zeros(t_long,nIdify);

CtrlK=[k(1) k(2)  k(3) k(4) k(5) k(6) k(7) k(8) k(9) k(10) k(11)];

OriginalValue=Diff_solution(IniState,u,t,t_long,CtrlK,dt,TNum);

dstep=0.01;

for i=1:11
   kCurrent=CtrlK;
   kCurrent(i)=kCurrent(i)+dstep;
   CurrentValue=Diff_solution(IniState,u,t,t_long,kCurrent,dt,TNum);
   JocbCtrl(:,i)=(CurrentValue-OriginalValue)/dstep;
End
```

4. Jacobian Matrix of stress subjects

```
%%%%%%%%%%%%%%%%%%%%%%%%%%%%%%%%%%%%
% File name: JocabStressFunction.m
% Author: Lei Lu
% Data: June 2006
% Function: getting Jacobian matrix of stress subjects
%%%%%%%%%%%%%%%%%%%%%%%%%%%%%%%%%%%%

function JocbStress=JocbbStressFunction(IniState,u,t,t_long,k,nIdify,dt,TNum)

JocbStress=zeros(t_long, nIdify);

OriginalValue=Diff_solution(IniState,u,t,t_long,k,dt,TNum);

dstep=0.01;

for i=1:11
   kCurrent=k;
   kCurrent(i)=kCurrent(i)+dstep;
   CurrentValue=Diff_solution(IniState,u,t,t_long,kCurrent,dt,TNum);
   if(i==11)
      JocbStress(:,12)=(CurrentValue-OriginalValue)/dstep;
   else
      JocbStress(:,i)=(CurrentValue-OriginalValue)/dstep;
   end
end
```

5. Solution of the model

```
%%%%%%%%%%%%%%%%%%%%%%%%%%%%%%%%%%%%
% File name: Diff_Matr.m
% Author: Lei Lu
% Data: June 2006
% Function: solving the model and storing the results
%%%%%%%%%%%%%%%%%%%%%%%%%%%%%%%%%%%%

function Diff_Matr(IniState, u, t, t_long, k, filename, dt, TNum)

fid=fopen(filename, 'w');
fprintf(fid,'%6.7f %6.7f %6.7f  %6.7f  %6.7f %6.7f %6.7f %6.7f  %6.7f\n', t(1), u(1), IniState(1), IniState(2),
IniState(3), IniState(4), IniState(5), IniState(6), IniState(7));

for j=1:(t_long-1)
   t1=j*dt;
   t2=(j+1)*dt;
   input=u(j);
   ka=[k(1) k(2) k(3) k(4) k(5) k(6) k(7) k(8) k(9) k(10)];
   [T, C]=ode15s(@ERG_model, [t1 t2], IniState, [], ka, input, TNum);
   [row_C column_C]=size(C);

   IniState=[C(row_C, 1)
          C(row_C, 2)
          C(row_C, 3)
```

```
            C(row_C, 4)
            C(row_C, 5)
            C(row_C, 6)
            C(row_C, 7)];
    T1=T(row_C, 1);
    fprintf(fid,'%6.7f %6.7f  %6.7f  %6.7f  %6.7f %6.7f %6.7f %6.7f %6.7f\n', T1, input, IniState(1), IniState(2),
IniState(3), IniState(4), IniState(5), IniState(6), IniState(7));

end;

fclose(fid);
```

6. Getting cG

```
%%%%%%%%%%%%%%%%%%%%%%%%%%%%%%%%%%%%
% File name: Diff_Matr.m
% Author: Lei Lu
% Data: June 2006
% Function: getting value of cG
%%%%%%%%%%%%%%%%%%%%%%%%%%%%%%%%%%%%

function Diff_solution=Diff_solution(IniState,u,t,t_long,k,dt,TNum)

Diff_Matr(IniState,u,t,t_long,k,'temp.tex',dt,TNum);

data=load('temp.tex');

[row, column]=size(data);

Diff_solution=zeros(row, 1);

for i=1:row

    Diff_solution(i)=k(11)*data(i,9)*data(i,9)*data(i,9)-k(11)*TNum(4)*TNum(4)*TNum(4);

end;
```

7. Identifying the Parameters

```
%%%%%%%%%%%%%%%%%%%%%%%%%%%%%%%%%%%%
% File name: simu_f12.m
% Author: Lei Lu
% Data: June 2006
% Function: indentifying the parameters when there is
%                only one stress subject.
%%%%%%%%%%%%%%%%%%%%%%%%%%%%%%%%%%%%

function [k_matr, imse]=simu_f(t,nIdify,IniState,k,Error_limit,u,f1,f2,f3,f4,t_long,dt,TNum)

CtrlK=[k(1),k(2),k(3),k(4),k(5),k(6),k(7),k(8),k(9),k(10),k(11)];
```

```
StressK=[k(1),k(2),k(3),k(4),k(5),k(6),k(7),k(8),k(9),k(10),k(12)];

ErrorMat_Ctrl1=zeros(t_long, 1);
ErrorMat_Ctrl2=zeros(t_long, 1);
ErrorMat_Ctrl3=zeros(t_long, 1);
ErrorMat_Stress=zeros(t_long, 1);

%%%%%%%%%%%%%%%%%%%%%%%%%%%%%%%%%%%%
% calculate the Jacobian Matrix
%%%%%%%%%%%%%%%%%%%%%%%%%%%%%%%%%%%%

cG_Ctrl=Diff_solution(IniState,u,t,t_long,CtrlK,dt,TNum);
cG_Stress=Diff_solution(IniState,u,t,t_long,StressK,dt,TNum);


ErrorMat_1=f1-cG_Ctrl;
ErrorMat_2=f2-cG_Ctrl;
ErrorMat_3=f3-cG_Ctrl;
ErrorMat_4=f4-cG_Stress;

Energy=(ErrorMat_1'*ErrorMat_1+ErrorMat_2'*ErrorMat_2+ErrorMat_3'*ErrorMat_3+ErrorMat_4'*Erro
rMat_4)/(t_long-2);

E_E0=Energy;

E_init=100000;
E_E1=E_init;
E_E2=E_init;
E_E3=E_init;

lamda=1000;

bContinue=1;

fid=fopen('temp.txt', 'w');
fprintf(fid,'%6.7f %6.7f %6.7f %6.7f %6.7f %6.7f %6.7f %6.7f %6.7f %6.7f %6.7f
%6.7f\n',Energy,k(1),k(2),k(3),k(4),k(5),k(6),k(7),k(8),k(9),k(10),k(11),k(12));

while ( Energy>Error_limit & bContinue>0)
   CtrlK=[k(1),k(2),k(3),k(4),k(5),k(6),k(7),k(8),k(9),k(10),k(11)];
   StressK=[k(1),k(2),k(3),k(4),k(5),k(6),k(7),k(8),k(9),k(10),k(12)];

   JocbCtrl=JocbCtrlFunction(IniState,u,t,t_long,CtrlK,nIdify,dt,TNum);
   JocbStress=JocbStressFunction2(IniState,u,t,t_long,StressK,nIdify,dt,TNum);

   delta_k=(lamda*eye(nIdify)+3*JocbCtrl'*JocbCtrl+JocbStress'*JocbStress)^(-
1)*(JocbCtrl'*ErrorMat_1+JocbCtrl'*ErrorMat_2+JocbCtrl'*ErrorMat_3+JocbStress'*ErrorMat_4);

   k_k0=k;
   delta_k=0.5*delta_k;
   k=k+delta_k';

   CtrlK=[k(1),k(2),k(3),k(4),k(5),k(6),k(7),k(8),k(9),k(10),k(11)];
   StressK=[k(1),k(2),k(3),k(4),k(5),k(6),k(7),k(8),k(9),k(10),k(12)];
```

```
   if (k(1)<0 | k(2)<0 | k(3)<0 | k(4)<0 | k(5)<0 | k(6)<0 | k(7)<0 | k(8)<0 | k(9)<0 | k(10)<0 | k(11)<0 |
k(12)<0)
      k=k_k0;
      Energy=E_E0;
      bContinue=0;
   end;

   cG_Ctrl=Diff_solution(IniState,u,t,t_long,CtrlK,dt,TNum);
   cG_Stress=Diff_solution(IniState,u,t,t_long,StressK,dt,TNum);

   ErrorMat_1=f1-cG_Ctrl;
   ErrorMat_2=f2-cG_Ctrl;
   ErrorMat_3=f3-cG_Ctrl;
   ErrorMat_4=f4-cG_Stress;


Energy=(ErrorMat_1'*ErrorMat_1+ErrorMat_2'*ErrorMat_2+ErrorMat_3'*ErrorMat_3+ErrorMat_4'*Erro
rMat_4)/(t_long-2)

   fprintf(fid,'%6.7f %6.7f %6.7f %6.7f %6.7f %6.7f %6.7f %6.7f %6.7f %6.7f %6.7f %6.7f
%6.7f\n',Energy,k(1),k(2),k(3),k(4),k(5),k(6),k(7),k(8),k(9),k(10),k(11),k(12));

   if Energy<E_E0
      lamda=lamda/4;
   else
      lamda=lamda*2;
      k=k_k0;
   end;

   E_E3=E_E2;
   E_E2=E_E1;
   E_E1=E_E0;
   E_E0=Energy;

   if (E_E0>E_E1)&(E_E1>E_E2)&(E_E2>E_E3)
       bContinue=0;
   end;

end;

fclose(fid);

data=load('temp.txt');

[row, column]=size(data);

if row>1
   data_Eng=zeros((row-1), 1);
   for i=1:(row-1)
      data_Eng(i)=data((i+1), 1);
   end;

   Eng_min=min(data_Eng);

   k_matr=zeros(1, nIdify);
   p=0;
```

```
    for j=1:(row-1)
        if data_Eng(j, 1)==Eng_min
            p=j+1;
        end;
    end;

    k_matr=[data(p,2) data(p,3) data(p,4) data(p,5) data(p,6) data(p,7) data(p,8) data(p,9) data(p,10)
data(p,11) data(p,12) data(p,13)];
    imse=data(p, 1);
else
    k_matr=[data(1,2) data(1,3) data(1,4) data(1,5) data(1,6) data(1,7) data(1,8) data(1,9) data(1,10)
data(1,11) data(1,12) data(1,13)];
    imse=data(1,1);
end;


%%%%%%%%%%%%%%%%%%%%%%%%%%%%%
% File name: simu_f32.m
% Author: Lei Lu
% Data: June 2006
% Function: identifying the parameters when there are
%               three stress subjects
%%%%%%%%%%%%%%%%%%%%%%%%%%%%%

function [k_matr, imse]=simu_f(t,nIdify,IniState,k,Error_limit,u,f1,f2,f3,f4,f5,f6,t_long,dt,TNum)

CtrlK=[k(1),k(2),k(3),k(4),k(5),k(6),k(7),k(8),k(9),k(10),k(11)];
StressK=[k(1),k(2),k(3),k(4),k(5),k(6),k(7),k(8),k(9),k(10),k(12)];

ErrorMat_Ctrl1=zeros(t_long, 1);
ErrorMat_Ctrl2=zeros(t_long, 1);
ErrorMat_Ctrl3=zeros(t_long, 1);
ErrorMat_Stress1=zeros(t_long, 1);
ErrorMat_Stress2=zeros(t_long, 1);
ErrorMat_Stress3=zeros(t_long, 1);

%%%%%%%%%%%%%%%%%%%%%%%%%%%%%
% calculate the Jacobian Matrix
%%%%%%%%%%%%%%%%%%%%%%%%%%%%%

cG_Ctrl=Diff_solution(IniState,u,t,t_long,CtrlK,dt,TNum);
cG_Stress=Diff_solution(IniState,u,t,t_long,StressK,dt,TNum);

ErrorMat_1=f1-cG_Ctrl;
ErrorMat_2=f2-cG_Ctrl;
ErrorMat_3=f3-cG_Ctrl;
ErrorMat_4=f4-cG_Stress;
ErrorMat_5=f5-cG_Stress;
ErrorMat_6=f6-cG_Stress;

Energy=(ErrorMat_1'*ErrorMat_1+ErrorMat_2'*ErrorMat_2+ErrorMat_3'*ErrorMat_3+ErrorMat_4'*ErrorMat_4+Err
orMat_5'*ErrorMat_5+ErrorMat_6'*ErrorMat_6)/(t_long-2);

E_E0=Energy;

E_init=100000;
E_E1=E_init;
E_E2=E_init;
E_E3=E_init;
```

```
lamda=1000;

bContinue=1;

fid=fopen('temp.txt', 'w');
fprintf(fid,'%6.7f %6.7f %6.7f %6.7f %6.7f %6.7f %6.7f %6.7f %6.7f %6.7f %6.7f %6.7f
%6.7f\n',Energy,k(1),k(2),k(3),k(4),k(5),k(6),k(7),k(8),k(9),k(10),k(11),k(12));

while ( Energy>Error_limit & bContinue>0)
   CtrlK=[k(1),k(2),k(3),k(4),k(5),k(6),k(7),k(8),k(9),k(10),k(11)];
   StressK=[k(1),k(2),k(3),k(4),k(5),k(6),k(7),k(8),k(9),k(10),k(12)];

   JacobMat_Ctrl=JocbCtrlFunction(IniState,u,t,t_long,CtrlK,nIdify,dt,TNum);
   JacobMat_Stress=JocbStressFunction2(IniState,u,t,t_long,StressK,nIdify,dt,TNum);
   delta_k=(lamda*eye(nIdify)+3*JacobMat_Ctrl'*JacobMat_Ctrl+3*JacobMat_Stress'*JacobMat_Stress)^(-
1)*(JacobMat_Ctrl'*ErrorMat_1+JacobMat_Ctrl'*ErrorMat_2+JacobMat_Ctrl'*ErrorMat_3+JacobMat_Stress'*ErrorM
at_4+JacobMat_Stress'*ErrorMat_5+JacobMat_Stress'*ErrorMat_6);

   k_k0=k;

   disp('**************************')
   delta_k=0.5*delta_k;

   k=k+delta_k';

   CtrlK=[k(1),k(2),k(3),k(4),k(5),k(6),k(7),k(8),k(9),k(10),k(11)];
   StressK=[k(1),k(2),k(3),k(4),k(5),k(6),k(7),k(8),k(9),k(10),k(12)];


   if (k(1)<0 | k(2)<0 | k(3)<0 | k(4)<0 | k(5)<0 | k(6)<0 | k(7)<0 | k(8)<0 | k(9)<0 | k(10)<0 | k(11)<0 | k(12)<0)
      k=k_k0;
      Energy=E_E0;
      bContinue=0;
   end;

   cG_Ctrl=Diff_solution(IniState,u,t,t_long,CtrlK,dt,TNum);
   cG_Stress=Diff_solution(IniState,u,t,t_long,StressK,dt,TNum);

   ErrorMat_1=f1-cG_Ctrl;
   ErrorMat_2=f2-cG_Ctrl;
   ErrorMat_3=f3-cG_Ctrl;
   ErrorMat_4=f4-cG_Stress;
   ErrorMat_5=f5-cG_Stress;
            ErrorMat_6=f6-cG_Stress;


Energy=(ErrorMat_1'*ErrorMat_1+ErrorMat_2'*ErrorMat_2+ErrorMat_3'*ErrorMat_3+ErrorMat_4'*ErrorMat_4+Err
orMat_5'*ErrorMat_5+ErrorMat_6'*ErrorMat_6)/(t_long-2)

   fprintf(fid,'%6.7f %6.7f %6.7f %6.7f %6.7f %6.7f %6.7f %6.7f %6.7f %6.7f %6.7f %6.7f
%6.7f\n',Energy,k(1),k(2),k(3),k(4),k(5),k(6),k(7),k(8),k(9),k(10),k(11),k(12));

   if Energy<E_E0
      lamda=lamda/4;
   else
      lamda=lamda*2;
      k=k_k0;
   end;

   E_E3=E_E2;
   E_E2=E_E1;
   E_E1=E_E0;
```

```
    E_E0=Energy;

    if (E_E0>E_E1)&(E_E1>E_E2)&(E_E2>E_E3)
        bContinue=0;
    end;

end;

fclose(fid);

data=load('temp.txt');

[row, column]=size(data);

if row>1
    data_Eng=zeros((row-1), 1);
    for i=1:(row-1)
        data_Eng(i)=data((i+1), 1);
    end;

    Eng_min=min(data_Eng);

    k_matr=zeros(1, nIdify);
    p=0;
    for j=1:(row-1)
        if data_Eng(j, 1)==Eng_min
            p=j+1;
        end;
    end;

    k_matr=[data(p,2) data(p,3) data(p,4) data(p,5) data(p,6) data(p,7) data(p,8) data(p,9) data(p,10) data(p,11) data(p,12)
data(p,13)];
    imse=data(p, 1);
else
    k_matr=[data(1,2) data(1,3) data(1,4) data(1,5) data(1,6) data(1,7) data(1,8) data(1,9) data(1,10) data(1,11) data(1,12)
data(1,13)];
    imse=data(1,1);
end;
```

APPENDIX B. Figures of Experimental and Estimated Data

1. Simulations of wild-type mice

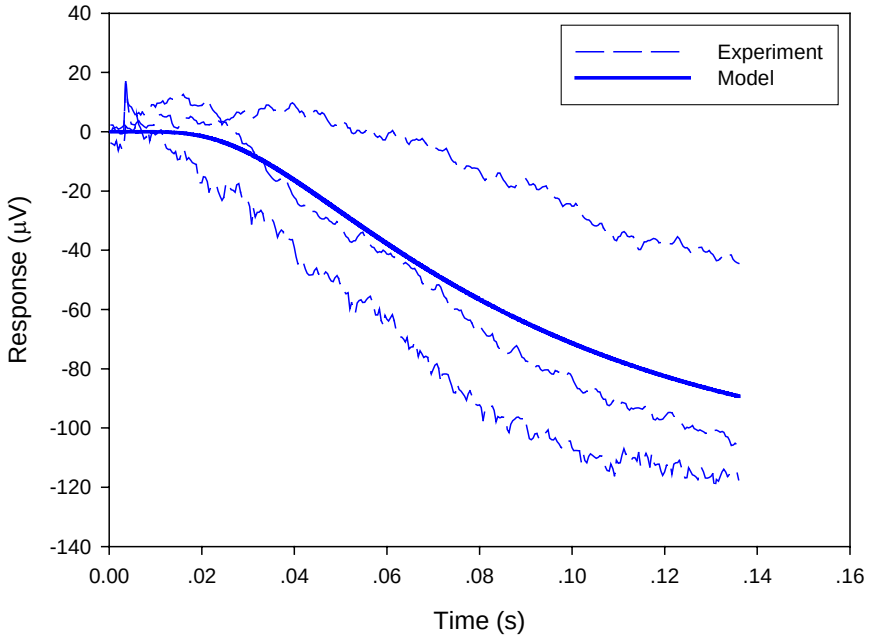

Fig. B1. Subjects: wild-type after APB. Stimulus: pulse. Light Intensity (Log): 12.997 photons cm^{-2} s^{-1}.

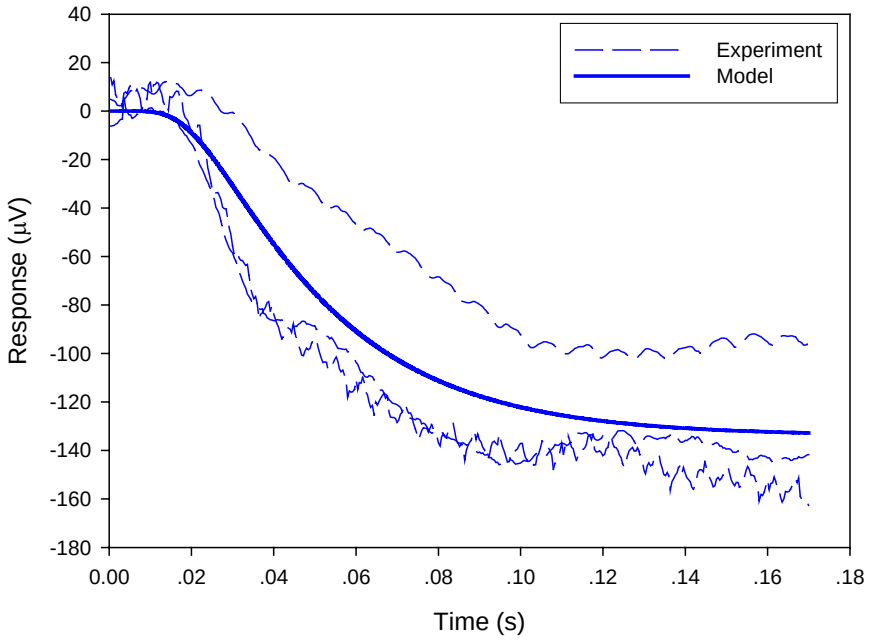

Fig. B2. Subjects: wild-type after APB. Stimulus: pulse. Light Intensity (Log): 13.891 photons cm^{-2} s^{-1}.

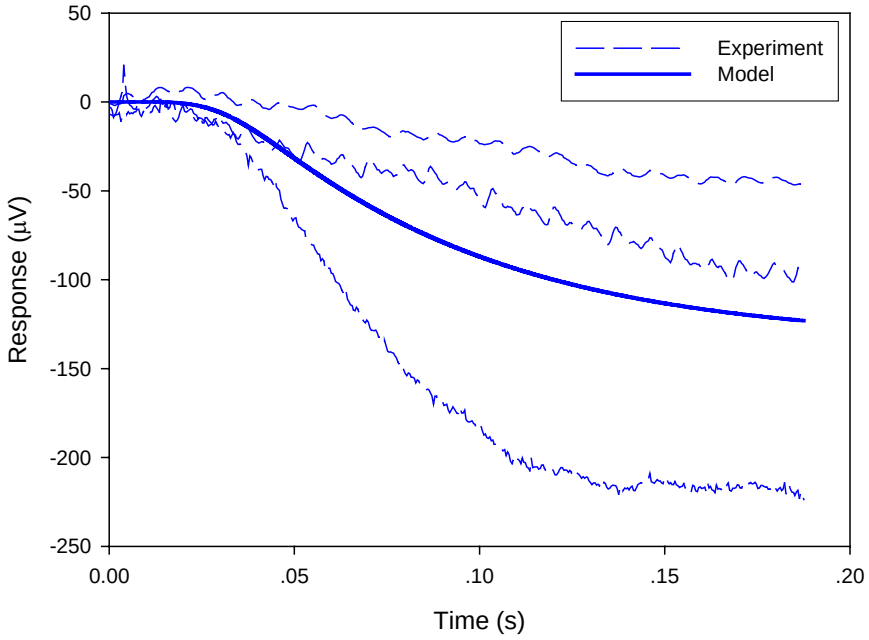

Fig. B3. Subjects: wild-type after APB. Stimulus: step. Light Intensity (Log): 12.407 photons cm^{-2} s^{-1}.

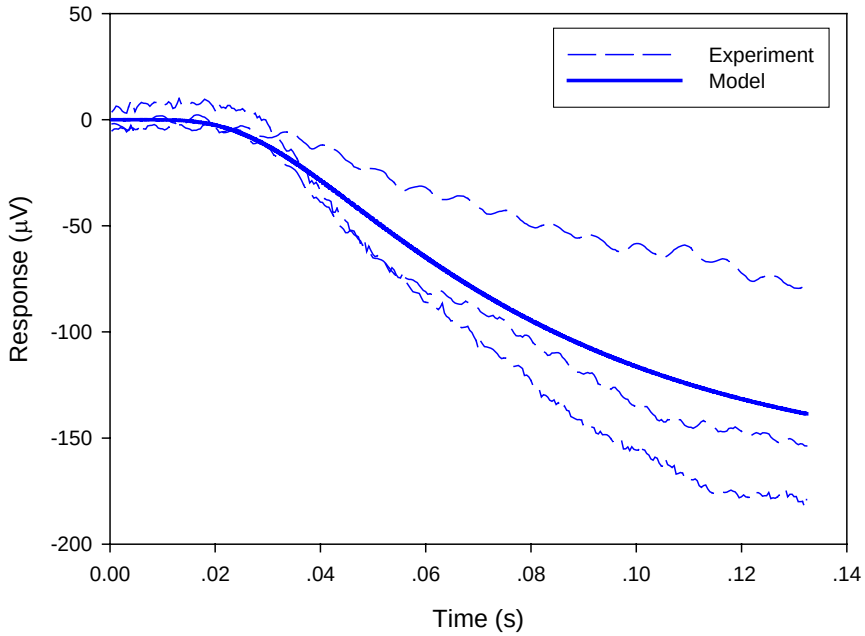

Fig. B4. Subjects: wild-type after APB. Stimulus: step. Light Intensity (Log): 12.997 photons cm^{-2} s^{-1}.

2. Simulations of wild-type and light-damaged mice

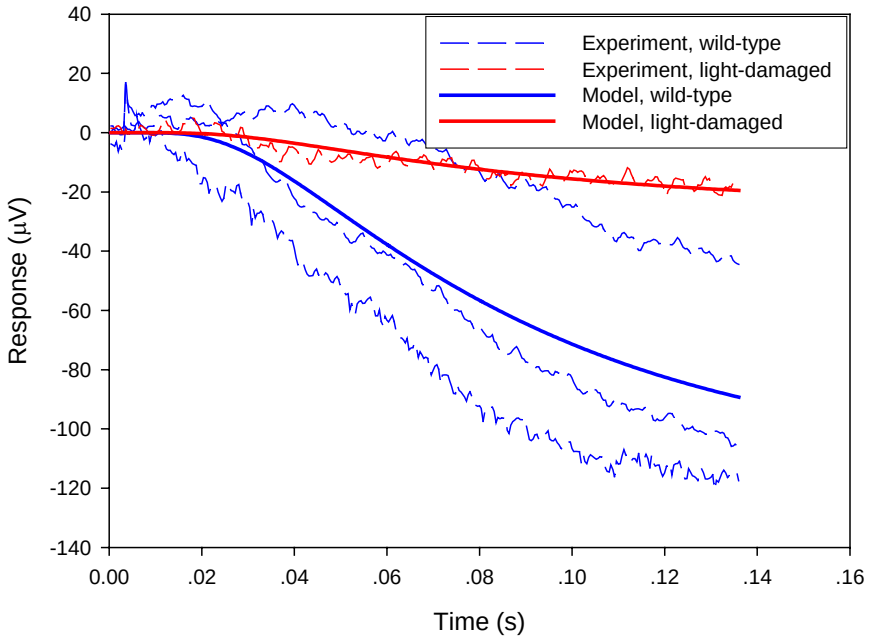

Fig. B5. Subjects: wild-type after APB and light-damaged wild-type after APB. Stimulus: pulse. Light Intensity (Log): 12.997 photons cm^{-2} s^{-1}.

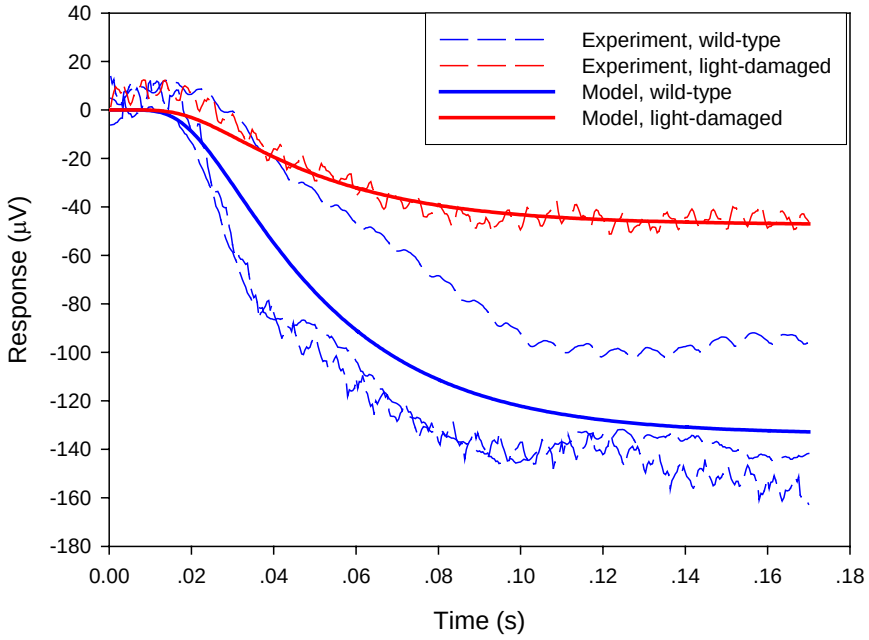

Fig. B6. Subjects: wild-type after APB and light-damaged wild-type after APB. Stimulus: pulse. Light Intensity (Log): 13.891 photons cm^{-2} s^{-1}.

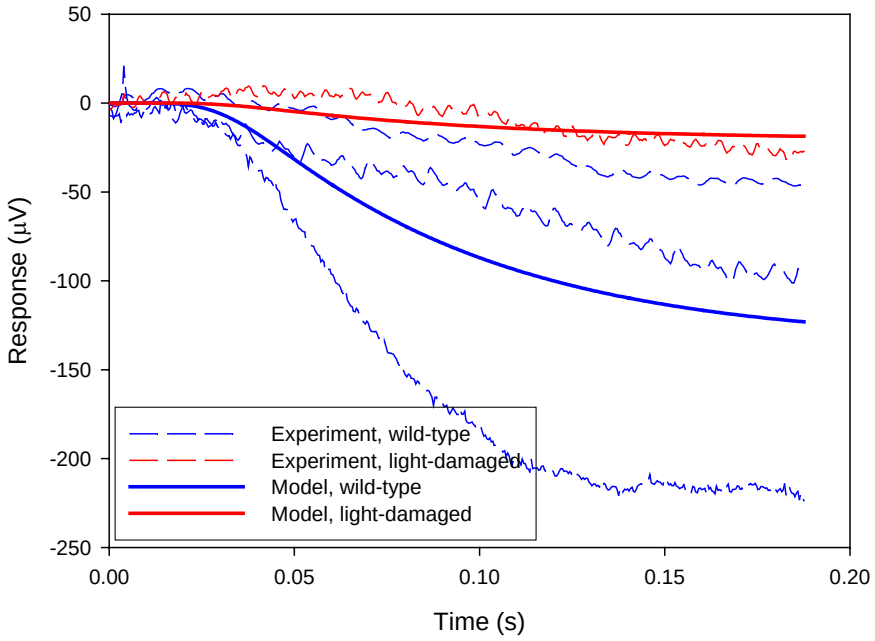

Fig. B7. Subjects: wild-type after APB and light-damaged wild-type after APB. Stimulus: step. Light Intensity (Log): 12.407 photons cm^{-2} s^{-1}.

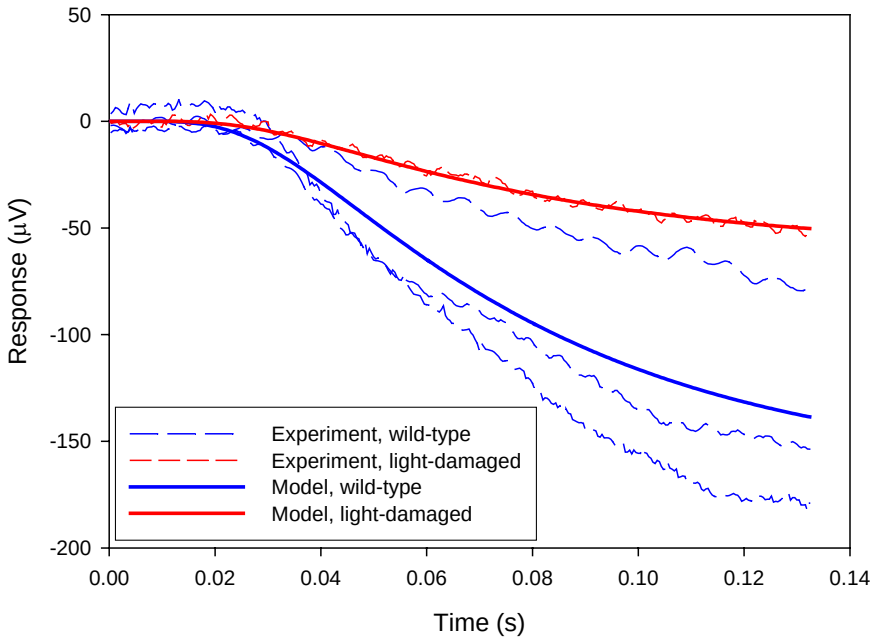

Fig. B8. Subjects: wild-type after APB and light-damaged wild-type after APB. Stimulus: step. Light Intensity (Log): 12.997 photons cm^{-2} s^{-1}.

3. Simulations of NOB1 and drug-damaged mice

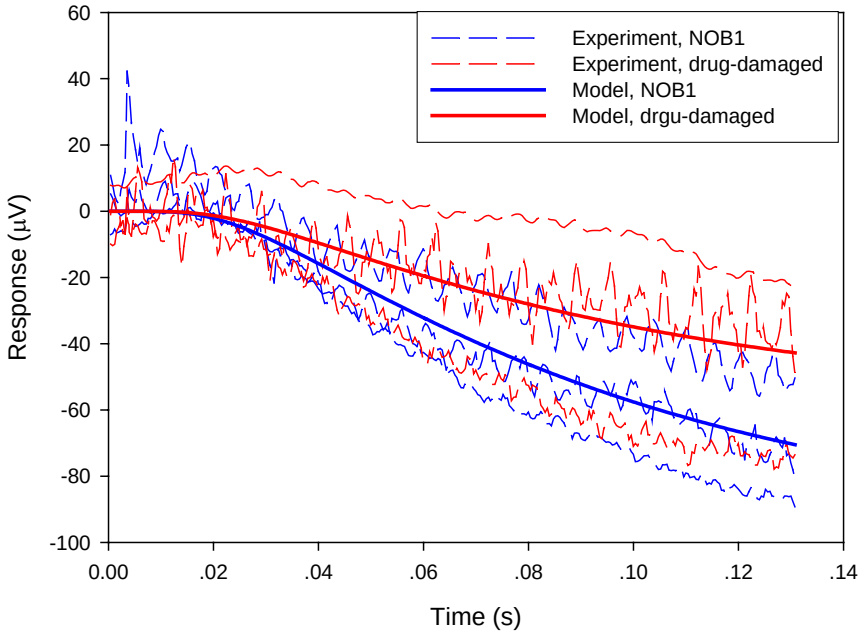

Fig. B9. Subjects: NOB1 and drug-damaged. Drug dose: 30 mg/kg body weight. Stimulus: pulse. Light Intensity (Log): 12.407 photons cm^{-2} s^{-1}.

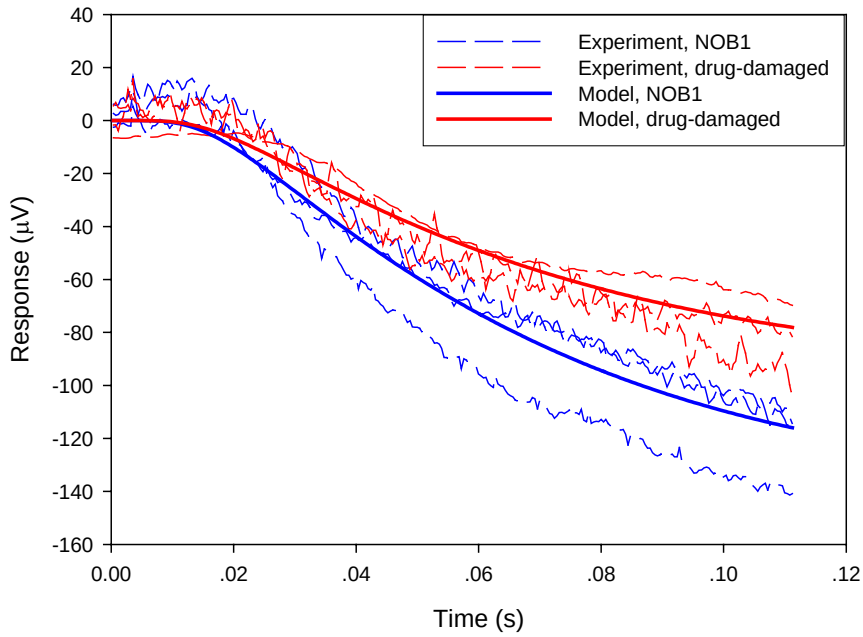

Fig. B10. Subjects: NOB1 and drug-damaged. Drug dose: 30 mg/kg body weight. Stimulus: pulse. Light Intensity (Log): 12.997 photons cm^{-2} s^{-1}.

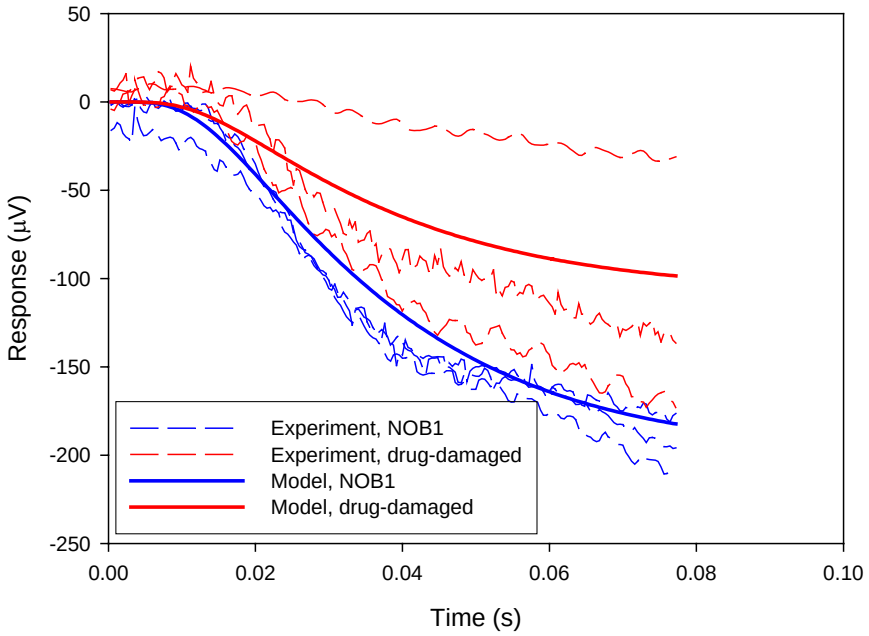

Fig. B11. Subjects: NOB1 and drug-damaged. Drug dose: 30 mg/kg body weight. Stimulus: pulse. Light Intensity (Log): 13.891 photons cm^{-2} s^{-1}.

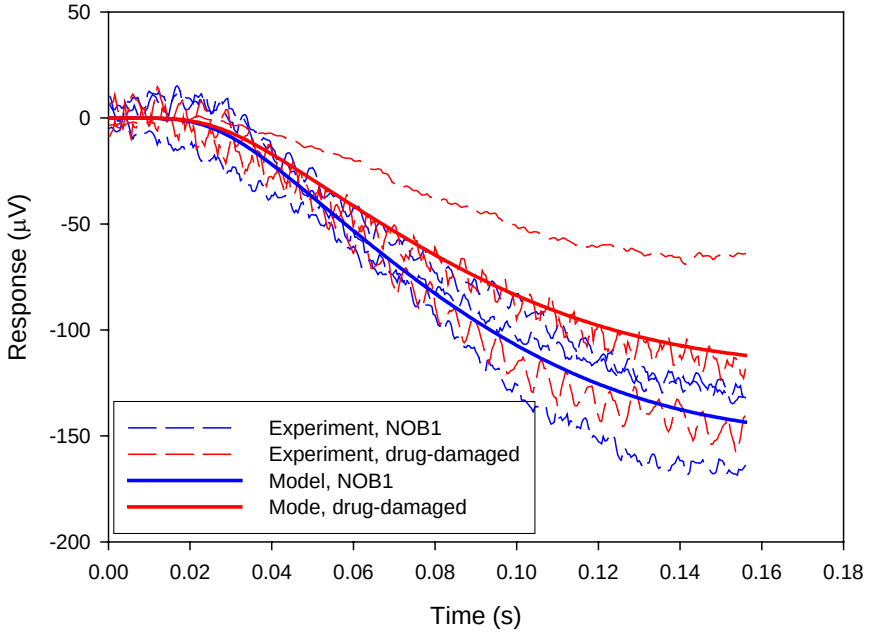

Fig. B12. Subjects: NOB1 and drug-damaged. Drug dose: 30 mg/kg body weight. Stimulus: step. Light Intensity (Log): 12.407 photons cm^{-2} s^{-1}.

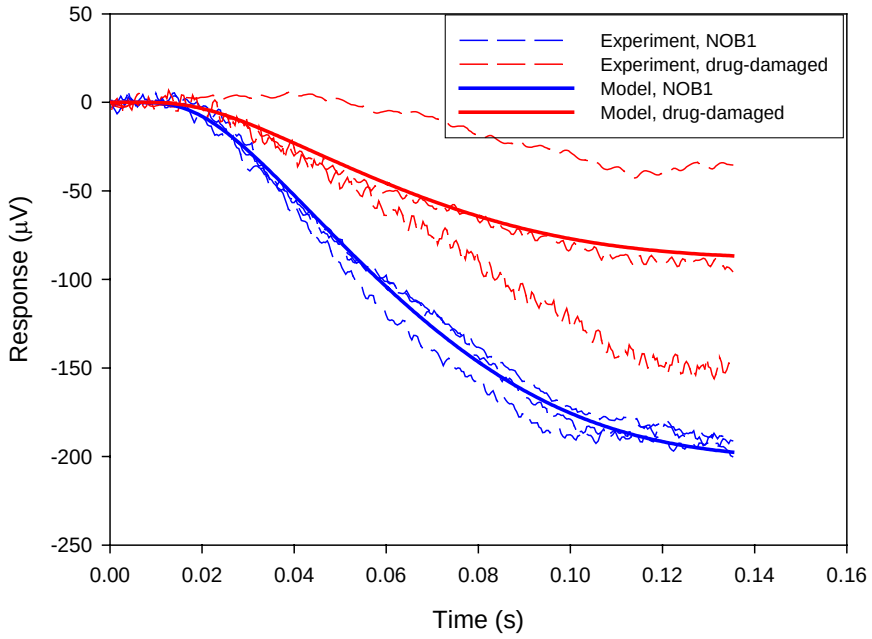

Fig. B13. Subjects: NOB1 and drug-damaged. Drug dose: 60 mg/kg body weight. Stimulus: step. Light Intensity (Log): 12.997 photons cm^{-2} s^{-1}.

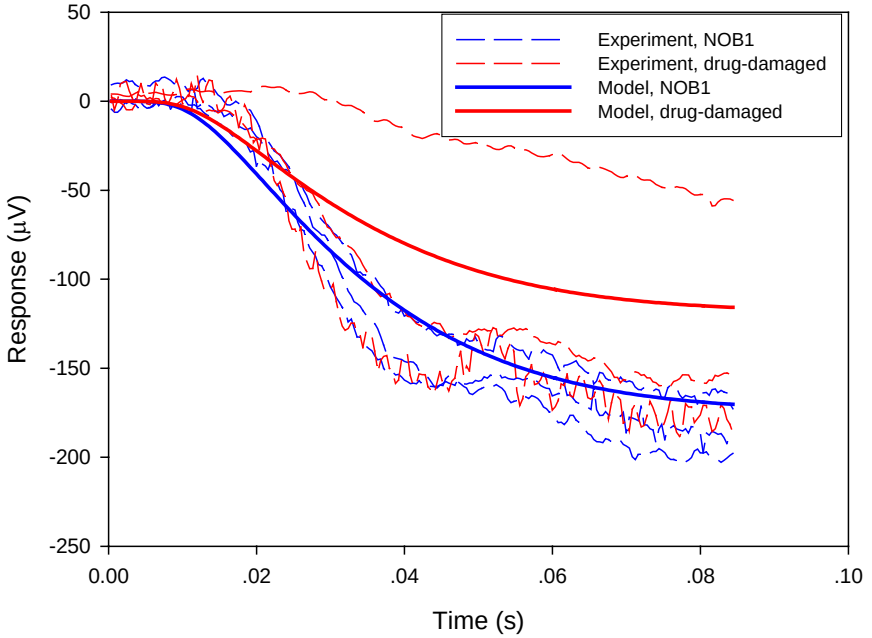

Fig. B14. Subjects: NOB1 and drug-damaged. Drug dose: 30 mg/kg body weight. Stimulus: step. Light Intensity (Log): 13.891 photons cm^{-2} s^{-1}.

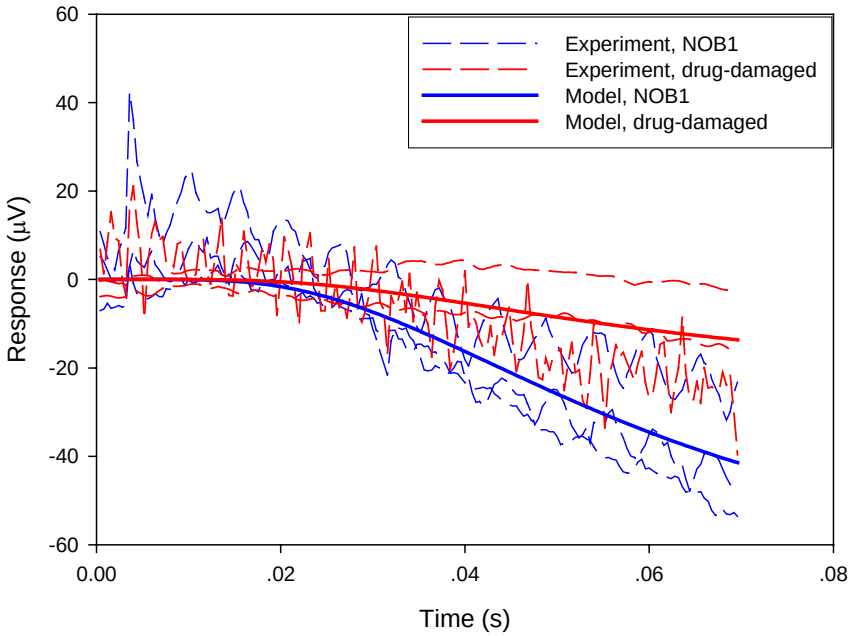

Fig. B15. Subjects: NOB1 and drug-damaged. Drug dose: 60 mg/kg body weight. Stimulus: pulse. Light Intensity (Log): 12.407 photons cm^{-2} s^{-1}.

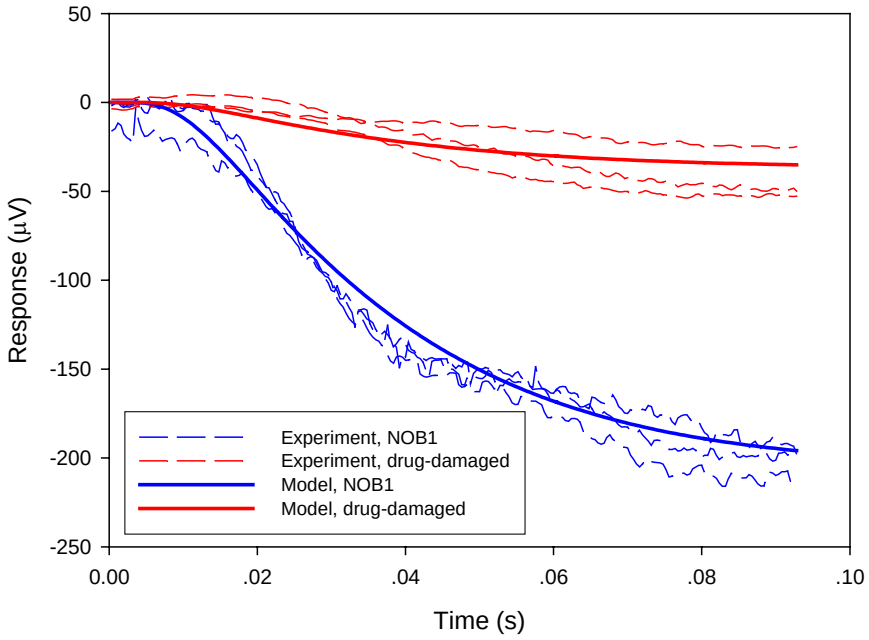

Fig. B16. Subjects: NOB1 and drug-damaged. Drug dose: 60 mg/kg body weight. Stimulus: pulse. Light Intensity (Log): 13.891 photons cm^{-2} s^{-1}.

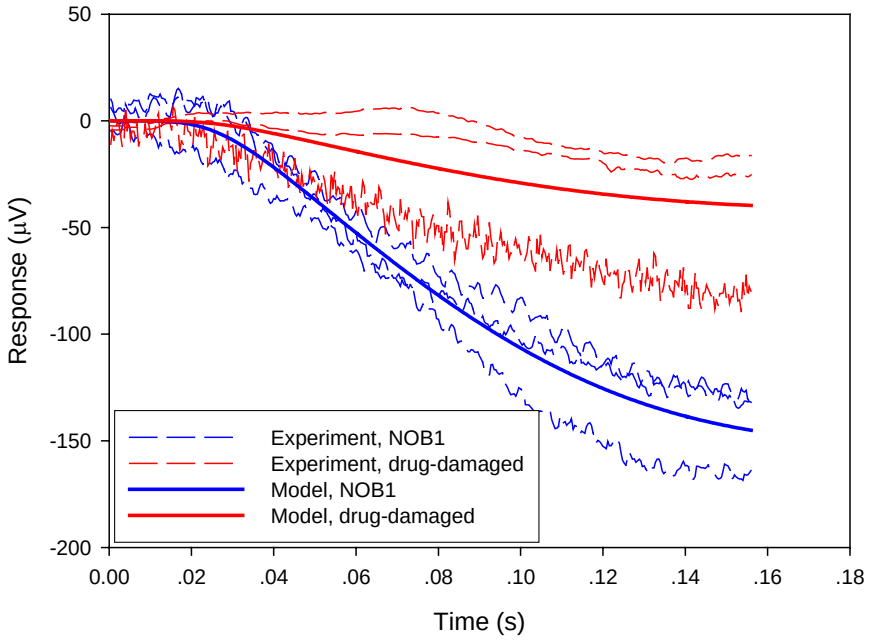

Fig. B17. Subjects: NOB1 and drug-damaged. Drug dose: 60 mg/kg body weight. Stimulus: step. Light Intensity (Log): 12.407 photons cm^{-2} s^{-1}.

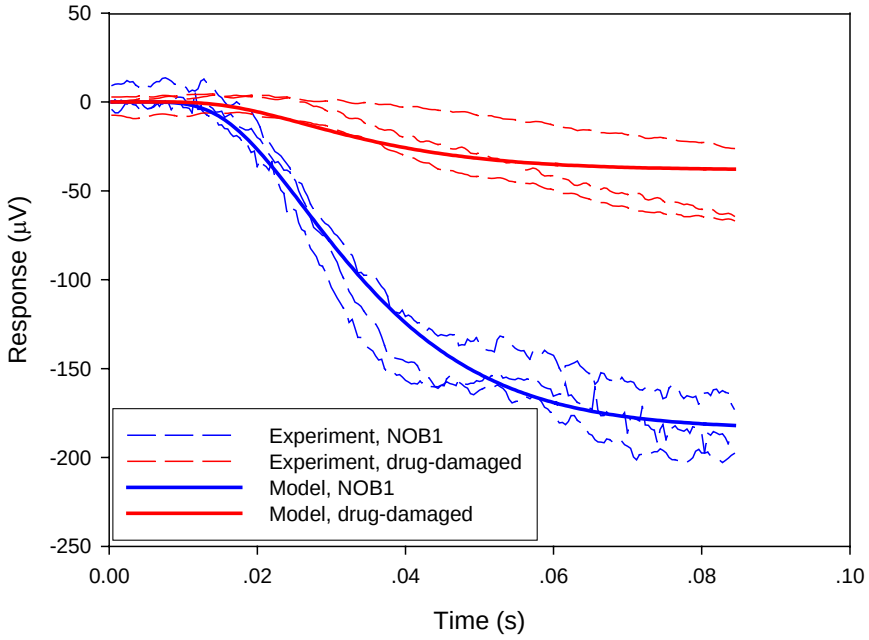

Fig. B18. Subjects: NOB1 and drug-damaged. Drug dose: 60 mg/kg body weight. Stimulus: step. Light Intensity (Log): 13.891 photons cm^{-2} s^{-1}.

BIBLIOGRAPHY

Armington, J.C. 1974. *The Electroretinogram*. Academic Press, New York.

Artemyev, N.O., R. Surendran, J. C. Lee & H. E. Hamm. 1996. Subunit Structure of Rod cGMP-phosphodiesterase. *Journal of Biological Chemistry,* **271**, 25382-25388.

Beavo, J.A. 1995. Cyclic Nucleotide Phosphodiesterases: Functional Implications of Multiple Isoforms. *Physiological Reviews*, **75**, 725-748.

Berson, E.L. 1975. Electrical Phenomena in the Retina. *Adler's Physiology of the Eye*, ed. Moses, R.A., pp.453-499. New York: C.V. Mosby Co.

Birch, D.G. 1989. Clinical Electroretinography. *Ophthalmology Clinics of North America*, ed. Stampfer, R.L., pp.469-498. New York: W.B. Saunders Co.

Bornancin, F., C. Pfister & M. Chabre. 1989. The Transitory Complex between Photoexcited Rhodopsin and Transducin. Reciprocal Interaction between the Retinal Site in Rhodopsin and the Nucleotide Site in Transducin. *European Journal of Biochemistry*, **184**, 687-698.

Brown, K.T. 1968. The Electroretinogram: its Components and their Origin. *Vision Research*, **8**, 633-677.

Brown, K.T. & M. Murakami. 1964. A new receptor Potential of the Monkey Retina with no Detectable Latency. *Nature*, **204**, 739-740.

Brown, K.T. & T.N. Wiesel. 1961a. Analysis of the Intraretinal Electroretinogram in the Intact Cat Eye. *Journal of Physiology (London)***, 158**, 229-256.

Brown, K.T. & T.N. Wiesel. 1961b. Localization of Origins of Electroretinogram Components by Intraretinal Recording in the Intact Cat Eye. *Journal of Physiology (London)*, **158**, 257-280.

Cajal, S.R. 1972. *The Structure of the Retina*. Thomas, Springfield I1.

Constantinides A. & N. Mostoufi. 2000. Numerical Methods for Chemical Engineers with Matlab Applications. *Prentice Hall PTR Upper Saddle River*, New Jersey.

de Rouck, A.F. 1991. History of the electroretinogram. *Principle and Practice of Clinical Electrophysiology of Vision,* ed. Heckendivel J.R. & G.B. Arden., pp 5-13. Mosby, Year Book., St. Louis.

Dewar J. & J. G. Mckendrick. 1873. On the Physiological Action of Light. *Trans R Soc Edinb*, **27**, 141-166.

Einthoven, W. & W.A. Jolly. 1908. The Form and Magnitude of the Electrical Response of the Eye to Stimulation by Light at Various Intensities. *Quaterly Journal of Experimental Physiology*, **1**, 373-416.

Enoch, J.M. & F.L. Tobey. 1981. *Vertebrate Photoreceptor Optics.* Springer, Berlin.

Fesenko, E.E., S.S. Kolesnikov & A.L. Lyubarsky. 1985. Induction by Cyclic GMP of Cationic Conductance in Plasma Membrane of Retinal Rod Outer Segment. *Nature*, **313,** 310-313.

Gorczyca, W.A., M.P. Gray-Kelly, P.B. Detwiler & K. Palczewski. 1994. Purification and Physiological Evaluation of a Guanylate-cyclase Activating Protein from Retinal Rods. *Proceedings of the National Academy of Sciences of the United States of America,* **91**, 4014-4018.

Gorczyca, W.A., A.S. Polans, I.G. Surgucheva, I. Subbaraya, W. Baehr & K. Palczewski. 1995. *Journal of Biological Chemistry*, **270**, 22029-22036.

Gotch, F. 1903. The Time Relations of the Photoelectric Changes on the Eyeball of the Frog. *J. Physiology (London)*, **29**, 388-416.

Gouras, P. 1970. Electroretinography: Some Basic Principles. *Invest Ophthalol,* **9**, 557-569.

Granit, R. 1933. The Components of the Retinal Action Potential in Mammals and their Relation to the Discharge in the Optic Nerve. *J. Physiology (London)*, **77,** 207-239.

Granit, R. 1947. *Sensory Mechanisms of the Retina*. London. Oxford University Press, London.

Granit, R. 1991. *Principles and Practice of Clinical Electrophysiology of vision: Introduction: A Personal Memoir*. Mosby Year Book. St. Louis.

Hamm, H.E. 1998. The Many Faces of G Protein Signaling. *Journal of Biological Chemistry* **273**, 669-672.

He, W., C.W. Cowan & T.G. Wensel. 1998. RGS9, a GTPase Accelerator for Phototransduction. *Neuron*, **20**, 95-102.

Hofmann, K.-P. 1986. Photoproducts of Rhodopsin in the Disc Membrane. *Photobiochemistry and Photobiophysics*, **13**, 309-327.

Hofmann, K.-P. 2000. Late Photoproducts and Signaling States of Bovine Rhodopsin. *Handbook of Biological Physics, Vol. 3*. Elsevier, Amsterdam, 1-72.

Holmgren, F. 1870. Om Retinastromme. *Ups Lakareforenings Forh*, **6**, 419-455.

Hood, D.C. & D.G. Birch. 1990. The a-wave of the Human ERG and Rod Receptor Function. *Investigative Ophthalology and Visual Science* **31**, 2070-2081.

Hood, D.C. & D.G. Birch. 1992. A Computational Model of the Amplitude and Implicit Time of the b-wave of the Human ERG. *Visual Neuroscience*, **8,** 107-126.

Hood, D.C. & D.G. Birch. 1993. Human Cone Receptor Activity: the Leading Edge of the A-wave and Models of Receptor Activity. *Visual Neuroscience*, **10,** 857-871.

Kahlert, M. & K.-P. Hofmann. 1991. Reaction Rate and Collisional Efficiency of the Rhodopsin- Transducin System in Intact Retinal Rods. *Biophysical Journal* **59**, 375-386.

Kahn, R. & A. Löwenstein. 1924. Das Elektroretinogramm. *Graefes Arch Ophthalmol,* **114**, 304-325.

Karpe, G. 1945. Basic of Clinical Electroretinography, *Acta Ophthaimol*, **24** (suppl), 1-118.

Kolb, H., R. Nelson and E. Fernandezs. 2000. Webvision, 'ww.webvision.med.utah.edu'.

Koutalos, Y., K. Nakatami, T. Tamura & K-W. Yau. 1995a. Characterization of Guanylate Cyclase Activity in Single Retinal Rod Outer Segments. *Journal of General Physiology* **106**, 863-890.

Koutalos, Y., K. Nakatami, T. Tamura & K-W. Yau. 1995b. The cGMP-phosphodiesterase and its Contribution to Sensitivity Regulation in Retinal Rods. *Journal of General Physiology* **106**, 891-921.

Lagnado, L., L. Cervetto & P.A. McNaughton. 1992. Cytoplasmic Free Calcium Concentration in Dark-adapted Retinal Rod Outer Segments. *Vision Research* **29**, 939-948.

Lamb, T.D. & E.N. Pugh, Jr. 1992. A Quantitative Account of the Activation Steps Involved in Phototransduction in Amphibian Photoreceptors. *Journal of Physiology*, **449**, 719-758.

LaVil, M.M., J.G. Hollyfield & R.E. 2003. *Retinal Degeneration: Mechanisms and Experimental Therapy.* New York : Kluwer Academic/Plenum Publishers.

Li, F., W. Cao & R.E. Anderson. 2001. Protection of Photoreceptor Cells in Adult Rats from Light-induced Degeneration by Adaptation to Bright Cyclic Light. *Exp Eye Res*, **73,** 569-577.

Liri, T., Z. Farfel & H. Bourne. 1998. G-protein Diseases Furnish a Model for the Turnon Switch. *Nature* **394**, 35-38.

Lyubarsky, A.L. & E.N. Pugh, Jr. 1996. Recovery Phase of the Murine Rod Photo-Response Reconstructed from Electroretinographic Recordings. *Journal of Neuroscience* **16**, 563-571.

Makino, E.R., J.W. Handy, T. Li & V.Y. Arshavsky. 1999. The GTPase Activating Factor for Transducin in Rod Photoreceptors is the Complex between RGS9 and Type 5 G Protein Beta Subunit. *Proceedings of the National Academy of Sciences of the United States of America*, **96**, 1947-1952.

Marc, R.E, B.W. Jones, C.B. Watt & E. Strettoi. 2003. Neural Remodeling in Retinal Degeneration. *Prog Retin Eye Res*, **22,** 607-655.

Miller, J.L. & J.L. Korenbort. 1994. Differences in Calcium Homeostasis between Retinal Rod and Cone Photoreceptors Revealed by the Effects of Voltage on the cGMP-gated Conductance in Intact Cells. *Journal of General Physiology* **104**, 909-940.

Molday, R.S. & U.B. Kaupp. 2000. Ion Channels of Vertebrate Photoreceptors. *Molecular Mechanisms in Visual Transduction.* ed. Hoff A.J., pp. 143-181. Amsterdam; New York; Elsevier.

Nikonov, S., N. Engheta & E.N. Pugh, Jr. 1998. Kinetics of Recovery of the Dark-adapted Salamander Rod Photoresponse. *Journal of General Physiology* **111,** 7-37.

Noell, W.K, V.S. Walker, B.S. Kang & S. Berman. 1966. Retinal Damage by Light in Rats. *Invest Ophthalmol,* **5,** 450-473.

Owen, W.G. 1987. Ionic Conductances in Rod Photoreceptors. *Annual Review of Physiology,* **49,** 743-764.

Palczewski, K., I. Subbaraya, W.A. Gorczyca, B.S. Helekar, C.C. Ruiz, H. Ohguro, J. Huang, X. Zhao, J.W. Crabb & R. S. Johnson. 1994. Molecular Cloning and Characterization of Retinal Photoreceptor Guanylyl Cyclase-activating Protein. *Neuron* **13**, 395-404.

Penn, R.D. & W.A. Hagins. 1969. Signal Transmission along Retinal Rods of the Electroretinographic a-wave. *Nature*, **223**, 201-205.

Perlman, I. 2005. http://webvision.med.utah.edu/ERG.html#Historical%20view.

Piper, H. 1911. Ueber die Netzhautströme. *Arch Anat Physiol Leipzig*, 85-132.

Pugh, E.N. Jr. & T.D. Lamb. 1990. Cyclic GMP and Calcium: the Internal Messengers of Stimulus and Adaptation in Vertebrate Photoreceptors. *Vision Research,* **26**, 1613-1643.

Pugh, E.N. Jr. & T.D. Lamb. 1993. Amplification and Kinetics of the Activation Steps in Phototransduction. *Biochimica et Biophysica Acta,* **1141,** 111-149.

Pugh, E.N. Jr. & T.D. Lamb. 2000. Phototransduction and Vertebrate Rods and Cones: Molecular Mechanisms of Amplification, Recovery and Light Adaptation. *Molecular Mechanisms in Visual Transduction.* ed. Stavenga, W.J., W.J.de Grip & E.N. Pugh, Jr., pp.183-255. Amsterdam; New York; Elsevier.

Smith, N.P. & T.D. Lamb. 1997. The A-wave of the Human Electroretinogram Recorded with a Minimally Invasive Technique. *Vision Research* **37**, 2943-2952.

Sprang, S. 1997. G Protein Mechanisms: Insights from Structural Analysis. *Annual Review of Biochemistry* **66**, 639-678.

Snyder, A.W. & R. Menzel. 1975. *Photoreceptor Optics*. Springer, Berlin.

Stroop, D.D. & J.A. Beavo. 1992. Sequence Homology and Structure-function Studies of the Bovine Cyclic-GMP-stimulated and Retinal Phosphodiesterases. *Advances in Second Messenger and Phosphoprotein Research*, **25**, 55-71.

Tomita, T. 1950. Studies on the Intraretinal Action Potential. I. Relation between the Localization of Micropipette in the Retina and the Shape of the Intraretinal Action Potential. *Journal of Physiology(Japanese)* **1,** 110-117.

Yau, K.-W. & D.A. Baylor. 1989. Cyclic GMP-actived Conductance of Retinal Photoreceptor Cells. *Annual Review of Neuroscience,* **12**, 289-327.